Argonne National Laboratory

DEVELOPMENT OF BRAZING TECHNIQUES AND PROCEDURES FOR FABRICATING FUEL SUBASSEMBLIES FOR THE ARGONNE ADVANCED RESEARCH REACTOR (AARR)

by

V. M. Kolba, C. V. Pearson,
and W. C. Kramer

The facilities of Argonne National Laboratory are owned by the United States Government. Under the terms of a contract (W-31-109-Eng-38) between the U. S. Atomic Energy Commission, Argonne Universities Association and The University of Chicago, the University employs the staff and operates the Laboratory in accordance with policies and programs formulated, approved and reviewed by the Association.

MEMBERS OF ARGONNE UNIVERSITIES ASSOCIATION

The University of Arizona	Kansas State University	The Ohio State University
Carnegie-Mellon University	The University of Kansas	Ohio University
Case Western Reserve University	Loyola University	The Pennsylvania State University
The University of Chicago	Marquette University	Purdue University
University of Cincinnati	Michigan State University	Saint Louis University
Illinois Institute of Technology	The University of Michigan	Southern Illinois University
University of Illinois	University of Minnesota	University of Texas
Indiana University	University of Missouri	Washington University
Iowa State University	Northwestern University	Wayne State University
The University of Iowa	University of Notre Dame	The University of Wisconsin

LEGAL NOTICE

Printed in the United States of America
Available from
Clearinghouse for Federal Scientific and Technical Information
National Bureau of Standards, U. S. Department of Commerce
Springfield, Virginia 22151
Price: Printed Copy $3.00; Microfiche $0.65

ANL-7458
Metals, Ceramics, and
Materials

ARGONNE NATIONAL LABORATORY
9700 South Cass Avenue
Argonne, Illinois 60439

DEVELOPMENT OF BRAZING TECHNIQUES AND PROCEDURES FOR FABRICATING FUEL SUBASSEMBLIES FOR THE ARGONNE ADVANCED RESEARCH REACTOR (AARR)

by

V. M. Kolba and C. V. Pearson

Reactor Engineering Division

W. C. Kramer

Metallurgy Division

August 1968

TABLE OF CONTENTS

TABLE OF CONTENTS

TABLE OF CONTENTS

LIST OF FIGURES

LIST OF FIGURES

LIST OF FIGURES

LIST OF FIGURES

LIST OF TABLES

DEVELOPMENT OF BRAZING TECHNIQUES AND PROCEDURES FOR FABRICATING FUEL SUBASSEMBLIES FOR THE ARGONNE ADVANCED RESEARCH REACTOR (AARR)

by

V. M. Kolba, C. V. Pearson, and W. C. Kramer

1.0 INTRODUCTION

The Title I design of the AARR Facility, as completed in fiscal 1966, featured a pressurized, light-water-cooled, beryllium-reflected reactor with a thermal output of 100 MW. Consistent with this power level, the reference Mark-I core was being developed to provide for experimental purposes, unperturbed thermal-neutron fluxes approaching 4×10^{15} n/(cm^2)(sec) in the Internal Thermal Column (ITC) and 10^{15} n/(cm^2)(sec) at the innermost tips of six horizontal beam tubes. Designed for unit replacement, the core consisted of 45 fuel subassemblies, 12 control and safety rods, and supporting structures disposed around the ITC.

As shown in Fig. 1, each fuel subassembly was rhomboidal in cross section and consisted of Type 347 stainless steel-clad fuel plates fabricated by the picture-frame technique. Each plate measured 20 in. long, 2.546 in. wide, and 0.040 in. thick. Five types of subassemblies were to be employed, differing only in the number of fuel plates, fuel content, and spacing.

A standard subassembly contained 27 plates of highly enriched (93% U^{235}), spheroidal uranium dioxide (37 w/o max) uniformly dispersed in a Type 347 stainless steel matrix. A sufficient amount of stable boron compound (ZrB_2) was included for additional reactivity holddown during initial reactor operation. To reduce power peaking at the inner and outer edges of the core, the subassemblies in these regions contained plates of varying fuel content and coolant-channel thickness. Figure 2 shows the fuel-plate spacing and arrangement of subassemblies comprising one quadrant of the core.

Physics requirements dictated a minimum of diluent material in the active core region. Accordingly, in lieu of side plates, the fuel plates were to be spaced and supported by square wires welded or brazed vertically at intervals along the edges and continuously along the axial centerline. Finally, rhomboidal end fittings, fabricated from Type 347 stainless steel, were to be welded to plate extensions at the top and bottom to ensure adequate division of coolant flow through the subassembly channels.

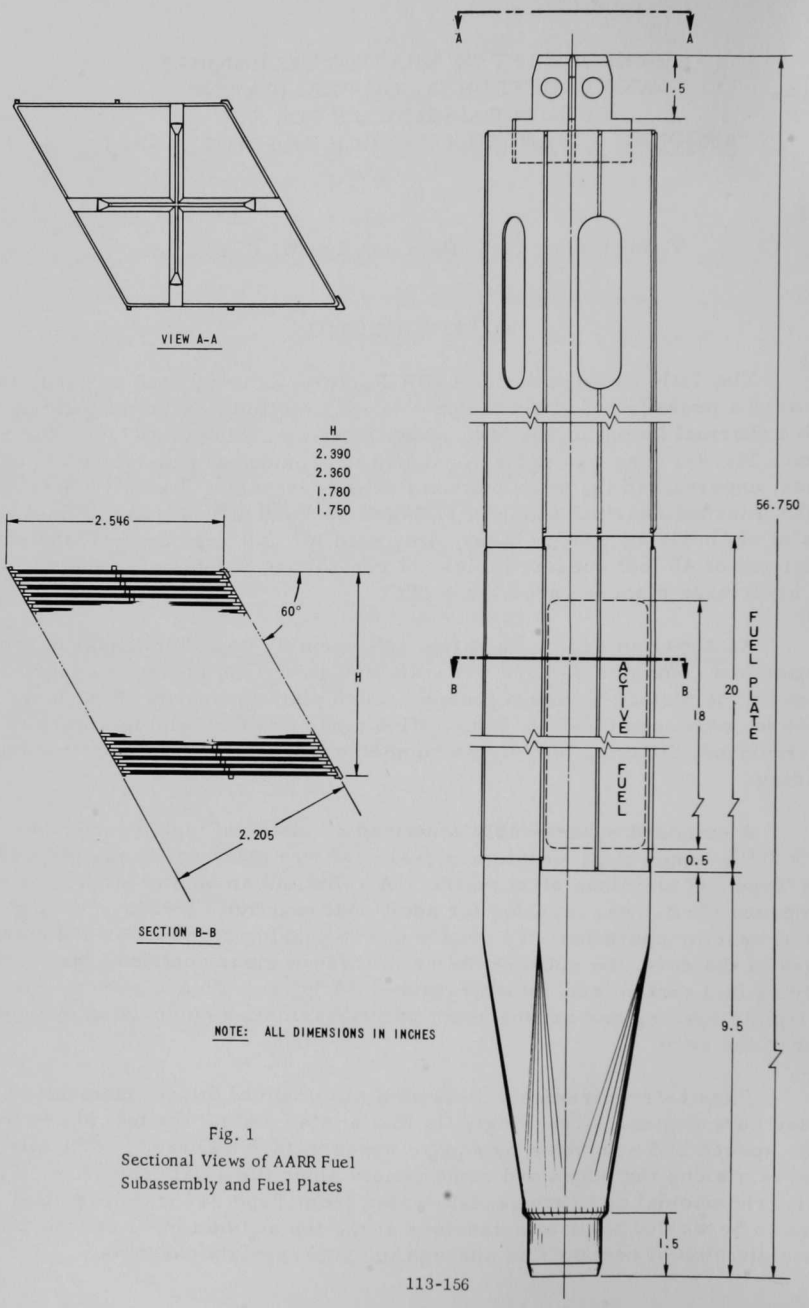

Fig. 1
Sectional Views of AARR Fuel Subassembly and Fuel Plates

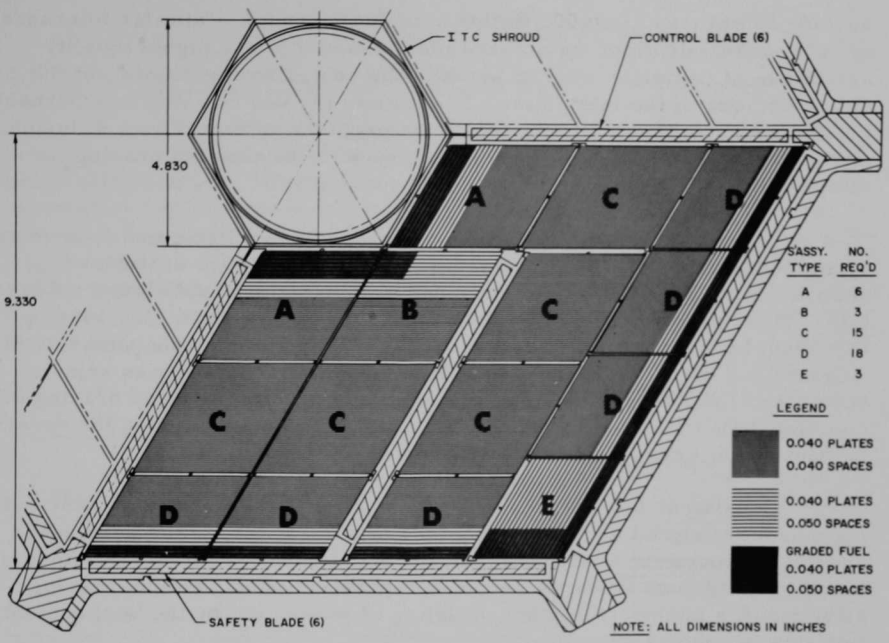

113-157

Fig. 2. Partial Plan View of AARR Core Showing Relative Positions of Standard and Graded Fuel Subassemblies, and Orientation of Control and Safety Blades

Brazing was selected as the method of fuel-plate assembly for several reasons. First, it represented the most feasible method for complete bonding of the center spacer wires to adjacent plates. Second, it had the potential of providing closer tolerances, with less distortion than would be incurred by welding. Third, it was amenable to batch processing. Finally, brazing techniques had been developed for assembly of reactor fuel elements of similar materials but of different designs. These included APPR-1, Core-II fuel elements developed at ORNL[1] and ALCO Products, Inc.; the BORAX-V superheater fuel element developed at ANL;[2] and the Fermi Core-B fuel-element design developed at ORNL.[3] The intent here was to utilize to best advantage the brazing technology evolved from the respective reactor programs.

However, a review of this technology revealed it had limited application to the AARR fuel subassembly. Not only was the design unique, but because of the higher power density and hydrodynamic considerations, the dimensional tolerances and other requirements were more stringent than those employed in the foregoing reactors. More specifically, these included

spacing tolerances of ±0.001 in. for a coolant channel, a similar tolerance for the overall depth of the stacked plate assembly, and higher-quality assurance of complete bonding between the center spacer wires and the active regions of the fuel plates. In addition, the use of a discrete burnable poison (ZrB_2) in these regions posed the problem of interaction, diffusion, and loss of the boron during prolonged exposure to elevated brazing temperatures.

Consequently, an independent program was implemented to develop optimized brazing process-product specifications for use in vendor-qualification tests and ultimate commercial fabrication of AARR fuel subassemblies. This program was conducted during the period from May 1964 to Oct 1966, by Pyromet Co., San Carlos, California, under subcontract with Argonne and direction of the AARR Project Staff. Pyromet was selected because of their extensive commercial experience in precision brazing of complex structures and their technological contributions during the development of the Fermi Core-B fuel element.

Consistent with the contract, Pyromet utilized their personnel and equipment, designed and constructed all brazing fixtures, and developed and/or improved the brazing techniques and processes. Process improvement included such areas as surface preparation, spot welding, brazing alloy binders and pretreatment, knurling of wires, and methods of controlling flow of the brazing alloy.

Throughout the development program, close liaison was maintained between ANL and Pyromet. Each phase of the various activities was evaluated by cognizant AARR Project personnel to ensure that all materials, preparatory steps, and processes were compatible with all other aspects of the fuel-technology program and the requirements of reactor performance.

In Oct 1966, a decision was made to revise the AARR Facility design to accommodate an aluminum-clad U_3O_8-aluminum cermet, involute-plate core which had been developed and successfully operated in the High Flux Isotope Reactor (HFIR) at ORNL. This revision is not reflected in the program described herein.

To the extent that the development and process-improvement efforts were completed, an optimized process specification was evolved. However, some aspects of the process are recommended for further investigation. Also included are recommendations with regard to completion of the AARR Mark-I core brazing effort (e.g., irradiation tests), since the potential for a higher-power core of longer life does exist.

2.0 EXPLORATORY STUDIES

2.1 Screening Tests of Braze Alloy Powders

A consideration of the required properties, anticipated core environmental conditions, and past applications indicated that Ni-Cr-Si-type braze alloy powders offered the most promise for brazing AARR fuel subassemblies. Boron-containing powders were excluded because of the nuclear-poisoning effect of the boron and the necessity for closely controlling the amount of burnable poison in the core. The nominal compositions and temperature characteristics of the specific alloys selected for screening tests are listed in Table I. It will be noted that the GE J8100 and Coast Metals 60 alloys are similar except for the iron content.

TABLE I. Nominal Compositions and Temperature Characteristics of Candidate Braze Alloy Powders

Alloy	Composition, %	Temperature, °F		
		Solidus	Liquidus	Brazing[a]
GE J8100	Ni-19Cr-10Si	1975	2075	2150
Coast 60	Ni-20Cr-10Si-3Fe	1975	2075	2150
Coast NP	Ni-30Fe-5Mo-11Si-3.5P	1750	1835	2050
Nicrobraz 50	Ni-13Cr-10P	1615	1640	1800

[a]Usual brazing temperature.

With respect to previous applications, GE J8100 alloy had been used to braze BORAX-V fuel subassemblies at ANL and, also, in Fermi Core-B braze-development studies at ORNL. Nicrobraz 50, developed by Wall Colmonoy Corp., Detroit, Michigan, under a U.S. Air Force-sponsored contract,[4] was used to braze components of the BONUS reactor superheater fuel elements.* Coast Metals NP was developed for brazing nuclear components and was used for the APPR-1 Core-II fuel elements by ORNL.

Preliminary screening tests were conducted with the GE J8100, Coast Metals 60, and Nicrobraz 50 alloys. Briefly, each alloy was used to prepare shear-test specimens consisting of a rectangular spacer wire (0.375 in. long, 0.060 in. wide, 0.040 in. high) brazed to a Type 347 plate (1.25 in. long, 0.375 in. wide, 0.040 in. thick). The brazed joints were prepared with zero, 0.001-, 0.002-, and 0.003-in. gaps between the spacer wire and plate. Subsequent peel tests and metallographic examination led to elimination of Coast Metals 60 alloy because joints greater than 0.002 in. had the lowest shear strengths and because a rough residue remained after brazing.

*G. M. Slaughter, ORNL, personal communication.

More definitive screening tests were then conducted with the GE J8100 and Nicrobraz 50 alloys. Coast Metals NP was added because of its lower brazing temperature. This characteristic is desirable from the standpoint of reducing interaction between the burnable poison (ZrB_2) and the stainless steel during a production brazing cycle.

Preparatory to these tests, the lots of respective alloy powders were analyzed (see Table II), and samples mounted for metallographic examination. As shown in Fig. 3, the GE J8100 and Coast Metals NP powders were spheroidal, whereas the Nicrobraz 50 particles were angular. All powders appeared clean and free of oxide or other nonmetallic impurities.

2.1.1 Test Specimens, Fixtures, and Procedures

Two types of test specimens were fabricated: braze-test assemblies and shear-test specimens. Each braze-test assembly (see Fig. 4) consisted of six plates (each 5.75 in. long, 1.25 in. wide, 0.040 in. thick) and five sets of spacer wires, all fabricated of Type 347 stainless steel. Each set included a 0.040-in. square center spacer wire and a rectangular, edge

TABLE II. Analysis of Braze Alloy Powders

Alloy:	GE J8100[a]	Coast NP[b]	Nicrobraz 50[b]
Chemical Analysis, %			
Nickel	69.15	49.1	75.5
Chromium	18.95	-	13.16
Silicon	10.10	11.05	-
Phosphorus	0.010	3.48	10.3
Iron	1.50	29.2	-
Molybdenum		4.7	-
Semiquantitative Spectrographic Analysis, %			
Nickel		Major	Major
Chromium		0.01	Major
Silicon		7	0.02
Iron	1.5	Major	0.3
Copper	-	0.03	0.01
Aluminum	0.015	0.01	0.007
Cobalt	0.045	0.10	0.15
Silver	-	0.0002	-
Magnesium	-	0.04	0.01
Molybdenum	-	3	0.002
Calcium	-	0.002	0.03
Titanium	0.005	0.007	0.002
Manganese	0.10	0.02	0.003
Zirconium	0.005	-	-
Boron	0.007	-	-
Carbon	0.038	-	-
Sulfur	0.004	-	-

[a]Vendor-certified analysis.
[b]Analysis performed by Anamet Laboratories, Inc.

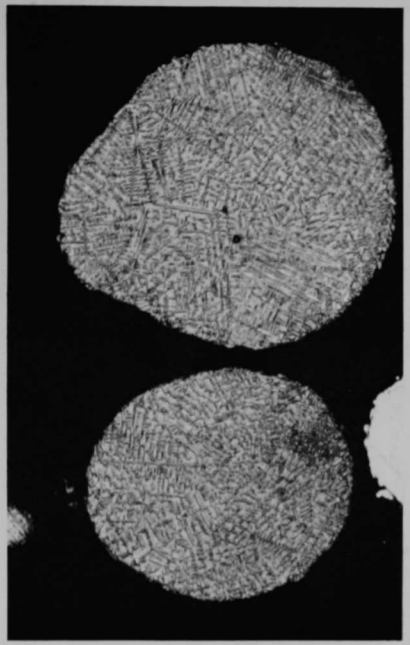

GE J8100

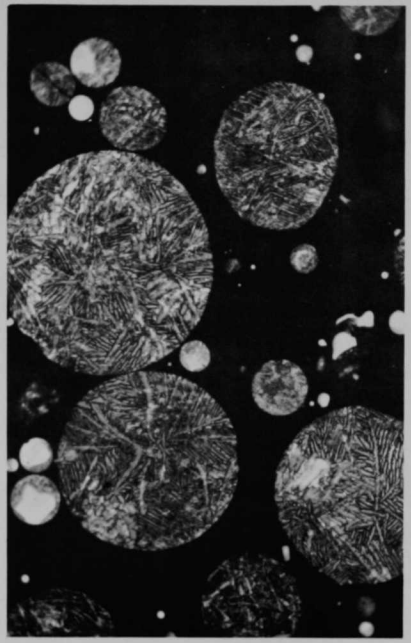

Coast NP

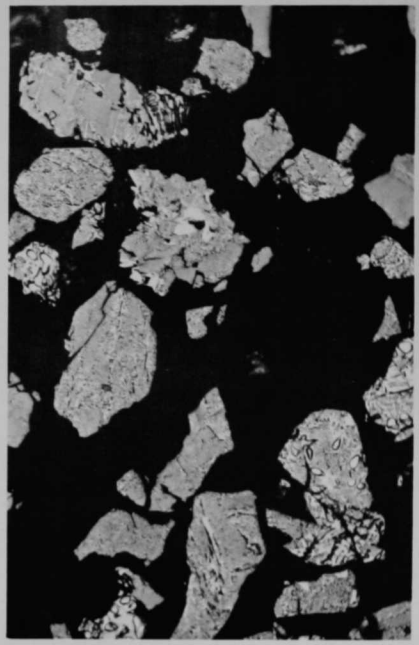

Nicrobraz 50

Fig. 3. Microstructures of Braze Alloy Powders

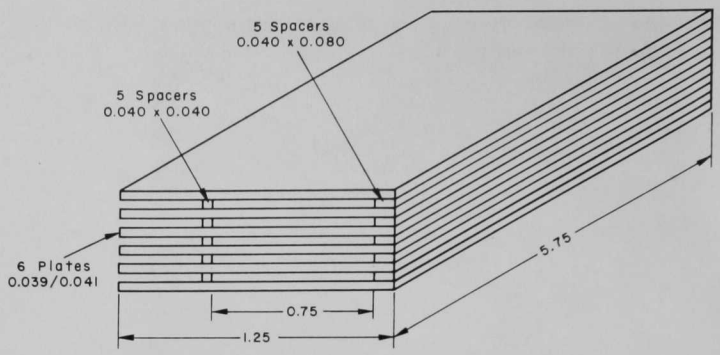

Fig. 4. Braze-test Assembly

spacer wire (0.080 in. wide and 0.040 in. high), both 5.75 in. long. All wires were knurled with 0.001-in. grooves approximately 1/64 in. apart. All wires and plates were cleaned with acetone. Then two spacer wires were spot welded to one surface of five plates. In each assembly, one of the braze alloy powders under consideration was applied adjacent to the spacer on the surface of each plate with the aid of a plastic loading bar containing a 0.030-in.-square groove. An acrylic binder, Wall Colmonoy Nicrobraz cement, was used to hold the powder in place. Nicrobraz Green Stopoff was applied to the plates to control the spread of the molten braze alloy at temperature. Each assembly was placed in a Type 347 stainless steel fixture (see Fig. 5) which held the plates horizontally and on edge during the brazing cycle. This oriented the joints in the same relative position as those of a full-scale subassembly.

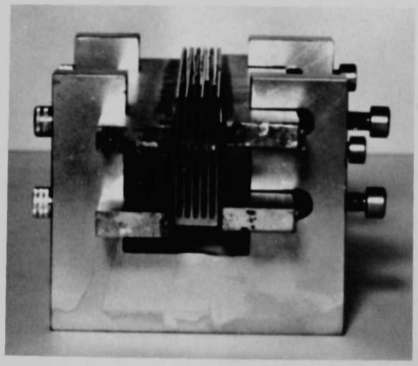

Fig. 5. Braze-test Assembly Positioned in Fixture

Three or four single shear-test plates [see Fig. 6(A)] prepared as above were also brazed in each experimental heat. On some plates, as shown in Fig. 6(B), the 0.375-in.-long spacer wire was rotated 90° so that the shearing load would be applied transverse to the wire axis.

All specimens were brazed in electric-resistance-heated, bell-type furnaces with weld-sealed retorts (of 20-in. ID and 20 in. long). The brazing atmosphere was dry hydrogen, having a maximum dew point of -80°F at the retort inlet. The

hydrogen was circulated at 100 ft^3/hr, providing approximately 27.5 atmosphere changes per hour.

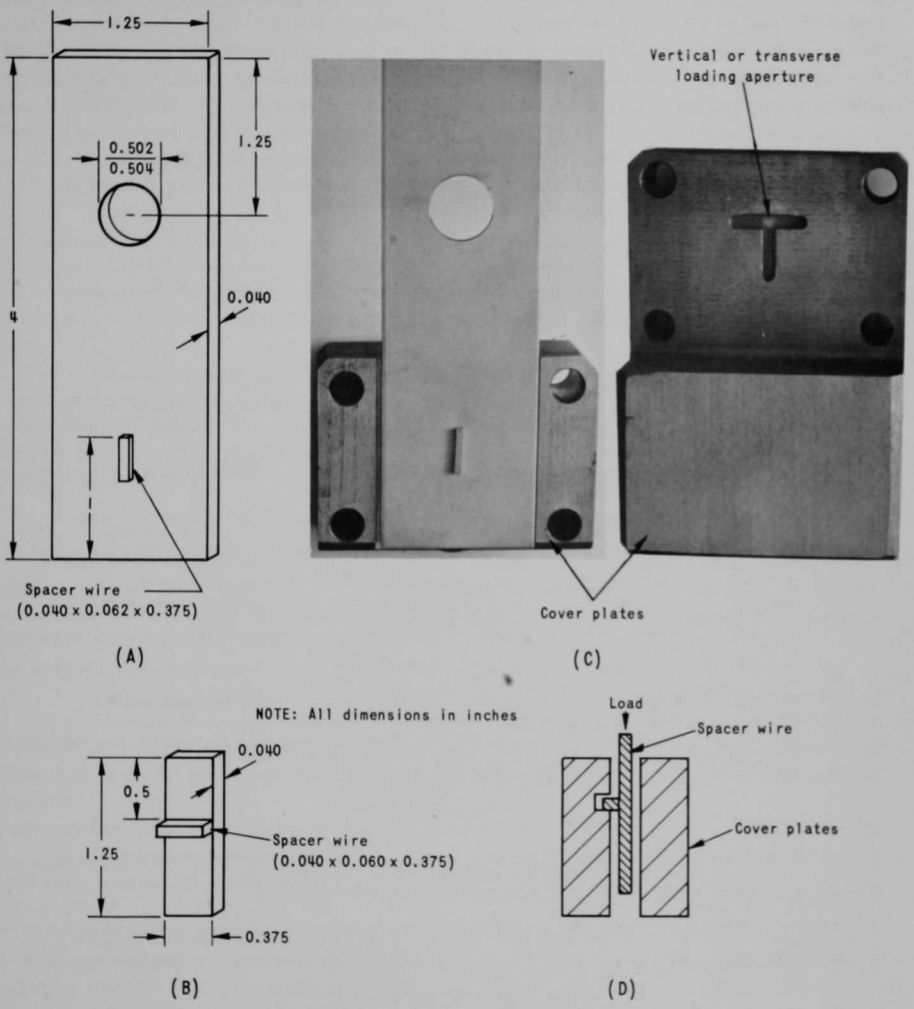

Fig. 6. Typical Shear Test Specimens and Postbraze Loading Fixtures

Each of the three braze alloys was tested at four brazing temperatures, with two holding times at each temperature. These holding times were: (1) 2 hr at the brazing temperature and (2) 10 min at the brazing temperature, followed by a 2- to 3-hr hold at a lower temperature.

Upon removal from the furnace, each braze-test assembly was examined visually at up to 30X magnification. Then the open edges were sealed and the unit pressurized internally with air to 50 psi. A soap solution was applied, and all brazed joints were checked for leaks. Subsequently, transverse and longitudinal sections were cut at random from each test assembly for metallographic examination. Sections were also taken from any defective areas observed visually or revealed by the leak test.

Shear-test plates were installed in appropriate fixtures [see Figs. 6(C) or (D)] and tested in a Tinius-Olsen tensile testing machine.

2.1.2 Results

The respective brazing conditions and the postbraze evaluations for the braze-test assemblies are summarized in Table III.

TABLE III. Summary of Screening Tests: Braze-test Assemblies

Test No.	Temp, °F	Time	Leak Test	Visual Examination of Outside Joints	Metallographic Examination of Random Sections
				GE J8100 Braze Alloy Powder	
1	2100	2 hr	None	Complete joints.	Sound, complete joints.
2	2100 2000	10 min 3 hr	Leak in P_3S_3	Incomplete flow; gaps in P_3S_3, S_4P_5, and S_5P_6 outside.	Some silicon-rich phase remains in joints. Voids observed in S_1P_1 inside, and S_4P_5 and S_5P_6 outside. P_3S_3 not bonded.
3	2120	2 hr	None	Incomplete flow; gaps in S_1P_2 and S_2P_3 outside.	Complete joints and fillets except on outside of S_2P_3 where gap was too large to be filled.
4	2120 2000	10 min 3 hr	None	Incomplete flow; gaps in S_3P_4.	Generally sound joints and fillets; inside S_5P_6 shows incomplete penetration of alloy. Partly diffusion bonded.
5	2130	2 hr	None	Complete joints.	Good fillets and complete joints; some excess hard phase, especially in fillets.
6	2130 2000	10 min 3 hr	None	Complete joints.	Good fillets and complete joints. Some hard phase, particularly in outside P_1S_1 joint.
7	2150	2 hr	None	Incomplete flow in outside S_5P_6.	Good fillets and complete joints except outside S_5P_6 wide gap not filled. Some excess hard phase in fillets.
8	2150 2000	10 min 3 hr	None	Complete joints.	Good fillets and complete joints. Filler alloy did not reach joint center in outside S_2P_3; diffusion bonded there.
9	2075	2 hr	None	Complete joints.	Good fillets and complete joints. Slight amount of excess hard phase in larger fillets.
10	2075	3 hr	None	Complete joints.	Inside: S_2P_3 80% bonded; other joints complete.
11	2090	3 hr	None	Complete joints.	Outside: S_4P_5 90% bonded; other joints complete, tight joints. Inside: S_2P_2 50% penetration, S_4P_5 65%, P_5S_5 70%; diffusion bonded where alloy did not penetrate.
18	2100	3 hr	None	Complete joints.	Outside: joints complete. Inside: S_1P_2 mostly diffusion bond; S_2P_3 25%, P_3S_3 30%; S_3P_4 and S_4P_5 did not penetrate; P_5S_5 did not penetrate 50% gap.
				Coast Metals NP Braze Alloy Powder	
12[a]	2075	2 hr	None	Partial flow in P_1S_1 and P_5S_5.	Hard phase in fillets. Joints complete except outside P_2S_2 and P_5S_5 mostly open but pressure tight.
13	2075	2 hr	Large leak in S_3P_4	Almost no flow in S_3P_4 outside. Large fillets inside.	Dendritic phase in fillets. Inside: S_5P_6 and S_1P_2 open (no alloy). Outside: S_3P_4 and S_2P_2 open. Longitudinal section S_2P_3 shows hard phases along joint.
14	2075 1800	10 min 3 hr	None	Satisfactory.	Joints thin but mostly complete; scattered hard phase.
15	2100	2 hr	S_2P_3 leak	No flow in S_2P_3 outside.	Some hard phase in fillets. Inside: P_1S_1, P_2S_2, P_5S_5 incomplete penetration; diffusion bond. No braze on S_4P_5. Outside: P_1S_1, P_2P_2, P_4S_4, P_5S_5 incomplete penetration; diffusion bond. No braze on S_2P_3.
16	2100 1800	10 min 3 hr	S_3P_4 leak	Alloy did not flow through S_3P_4 and S_5P_6.	Hard phase in fillets. No braze on S_4P_5 inside and S_3P_4 outside. Some voids in P_2S_2 outside and P_1S_1 inside.
				Nicrobraz 50 Braze Alloy Powder	
17	1825	2 hr	None	Incomplete flow in P_1S_1, P_2S_2, P_3S_3, P_4S_4.	Outside: incomplete penetration P_1S_1, S_1P_2, P_2S_2, S_2P_2, P_3S_3, P_4S_4, P_5S_5, S_5P_6. Inside: incomplete penetration P_1S_1, S_1P_2, P_2S_2, S_2P_3, P_4P_4, S_4P_5, P_5S_5, S_5P_6; some hard phase where alloy did penetrate.
19	1850	2 hr	Large leaks	Porous area 1 in. long.	Filler alloy did not flow into joints.
20	1850 1700	10 min 3 hr	None	Incomplete flow in P_3S_3, P_4S_4, P_5S_5.	Large amount of NiP compound, especially at fillets. Alloy did not penetrate consistently into joint on welded side.
21	1875	2 hr	None	Complete joints.	Large amount of NiP compound, almost continuous through joints, and especially heavy in fillets.
22	1875 1700	10 min 3 hr	None	Incomplete flow.	NiP compound present. Outside: P_2S_2 65% penetration, S_2P_3 75%, S_3P_4 and P_4S_4 65%, S_4P_5 and P_5S_5 50%. Inside: P_1S_1 30%, S_1P_2 cracked, P_2S_2 65%, P_4S_4 50%, S_5P_5 75%, P_5S_5 25%, S_5P_6 30%.
23	1900	2 hr	None	Generally good; some incomplete flow through joint.	Outside: P_1S_1, P_2S_2, and S_4P_5 did not penetrate to center of joint; scattered to heavy hard phase. Inside: P_2S_2 did not penetrate to center; S_2P_3 cracked; hard phase present.
24	1900 1700	10 min 3 hr	None	Incomplete flow.	Hard phase along most of joints. Outside: P_1S_1 void at center; S_1P_2 and P_2S_2 incomplete penetration; S_2P_3 small void; P_3S_3, S_3P_4, P_4S_4, S_4P_5 incomplete penetration. Inside: S_2P_2 cracked; P_4S_4 incomplete penetration.

[a]Coast Metals Plastibond binder substituted for Wall Colmonoy Nicrobraz cement.

Completely brazed joints were produced using GE J8100 alloy heated for 2 hr at temperatures ranging from 2075 to 2150°F. At lower temperatures, some residual unmelted phases were noted.

Attempts to reduce the time at brazing temperature using a second cycle (i.e., 10 min at braze temperature followed by a 3-hr hold at a lower temperature) were only partially successful. Three out of four assemblies tested each had one joint out of ten with incomplete flow of alloy across the joint. Also, one of these assemblies leaked during the pressure test.

Joint clearance has an influence on braze quality. Wide joints lead to excess amounts of hard silicon-rich phases which do not diffuse away, even at long hold times. Joints that are too thin may cause incomplete penetration of the braze alloy; however, they may be partially diffusion bonded.

The optimum cycle for the GE J8100 braze alloy appeared to be at temperatures from 2090 to 2120°F, with a 2-hr hold at temperature. Increasing the hold time to 3 hr at 2100°F did not significantly improve the braze joints. Microstructures of typical joints brazed with this alloy are shown in Fig. 7.

The phosphorus-containing alloys exhibited problems of penetration of joints with small clearances, and excessive hard, brittle phases in wider joints. The latter joints were susceptible to cracking. Alloying reactions between these braze materials and stainless steel was greater than observed with the GE J8100 alloy.

Three out of five assemblies brazed with Coast Metals NP leaked when pressure tested. The alloy tended to pile up and form large fillets, even at 2100°F. No significant improvement in joint quality was noted when Coast Alloys Plastibond cement was substituted for the standard Nicrobraz cement.

Typical microstructures of joints brazed with Coast Metals NP alloy and Nicrobraz 50 alloy are shown in Figs. 8 and 9, respectively.

Metallographic examination of the shear-test specimens revealed (1) complete penetration of all joints by the GE J8100 and Coast Metals NP alloys, and (2) a high incidence of defects (e.g., incomplete penetration, cracking, and hard phase) in joints brazed with the Nicrobraz 50 alloy.

Results of the shear tests are summarized in Table IV. Reliability of the shear strengths listed for the respective braze alloys is limited by the problems and variables encountered during these tests. For example, the combination of relatively thin spacer wires brazed parallel (axial) with the loading direction created problems in stress measurements, particularly

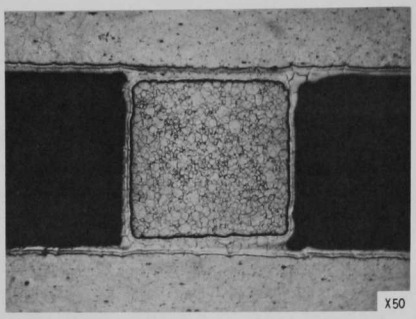

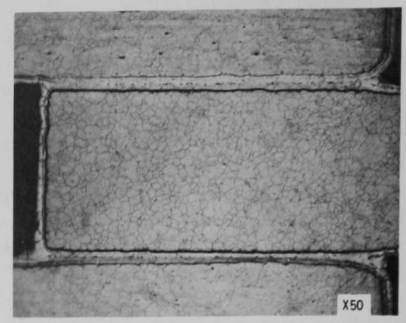

(Left) Center spacer joint and (Right) edge spacer joint from Assembly S/N 452-IA-1. Brazed at 2100°F for 2 hr. Electroetched with 50% HNO_3.

Longitudinal cross section of center spacer joint from Assembly S/N 452-IA-7. Brazed at 2150°F for 2 hr. Electroetched with 10% oxalic.

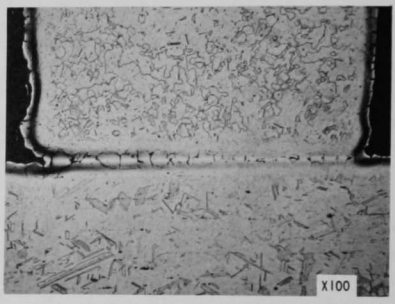

Center spacer joint on Assembly S/N 452-IA-1 showing undercutting at fillet. Brazed at 2100°F for 2 hr. Electroetched with 10% oxalic.

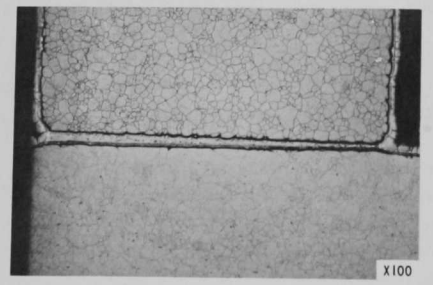

Edge spacer joint on Assembly S/N 452-IA-6. Brazed by dual temperature cycle: 2130°F for 10 min, then 2000°F for 3 hr. Silicon-rich phases have been eliminated by diffusion. Incomplete filling of other joints occurred under these conditions. Electroetched with 50% HNO_3.

Fig. 7. Microstructures of Joints Brazed with GE J8100 Alloy.
(Figures reduced by 35% photographically.)

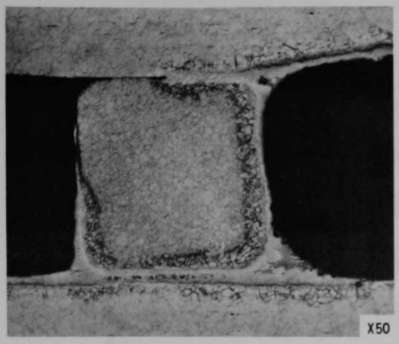

Center spacer joint of Assembly S/N 452-IA-13 showing large fillets and incomplete bonding. Brazed at 2075°F for 2 hr.

Edge spacer joint of Assembly S/N 452-IA-15 showing incomplete brazing. Brazed at 2100°F for 2 hr.

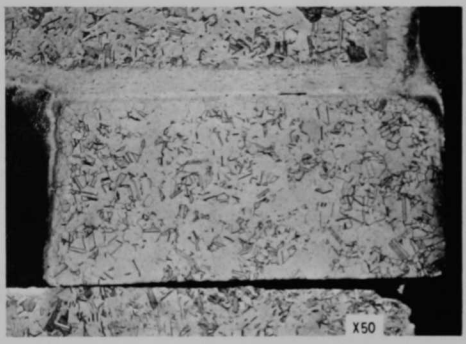

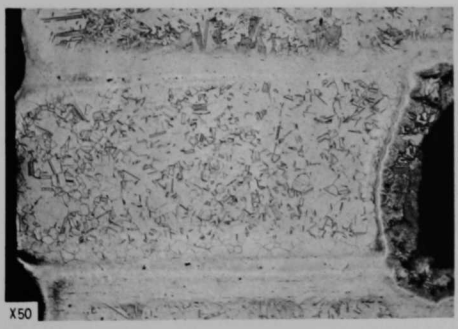

Edge spacer joint of Assembly S/N 452-IA-15. Joint completely brazed, but shows excessive alloying reaction between braze material and stainless steel. Brazed at 2100°F for 2 hr.

Fig. 8. Microstructures of Joints Brazed with Coast Metals NP Alloy. All specimens electroetched with 10% oxalic acid. (Figures reduced by 30% photographically.)

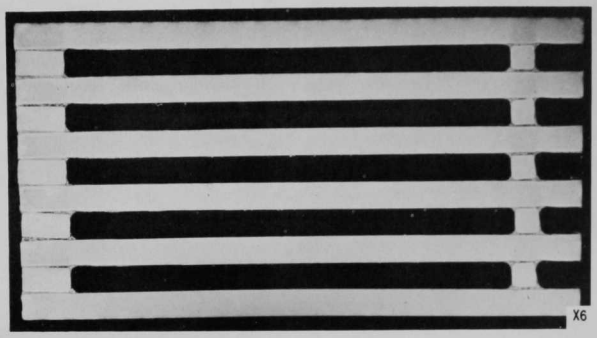

Assembly S/N 452-IA-21 brazed at 1875°F for 2 hr. All joints are complete, but with some excessively large fillets.

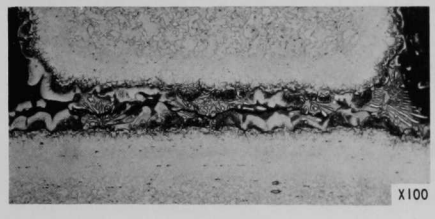

Center spacer wire in Assembly S/N 452-IA-23 showing extensive cracking in ~0.005-in.-wide joint brazed at 1900°F for 2 hr. Electroetched with 10% oxalic.

Closeup of joint in Assembly S/N 452-IA-22 showing alloy flow through knurled grooves in spacer wire but not in tight gaps in between. Brazed at 1875°F for 10 min, then at 1700°F for 3 hr. Electroetched with 10% oxalic.

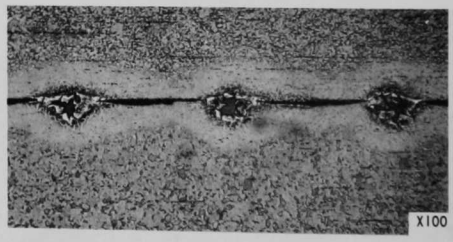

Fig. 9. Microstructures of Joints Brazed with Nicrobraz 50 Alloy. (Figures reduced by 30% photographically.)

TABLE IV. Summary of Screening Tests: Shear-test Specimens

Specimen[a] No.	Brazing Conditions	Load, lb	Calc Stress, psi	Average Stress, psi	Mode of Failure
		GE J8100 Alloy[b]			
1-1	2100°F, 2 hr	1350	63,945		Buckle
1-2		1165	55,182		Buckle
1-3		1400	66,313	61,813	Buckle
2-1	2100°F, 10 min;	672	31,830		Shear-buckle
2-2	2000°F, 3 hr	645	30,551		Shear
2-3		794	37,609	33,330	Shear-buckle
3-1	2120°F, 2 hr	520	24,631		Shear
3-2		488	23,115		Shear
3-3		550	26,052	24,600	Shear
3-1T[c]		1220	57,787		Shear-buckle
3-2T		1564	74,081		Shear
3-3T		1697	80,381	70,750	Shear
4-1	2120°F, 10 min;	785	37,183		Buckle
4-2	2000°F, 3 hr	1095	51,866		Buckle
4-3		770	36,472	41,840	Buckle
5-1	2130°F, 2 hr	804	38,083		Shear-buckle
5-2		864	40,295		Shear-buckle
5-3		860	40,735	39,704	Shear-buckle
6-1	2130°F, 10 min;	790	37,419		Shear-buckle
6-2	2000°F, 3 hr	890	42,156		Shear-buckle
6-3		1050	49,735	43,103	Shear-buckle
7-1	2150°F, 2 hr	667	31,593		Shear
7-2		912	43,198		Shear-buckle
7-3		806	38,177	37,656	Shear-buckle
8-1	2150°F, 10 min;	975	46,182		Shear-buckle
8-2	2000°F, 3 hr	1013	47,982		Shear-buckle
8-3		850	40,261	44,408	Shear-buckle
9-1	2075°F, 2 hr	1205	57,077		Shear-buckle
9-2		1600	75,786		Shear-buckle
9-3		1480	70,102	67,655	Shear-buckle
9-1T		2270	107,522		Shear
9-2T		2205	104,443		Shear
9-3T		2300	108,943		Shear
9-4T		2335	110,600		Shear
10-1	2075°F, 3 hr	1390	65,839		Shear-buckle
10-2		1245	58,971		Shear-buckle
10-3		1325	62,760	62,523	Shear-buckle
10-1T		2135	101,127		Shear
10-2T		1910	90,470		Shear
10-3T		2050	97,101		Shear
10-4T		2050	97,101	96,450	Shear
11-1T	2090°F, 3 hr	1990	94,259		Shear
11-2T		2170	102,785		Shear
11-3T		2120	100,417	99,154	Shear
18-1T	2100°F, 2 hr	2010	95,206		Shear
18-2T		2000	94,733		Shear
18-3T		1995	94,496	94,812	Shear

Specimen[a] No.	Brazing Conditions	Load, lb	Calc Stress, psi	Average Stress, psi	Mode of Failure
		Coast Metals NP Alloy[d]			
12-1T	2075°F, 2 hr;	2080	72,595		Shear
12-2T	Plastibond	2115	73,817		Shear
12-3T	binder	2145	74,864		Shear
12-4T		2090	72,944	73,555	Shear
13-1	2075°F, 2 hr	1347	37,218		Shear-buckle
13-2		923	25,503		Shear-buckle-shear
13-3		1780	49,182	37,301	Shear-buckle
14-1	2075°F, 10 min;	798	22,049		Buckle
14-2	1800°F, 3 hr	877	24,432		Buckle
14-3		1129	31,195	25,892	Buckle
15-1	2100°F, 2 hr	1100	30,393		Buckle
15-2		1185	32,742		Buckle
15-3		1385	38,268	33,801	Buckle
15-1T		1565	54,621		Shear
15-2T		1790	62,474		Shear
15-3T		1975	68,931	62,009	Shear
16-1	2100°F, 10 min;	1114	30,780		Shear-buckle-shear
16-2	1800°F, 3 hr	880	24,315		Shear-buckle-shear
16-3		1800	49,735	34,943	Buckle
		Nicrobraz 50 Alloy[e]			
17-1	1825°F, 2 hr	390	15,674		Shear
17-2		341	13,705		Shear
17-3		403	16,196	15,192	Shear
19-1	1850°F, 2 hr	316	12,700		Shear
19-2		260	10,449		Shear
19-3		354	14,227	12,459	Shear
20-1	1850°F, 10 min;	380	15,272		Shear
20-2	1700°F, 3 hr	453	18,206		Shear
20-3		454	18,246	17,241	Shear
21-1	1875°F, 2 hr	520	20,899		Shear
21-2		522	20,979		Shear
21-3		394	15,835	19,238	Shear
22-1	1875°F, 10 min;	394	15,835		Shear
22-2	1700°F, 3 hr	454	18,246		Partial shear
22-3		359	14,428		Shear
22-4		482	19,371	16,970	Partial shear
23-1	1900°F, 2 hr	384	15,433		Shear
23-2		434	17,442		Shear
23-3		557	22,386	18,420	Shear
24-1	1900°F, 10 min;	525	21,100		Shear
24-2	1700°F, 3 hr	425	17,081		Shear
24-3		547	21,984	20,055	Shear

[a]First number identifies the brazing experiment (see Table III), and the second the individual shear test specimen within the group.
[b]Calculated stress based on brazed joint 0.056 in. wide and 0.378 in. long.
[c]Suffix letter T denotes spacer wire transverse to loading direction.
[d]Stress for longitudinally loaded specimens based on joint area including fillets; AL = 0.096 x 0.377. For transverse specimens, effective joint area was assumed arbitrarily to include one-half the fillet width; AT = 0.076 x 0.377.
[e]Joint area (0.006 x 0.377 in.) for calculation of stress included total fillet width which averaged 0.005 in.

in the high-strength joints. In these instances, initial failure occurred by shear at the loaded end of the spacer. This was followed by buckling of the spacer until it wedged in the fixture, giving spurious data. By comparison, no buckling was experienced with specimens having spacer wires brazed perpendicular (transverse) to the loading direction; hence, the stress values were more consistent.

The test data were also influenced by fillet geometry and size. Fillets were small with the GE J8100 alloy, medium with the Nicrobraz 50 alloy, and large or full (avg width = 0.020 in.) with the Coast Metals NP alloy.

Accordingly, a representative fillet size was measured from metallographic sections. On the axially loaded test specimens, the effective joint area included the full fillet thickness on both sides of the spacer. On the transversely loaded specimens, one-half the fillet size was arbitrarily assumed as effective support for the applied loads.

Under these conditions, joints brazed with GE J8100 alloy showed the highest strengths, followed by Coast Metals NP alloy, with Nicrobraz 50 joints having the lowest strengths because of the defects cited above.

To reduce the number of variables in the ensuing exploratory studies, all spacer wires, dummy plate assemblies, and brazing fixtures were fabricated from Type 347 stainless. Except where noted otherwise, the following "standard" brazing cycle was used:

(1) Preheat test assembly and hold for ~15 min at 800-900°F in dry hydrogen atmosphere having a dewpoint of -80 to -100°F at the retort inlet.

(2) Heat at <200°F/hr to 1950°F and hold for 0.5 hr.

(3) Heat to 2135-2145°F and hold for 2 hr.

(4) Decrease furnace temperature at 100°F/hr to 1800°F.

(5) Turn off furnace power and allow assembly to cool to 800°F.

(6) Remove furnace and expose retort to ambient air.

(7) When assembly has cooled to 200-250°F, purge hydrogen from retort with exothermic gas or nitrogen; open retort and remove assembly.

2.2 Evaluation of Braze Alloy Binders

An effort was made to determine what effects, if any, the organic binder used to hold the braze alloy powder in place might have on the quality of the brazed joint. Four different binders were evaluated, using six-plate test assemblies with GE J8100 as the braze alloy: Wall Colmonoy Nicrobraz cement, Coast Metals Plastibond, and two paste compositions (C81-AT and CBL-71 #5) made by Fusion, Inc. The latter two were of interest because they combine the braze alloy powder and binder into a paste that can be dispensed from automatic machines of the type supplied by Fusion, Inc. or Handy and Harman.

Each test assembly was exposed to the standard brazing cycle, then pressure tested with air at 50 psig and visually examined. Longitudinal and transverse sections were removed for metallographic examination.

No significant difference was noted in the brazed joints of the four assemblies. However, the paste binders left a slightly greater amount of

a whitish residue. It was learned that these pastes contain some water in their formulation and may require a prebraze bake-out or drying cycle.

Because these tests provided no contraindicative evidence, it was decided to continue using the Nicrobraz cement as a braze alloy binder.

2.3 Methods of Controlling Alloy Placement

Five methods of placing and controlling the amount of braze alloy per joint were investigated: grooved spacer wires, plasma spraying, sintered wires, electroless nickel, and the use of a grooved plastic bar.

2.3.1 Grooved Spacer Wires

This method was evaluated using an assembly of seven plates (each 3 in. square and 0.040 in. thick), spaced with six wires (each 0.040 in. square and 3 in. long). A longitudinal groove was machined along the centerline of two opposing surfaces of each wire. Two wires were machined with 0.008 x 0.010-in. grooves, two with 0.010-in. square grooves, and two with 0.012 x 0.010-in. grooves. The grooved surfaces were knurled, and the grooves were filled with powdered GE J8100 brazing alloy (-400 mesh), which was held in place with Nicrobraz cement. It was quite difficult to fill the grooves uniformly with the -400-mesh powder, and impossible with a -150-mesh particle size.

Each wire was spot welded along the centerline of a plate, with a grooved surface against the plate. The six plates, along with the closure plate, were then clamped in a Type 347 stainless steel fixture and exposed to the standard brazing cycle.

Subsequent metallographic examination revealed sound, complete joints in all bond areas. Braze alloy flow was observed along the plate surfaces at 1/16 and 1/4 in. distant from the joints. However, this method was removed from consideration because, as shown in Fig. 10, the alloy flow from the groove results in a built-in void, which is detrimental.

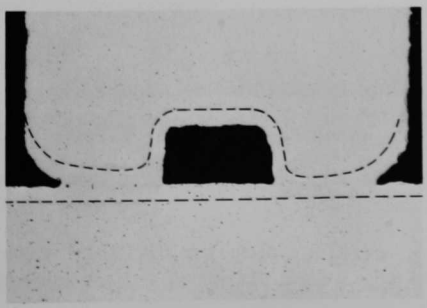

Fig. 10

Unetched Cross Section of Grooved Spacer Wire-plate Joint Brazed with GE J8100 Alloy Powder at 2135-2145°F for 2 hr. Dashed lines have been added for clarity. Dark rectangular area is built-in void caused by flow of molten braze alloy from 0.008 x 0.010-in. groove in spacer wire.

2.3.2 Plasma Spraying

Several tests were conducted to determine if the braze alloy could be applied by plasma spraying, thus making possible accurate control and uniformity of the deposit. Two procedures were investigated. The first involved spraying the alloy onto the wires before spot welding them to the plates. In the second procedure, the plates and wires were spot welded, clamped together, and the braze alloy sprayed onto the exposed edges of both the plates and wires. This section describes the problems encountered with adherence of the sprayed coating and the solutions that were effected.

Five spacer wires were degreased, cleaned with acetone, butted together side by side, and the top surfaces plasma sprayed with -150-mesh GE J8100. This operation revealed the need for additional surface preparation. The adherence of the sprayed alloy was so poor that it peeled off spontaneously when the coating reached a thickness of ~0.005 in.

In an effort to resolve this problem, the wire surfaces were grit-blasted with silicon carbide particles prior to plasma spraying. Afterwards, the coated wires were sintered for 30 min in dry hydrogen at 1800°F. Good adherence of the coating was achieved; however, carbide precipitation was encountered in the wires as a result of residue from the blasting grit.

Next, chilled iron shot was substituted for the silicon carbide. After grit blasting, the wires were first pickled in a 40% nitric acid-4% hydrofluoric acid solution to remove residual contamination, and then plasma sprayed and sintered as before. Adherence of the coating was good, and there was no evidence of carbide precipitation. The coating, however, could not be confined to the top surface of each wire; a small amount of overhang occurred at the edges and interfered with plate joint fit-up.

An assembly of six plates (each 3 in. square and 0.040 in. thick) with spacer wires (0.040 in. square and 3 in. long) plasma-spray-coated with GE J8100 alloy (0.008 in. thick) was exposed to the standard brazing cycle. The brazing characteristics of this assembly were essentially identical to those of previous test assemblies brazed with acrylic-bonded GE J8100 alloy powder.

The results of plasma spraying the braze alloy on exposed edges of a full-scale, plate-spacer wire assemblies and measures employed to confine the coating, are described in Sect. 3.2.

2.3.3 Electroless Nickel Plating

One test was conducted using electroless nickel plate (Ni-P alloy) as the braze alloy. Five spacer wires were each plated to a thickness of

0.0005 in. and then spot welded to 3-in.-square plates. These plates, along with a closure plate, were clamped in a fixture and brazed for 10 min in dry hydrogen at 2000°F. The results were not encouraging: no fillets were evident and there were large unbonded areas.

2.3.4 Sintered Braze Alloy Wires

An attempt was made to produce sintered wires of braze alloy, using the technique developed at ORNL to fabricate Ni-Cr-B rings. Accordingly, grooves corresponding to spacer-wire dimensions were cut into a graphite block and filled with dry GE J8100 braze alloy powder. The block containing the alloy was then heated to and held for 30 min in a dry hydrogen atmosphere at 1950°F.

The product was short pieces of wires that were too fragile to offer any advantages over use of the braze alloy as loose powder. Attempts to spot weld the wires to plates were partially successful: relatively strong welds could be made, but arcing occurred frequently.

2.3.5 Loading Bar

In preliminary scoping tests, the GE J8100 braze alloy powder was applied as a slurry in an acrylic binder, using an eyedropper. Fairly uniform and reproducible placement of the braze alloy was achieved with this technique. To improve the control of alloy quantity, the grooved Plexiglas loading-bar technique developed at ORNL[2] was also employed.

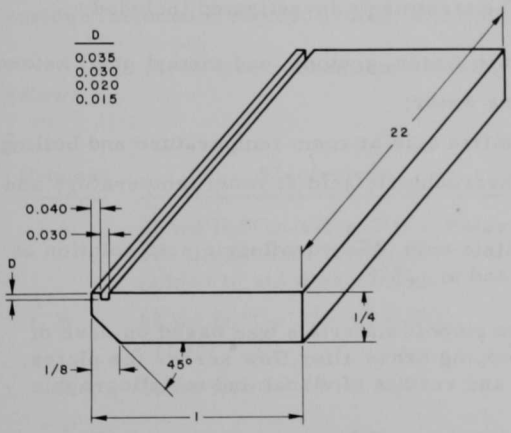

Fig. 11. Plexiglas Loading Bar

Four bars (see Fig. 11) were fabricated, differing only in the depth of the longitudinal groove; the width was held constant at 0.030 in. Each bar was used to apply the braze powder in different quantities on one side and on both sides of spacer wires in test plate assemblies. Examination of the brazed joints showed that the quantity of alloy contained in the 0.030-in.-square groove applied to one side of the spacer wire was satisfactory.

Application of braze alloy slurry to short edge spacers with an eyedropper was continued since the technique proved satisfactory for this type of joint.

2.4 Methods of Controlling Braze Alloy Flow

Excessive flow of braze alloy across fuel-plate surfaces is undesirable because of its adverse effects on heat transfer and coolant flow. Therefore, various techniques for confining the braze alloy near the spacer wire were studied, using placement methods discussed previously and materials which arrest or contain the liquid alloy. These techniques included use of commercial brazing stopoff materials, addition of nickel powder to the braze alloy, nickel plating, variation of the brazing cycle, scribing, and vapor deposition of aluminum and titanium.

2.4.1 Stopoff Materials

Four commercially available stopoff materials--Wall Colmonoy Standard Green, Green Type II, Red, and White--were evaluated in a series of tests. These tests were made on single-plate specimens and the six-plate braze test assemblies, using GE J8100 braze alloy powder (-150 mesh). Each stopoff material was applied in stripes (~1/8 in. wide) with a cotton-tipped stick and as close as possible to the wires (~1/16 in.). The assembly was then clamped in a fixture and exposed to the standard brazing cycle.

Subsequent tests were made to determine the postbraze treatment which would remove the stopoff material from the plate without harmful effects on the brazed joints. The treatments investigated included:

(1) ultrasonic agitation in Freon, acetone, and methyl ethyl ketone;

(2) immersion in boiling water;

(3) immersion in 50% nitric acid at room temperature and boiling;

(4) immersion in 50% hydrochloric acid at room temperature and boiling;

(5) pickling in a 40% nitric acid, 4% hydrofluoric acid solution at room temperature and at 125°F.

Overall evaluation of the stopoff materials was based on ease of application, effectiveness in stopping braze alloy flow across the plates, ease of removal after brazing, and results of visual and metallographic examination.

On these bases, Standard Green Stopoff was adjudged the easiest to apply and the most effective material for controlling braze alloy flow. It was found that even when diluted extensively, so long as the stripes were visible after drying, it would arrest the alloy flow. However, it was the most difficult one to remove, requiring pickling for ~15 min in a 40% nitric acid-4% hydrofluoric acid solution at 125°F. This treatment is undesirable because, as shown in Fig. 12, it results in chemical attack on the brazed joints.

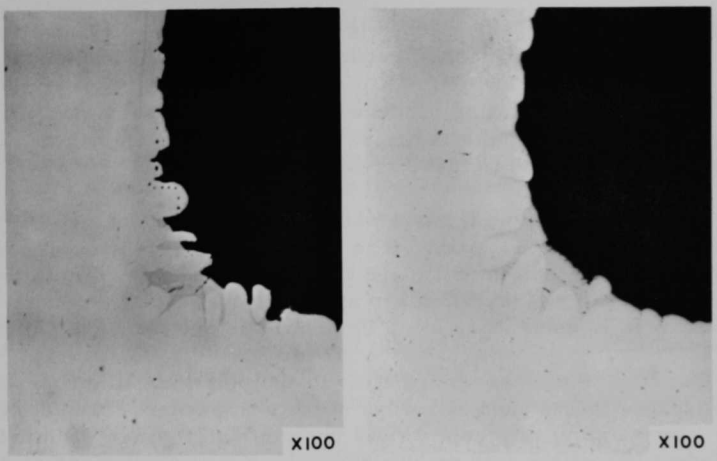

Fig. 12. (Left) Cross Section of Joint Brazed with GE J8100 Alloy and Then Pickled for ~15 min in 40% Nitric Acid-4% Hydrofluoric Acid Solution at 125°F to Remove Green Stopoff. (Right) Brazed Joint before Pickling.

A typical problem associated with the Standard Green Stopoff is the tenacious residue left on the stainless steel surface. Efforts to clean this residue included electropolishing, pickling, and abrasive grit blasting.

The three electrochemical cleaning processes used are tabulated below:

Process	Electrolyte	Temp, °F	Voltage, V	Time, min
A	55 ml H_2SO_4: 300 g Citric Acid; 125 ml Ethanol; 60 ml Glycerol (added to aid dissolution).	180-190	7	3
B	62 ml H_2SO_4; 325 ml H_3PO_4; 113 ml H_2O.	180-190	8-10	5
C	25 ml H_3PO_4; 75 ml H_2O.	Room	4	5

Each process successfully removed the stopoff residue from test plates; Process A produced a satin finish; B a shiny finish; C a frosty finish. Although considered feasible, cleaning by this technique is complex and tedious; each process would require a special cathode that could be inserted into the channel formed by the plates.

With respect to pickling, concentrated H_2SO_4 at 210°F slowly attacked the stopoff residue and left a smut that could be wiped off with a cotton swab.

This procedure also appeared feasible for cleaning full-scale fuel-plate subassemblies, although it would require swabbing of the individual channels.

Abrasive grit blasting produced clean, smooth surfaces, but would have required development of a means to protect the plate edges. Localized erosion was encountered in these areas.

Green Stopoff Type II has a water-soluble base and a consistency similar to latex-base wall paint. It is reportedly easier to apply and to remove after brazing than the Standard Green Stopoff. However, in these tests it was considerably more difficult to apply, it was equally effective as the Standard Green in controlling alloy flow, but was not easier to remove.

The Red Stopoff was more difficult to apply than either Green materials because the refractory oxides in the suspension settle out more rapidly. Braze alloy flow control was completely effective with this material. Either 50% nitric acid or 50% hydrochloric acid solutions at room temperature or boiling will remove Red Stopoff. However, hydrochloric acid is not recommended since it attacks the stainless steel, especially a hot solution. Visual and metallographic examinations revealed no harmful effects from the use of nitric acid; however, a slight stain from the stopoff was observed on the plate surface.

An experiment was performed to determine if, after the Red Stopoff suspension had settled, the relatively stable liquid phase remaining retained enough stopoff compound to effectively control alloy flow. When dried, the density of the applied stripe appeared similar to that of the diluted Green Stopoff mentioned earlier. However, unlike the latter, the Red Stopoff was completely ineffective when applied in this manner.

A combination of Red and White Stopoffs was almost as effective as the Red Stopoff alone, but was more difficult to apply. Removal of the Red-White combination required the same treatments as for Red alone.

The White Stopoff was also difficult to apply due to rapid settling of the refractory oxide powders. Control of braze alloy flow was very poor. Ultrasonic agitation and boiling water were effective in removing about 90% of the stopoff residue.

2.4.2 Addition of Nickel Powder to the Braze Alloy

Attempts were made to control excess flow of braze alloy by adding nickel powder to make the alloy more sluggish. All tests were made on single-plate specimens, with spacer wires attached by spot welding, then clamped in a fixture and exposed to the standard brazing cycle. Each specimen was oriented with the plate on edge and the spacer horizontal; this places the joints in the same position as those of the full-scale subassemblies during the brazing cycle.

Initial tests were made with blended mixtures of GE J8100 braze alloy powder with 5, 10, and 20 w/o additions of high-purity nickel powder (-200 to +325 mesh size). Additional tests were made with the nickel powder added to either one or both sides of the spacer wires adjacent to the plate. The braze alloy powder was placed on top of the nickel powder, except where the nickel was placed on both sides of the spacers. In this case, the braze alloy was placed over the nickel only on the upper side of the spacer.

Additions of 10 and 20 w/o nickel powder to the GE J8100 alloy restricted the flow on the bottom of the spacers but not on top where the braze alloy-nickel mixture was preplaced. Placement of nickel powder alone had the same effect. The nickel placed below the spacer stopped the alloy as it came through the joint. On the top side, the extent of braze alloy flow away from the joint was similar to that on a control specimen which was brazed with no addition of nickel.

Whether mixed with the braze alloy powder or placed directly on the joint area, the additions of nickel powder resulted in rough and porous braze fillets, i.e., the nickel alloyed partially with the molten braze metal, leaving unmelted nickel particles. Because of this fillet roughness, the addition of nickel powder would be feasible only on external joints, which would be machined after brazing.

2.4.3 Nickel Plating

Nickel plating had been tested earlier as a means of controlling alloy placement. In those tests, the nickel plating was applied to the spacer-wire surface adjacent to the plate. It was observed that the braze alloy flowed to the edge of the plated strip and stopped in many areas.

This observation was investigated further by tests with single-plate specimens and six-plate braze test assemblies, using nickel-plated strips to replace the stopoff lines. The plating was applied by two techniques: (1) standard electroplating in a sulfamate bath, and (2) brush or Dalic plating, in which the electrolyte is held in a cotton swab and brushed across the surface to be plated. Plating thickness ranged from 0.0001 to 0.0004 in. The brazed specimens were first examined visually; then transverse sections were prepared for detailed metallographic examination.

It was found that nickel plate 0.0002 to 0.0003 in. thick, or thicker, effectively controlled the flow of braze alloy. In the joint illustrated in Fig. 13 the upper spacer wire was located so that there was a 1/8-in. gap between the lower edge of the plated strip and the top edge of the wire. The lower, wide spacer was located so that its edge coincided with the edge of the plated strip. It can be seen that the nickel plating neatly defined the extent of braze alloy flow in the brazed joint of the lower spacer.

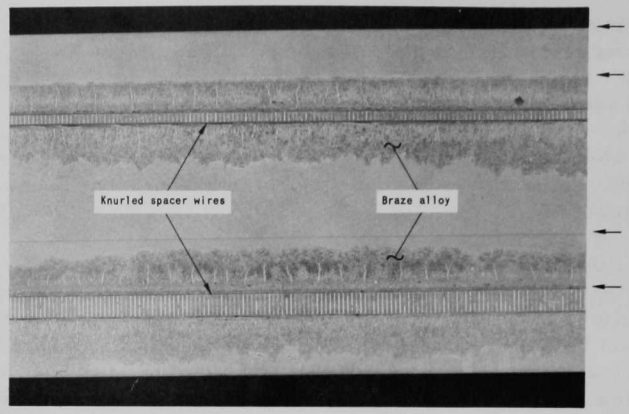

X2

Fig. 13. Brazed Test Specimen, Using Nickel-plated Strips for Flow Control of Braze Alloy. Arrows on right indicate original edges of plated area.

The mechanism of control of alloy flow is postulated to involve an alloying reaction between the braze metal and the nickel plating. When the plating is separated some finite distance from the joint, the molten braze alloy flows as a relatively thin film until it meets the plating, the nickel-to-braze alloy ratio at the interface being sufficient to raise the melting point and retard the flow. On the other hand, when the plating is adjacent to the joint, there is a relatively large amount of braze alloy in that area and the proportion of nickel taken into solution is insufficient to significantly affect the melting point or flow. Eventually, enough nickel is picked up to make the flow sluggish, but the outline of the flow area is irregular; this is illustrated in Fig. 14.

Fig. 14. Edge of Flow Area in Lower-spacer Joint of Nickel-plated Flow-control Specimen, Showing Irregular Flow of Braze Alloy. Electroetched with 10% oxalic acid.

The cost of nickel plating strips (1/8 to 1/16 in. wide, and 0.0003 to 0.0004 in. thick) on both sides of each plate of a full-scale, 27-plate fuel assembly was estimated to be less than $75.00. A major cost item would be the labor required to mask the areas that are not to be plated.

2.4.4 Variation of Brazing Cycle

A test was made to ascertain if excessive flow of the braze alloy could be controlled by limiting the

time that the assembly is held above the liquidus temperature of the alloy during the brazing cycle.

A single-plate assembly prepared with GE J8100 alloy was heated to and held for 2 min at the normal brazing temperature (2135-2145°F). The temperature was then lowered to 2050°F and held for 2 hr to diffuse the silicon away from the joint area. On examination, the brazed joint was found to be complete, sound, and free of microcracks. Alloy flow across the plate surfaces was reduced to between 1/8 and 1/4 in. distant from the joint; however, this distance was still considered excessive.

2.4.5 Scribing of Plates

Other programmatic efforts involving brazed components had shown that abrading the surfaces parallel to the brazed area with a stiff, sharp-bristled, stainless steel wire brush was effective in controlling braze alloy flow. This technique did not provide adequate control in the present program. Parallel grinding with coarse emery paper also was ineffective.

2.4.5.1 Stainless Steel Rods

To achieve close control of the location and depth of the abrasions, a comb-like scribing tool was designed and fabricated. It consisted of four, spring-loaded, stainless steel drill rods, each sharpened to a needle point, which scribed four grooves 1/32 in. apart and parallel to the brazed joint.

This technique provided uniform grooves and was effective in controlling the alloy flow; however, it resulted in a reduction of fuel-plate clad thickness locally at the grooves and, consequently, was abandoned.

2.4.5.2 Aluminum Rods

Alloys containing aluminum are difficult to braze in a dry hydrogen atmosphere due to formation of refractory aluminum oxide films. For example, at a brazing temperature of 2500°F, a hydrogen dewpoint of -140°F would be required to prevent oxidation of the aluminum. The equilibrium dewpoint would be even lower at a braze temperature of 2140°F. In this program a hydrogen dewpoint of -80 to -100°F was maintained at the retort inlet. This atmosphere is considered to be of extremely high quality by any hydrogen brazing standards. In any event, this characteristic behavior of aluminum in dry hydrogen was the basis for evaluating the use of aluminum scribes.

Briefly, the ends of 1/8-in.-dia aluminum welding rods were ground to a point. Two aluminum compositions--1100 (unalloyed) and 4043 (Al-5% Si)--were used in the annealed condition. With the aid of a straight edge,

each rod was used manually to scribe a film of aluminum on the plate surfaces parallel to the joint area. During the brazing cycle, this film oxidized and restricted braze alloy flow.

The condition of the stainless steel surface strongly influenced the effectiveness of the aluminum scribing. Fingerprints, acrylic binder traces, or other surface contaminants caused occasional discontinuities in the aluminum film transferred to the stainless steel. In an effort to eliminate these discontinuities during scribing, the rods were chucked in an air-actuated grinder and mechanically rotated. A vibratory engraver was also tried. In addition, some of the test plate assemblies were scribed before the braze alloy and binder were applied. Tests were made on single-plate specimens, six-plate braze test assemblies, and two full-scale dummy fuel assemblies. In each case, the braze alloy was GE J8100 with a Nicrobraz binder, and the brazing cycle was 2110°F, with a 2-hr hold at temperature.

In general, the Type 1100 aluminum rod worked better than the Type 4043 rod, i.e., the softer material rubbed off and transferred more easily. Typical examples of the effects of surface condition and aluminum hardness are illustrated in Fig. 15. Test plates scribed after application of the braze alloy and binder exhibited more frequent flow of alloy past the scribed film. Despite attempts to remove the excess binder with acetone, some traces remained and caused skips in the scribed film. As shown in Fig. 15, plates scribed with the harder, Type 4043 aluminum rods before application of braze alloy and binder also evidenced more frequent breakthrough of the braze alloy.

Use of a mechanically rotated aluminum scribe did not eliminate discontinuities in the stopoff film; rather, such a scribe had the potentially detrimental effect of depositing, intermittently, heavy layers of aluminum. As shown in the composite Fig. 16, when the aluminum layer was heavy, a reaction occurred with the surface of the stainless steel which was manifest as an etching reaction. Usually, no reaction layer is observed.

Of the two full-scale assemblies tested, the one whose plates had been scribed after application of the braze alloy and binder showed the higher incidence of alloy flow across the stopoff films. The plates in the other subassembly were first cleaned thoroughly with acetone, and then scribed before application of the alloy and binder. Postbraze examination revealed occasional areas where the alloy extended across the stopoff film. It is believed that the flow could be confined by scribing closely spaced multiple films.

2.4.6 Vapor Deposition of Aluminum and Titanium

In a series of tests, two parallel strips of aluminum and of titanium (each 1/8 in. wide and 1/4 in. apart) were vacuum vapor deposited on

specimen plates (6.125 in. long, 2.810 in. wide, and 0.040 in. thick). Three deposit thicknesses--100 Å (0.4×10^{-6} in.), 300 Å (1.2×10^{-6} in.), and 1000 Å (4×10^{-6} in.)--of each metal were evaluated. The titanium strips did not extend the length of the plates; Nicrobraz Green Stopoff was applied to complete the barriers. A single spacer wire was welded between the strips on each plate, and GE J8100 braze alloy was applied in the usual manner. All plates were brazed at 2120°F, with a 2-hr hold at temperature.

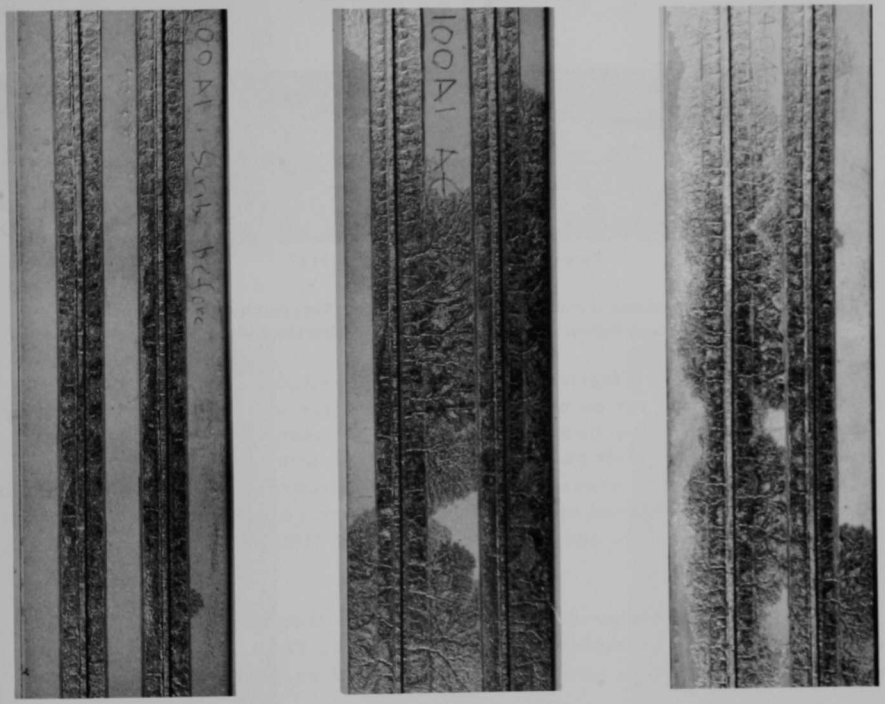

Type 1100 (Before) | Type 1100 (After) | Type 4043 (Before)

Fig. 15. Brazed Test Plates Scribed with Type 1100 and 4043 Aluminum Stopoffs, Showing Effect of Acrylic Binder Residue and Hardness of Aluminum Scribe on Braze Alloy Flow. Plate marked (After) was scribed with the softer Type 1100 aluminum rod after braze alloy and binder were applied.

Heavy aluminum-scribed deposit

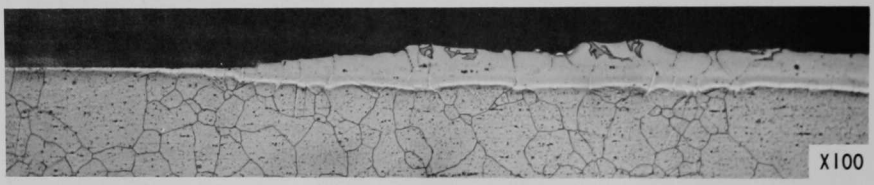

Normal aluminum-scribed deposit

Fig. 16. Surfaces of Stainless Steel Plates Showing (Top) Reaction Incurred by Heavy Deposit of Scribed Aluminum. Electroetched with 50% HNO_3.

The relative effectiveness of these deposited strips is shown in Fig. 17. Aluminum strips were partially effective at 300 Å, and completely stopped the braze alloy flow at the 1000-Å thickness. By comparison, the thinnest titanium deposit stopped the alloy flow; this is evidenced by the extent of alloy flow in areas outlined by the Nicrobraz Green Stopoff. Photomicrographs of sectioned specimens revealed no reaction between the stainless steel plate surface and either aluminum or titanium strips, even at the 1000-Å thickness.

The cost of vapor-depositing strips of either metal on a 27-plate, full-scale, fuel subassembly was estimated to be $2 to $3 per plate. For a large production run, special equipment could be built to reduce the cost.

2.5 Knurling of Spacer Wires

The surfaces of each wire adjoining the plates were knurled because preliminary braze tests with as-drawn wire showed incomplete flow of the braze alloy.

Knurling was accomplished in a machine consisting of two precision-ground, knurled wheels mounted one above the other. The upper one could be adjusted and locked with a set screw; the lower was driven manually with a crank. Except for a slight amount of twisting and bending of the wires, these wheels could knurl 64 transverse grooves per inch of wire, with groove depths ranging from 0.001 to 0.002 in. Typical grooves in an as-knurled wire and a microstructure of the brazed joint are shown in Fig. 18.

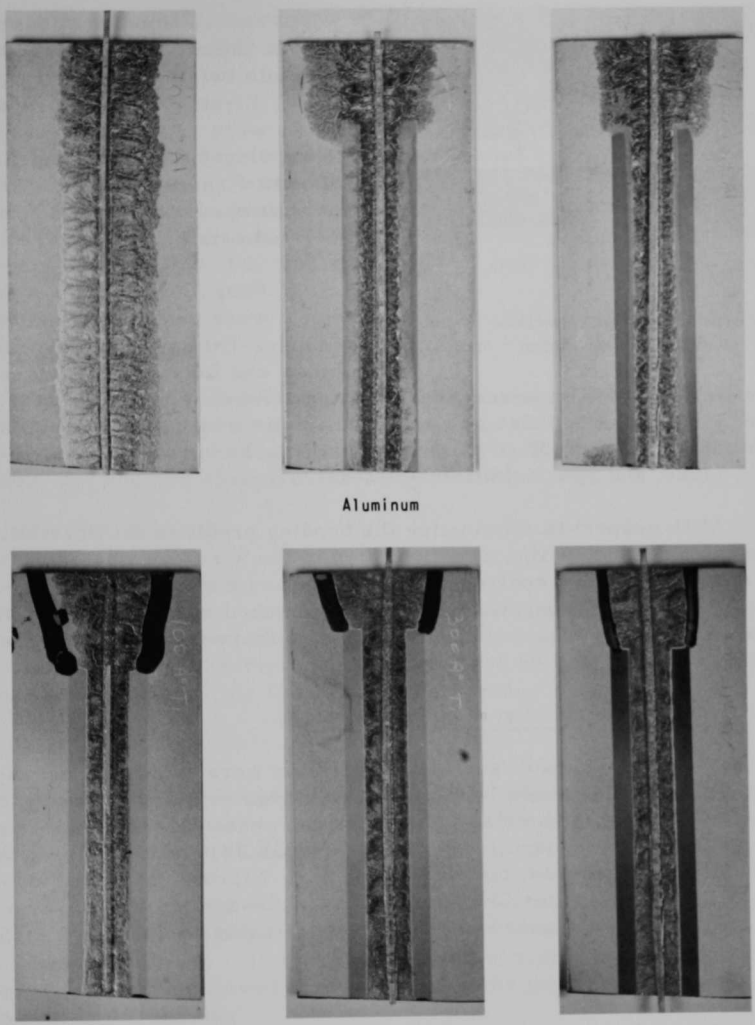

Fig. 17. Relative Effectiveness of Vapor-deposited Thicknesses of Aluminum and Titanium Strips as Braze Alloy Stopoffs. Irregular, darker outlines on titanium specimens are Nicrobraz Green Stopoff.

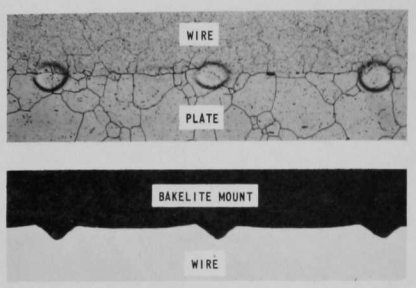

Fig. 18. (Bottom) Polished Specimen of Knurled Wire. (Top) Cross Section of Brazed Joint.

Several modifications were made in the machine components to eliminate twisting and bending of the wires. First, the straight-grooved wheels were replaced with wheels having diagonal grooves machined in opposite directions. Subsequent knurling operations resulted in aggravated twisting of the wires.

Next, the straight-grooved wheels were reinstalled and two sets of closer-fitting guides were fabricated: one for 0.040-in. wires and the other for 0.080-in. wires. By directing the wires precisely over the center of the wheels, these guides virtually eliminated the twisting, but not the bending. As a result of this improvement, the wires were much easier to cut, taper, and spot weld to the plates.

With respect to eliminating the bending problem, the possibility of incorporating the knurling as a final step in the wire-drawing operation was also considered. The knurled wires could then be straightened, if necessary, and cut precisely to length. However, this method was not pursued since it was shown that satisfactory knurled wires could be produced with the machine as modified above.

2.6 Effects of Preparation of Plate Surface

Five techniques of surface preparation were evaluated on respective six-plate braze test assemblies: wire brushing, chemical cleaning, electropolishing, sanding, and nickel plating. In each assembly, the spacer wires were knurled, spot welded to the plates, and GE J8100 braze alloy powder applied with the grooved, plastic loading bar. Nicrobraz Green Stopoff was used to confine the alloy flow on each side of the spacer wires. Finally, each assembly was exposed to the standard brazing cycle.

2.6.1 Wire Brushing

Approximately 1/4-in.-wide strips on both sides of each plate (braze area) were cleaned using a stainless steel brush. After brushing, each plate was thoroughly cleaned in acetone. The spacer wires were knurled and then cleaned in acetone before spot welding.

2.6.2 Chemical Cleaning

Prior to assembly, the plates and knurled spacer wires were pickled for 15 min in an aqueous solution containing 40% HNO_3 and 3% HF at 120°F.

After pickling, the parts were first rinsed in a hot water bath, then in cold running water, and dried with acetone.

2.6.3 Electropolishing

The plates and knurled wires were cleaned by Nicrolytics (West Los Angeles, California), using their "Select-O-Polish" electrolytic process system. This system is designed to permit electropolishing of the entire plate by immersion in a tank, or of localized areas with a remote cleaning head. Approximately 0.00025 in. of metal was removed from each surface, leaving a bright, shiny, finish.

2.6.4 Sanding

One-quarter-inch-wide strips (braze areas) on both sides of each plate were sanded with 180-grit, silicon carbide abrasive paper. After sanding, the plates were cleaned ultrasonically in Freon to remove the grit residue. The knurled spacer wires were cleaned in acetone.

2.6.5 Nickel Plating

Three combinations of nickel-plated surfaces were evaluated: (1) both plates and spacer wires plated; (2) spacer wires only; and (3) plates only. The spacers were plated to a thickness of 0.0003-0.0005 in. in a sulfamate bath. Nickel strips (3/16 in. wide and ~0.0002 in. thick) were applied to the plates by the Dalic (brush) process.

2.6.6 Results

Each brazed assembly was evaluated by visual examination at up to 30X magnification, pressure testing with air at 50 psia, and metallographic examination of transverse and longitudinal sections.

No significant differences were noted. Visual examination showed complete flow of braze alloy in all of the joints. None of the assemblies leaked during pressure testing. Metallographic examination revealed that the braze alloy either flowed through the joint or the fit was tight enough to achieve diffusion bonding.

From the viewpoint of brazed joint quality, none of the cleaning techniques offered a clear-cut advantage over the others; therefore other factors were considered. Chemical cleaning was selected because the process was relatively simple and inexpensive to set up, the results were reproducible, and there was no evidence of surface attack or other detrimental effects on the stainless steel.

2.7 Spot-welding Studies

Based on previous experience at ANL and ORNL, spot welding was selected as the method for tacking the spacer wires to the plates prior to brazing. A fixture was designed and fabricated for locating and holding the wires in position on the plates during this operation. As shown in Fig. 19, this fixture was machined from a Micarta-type plastic and featured a recess to hold the plate, and grooves to locate and hold the spacer wires. Spacing between the edge spacers was established by inserting wires machined to the exact length required. Matching holes were drilled in both halves of the fixture to permit insertion of the welding electrodes. With this fixture, the spacing between the center and edge spacers was maintained consistently within the specified tolerance of ±0.002 in.

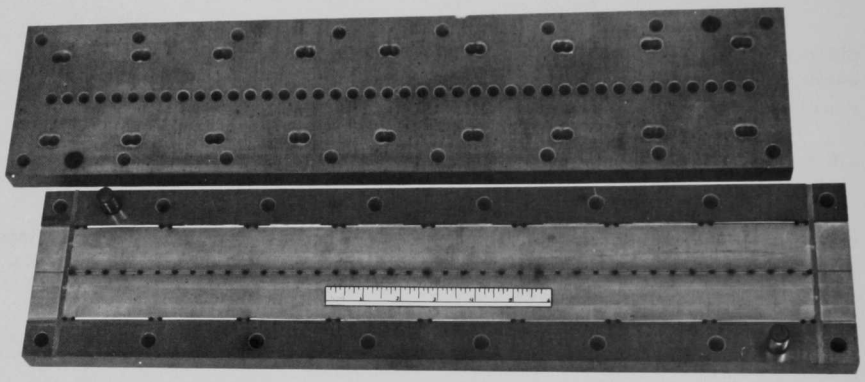

Fig. 19. Initial Fixture for Spot Welding Spacer Wires to Dummy Fuel Plates

Two spot-welding machines were investigated. One was a stored-energy type, the other an electronically controlled unit. With the latter, it was found that the power-time-pressure conditions required to produce spot welds of adequate strength resulted in slight, but perceptible, distortion of the spacers and plates. This distortion appeared to be caused by shrinkage of the weld nugget. Less distortion was incurred with the stored-energy capacitor-discharge machine; hence, it was selected.

Initially, difficulty was encountered in firmly attaching the spacer wires, even at the maximum output (250 Wsec) of the welding machine. This problem was partially solved by slightly notching the wires so that the points protruded and provided contacts for the probe-type welding electrode that was used.

When knurling of the spacer wires was introduced to solve the problem of braze alloy flow through the joint, it also alleviated the spot-welding

problem. With the knurled wires, firm attachment to the plates was achieved at low power levels (30-60 Wsec). Also, tweezer electrodes were found to be more satisfactory than the probe type.

New fixtures were fabricated for use with the tweezer electrodes. The fixture for attaching the center spacer wire consisted of a grooved Plexiglas plate to locate the wire, and two, adjustable, parallel plates attached to the sides for fuel-plate location. In operation (see Fig. 20), the wire was welded behind the fixture as it moved along the plate.

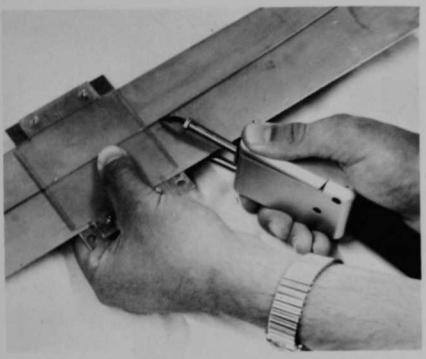

Fig. 20. Fixture for Spot Welding Center Spacer Wire to Plate with Tweezer Electrode

After spot welding the center spacer wire, the edge spacers were attached, using a fixture machined to the desired channel width, with edge cut-outs corresponding to the spacer-wire interval along the plate. This fixture accurately located the edge spacers with respect to the center spacer and to each other; it also provided channel width tolerances of ±0.002 in., or better. Except for adjustments in dimensions, similar fixtures were used for dummy fuel-plate subassemblies which required dual center spacers.

An air-actuated welding head (Stryco Manufacturing Company Model WH-250A) was attached to the 100-Wsec-capacity welder. This welding head was equipped with a spring-controlled switch mechanism whereby the welder could be adjusted to fire at a given electrode contact pressure. Figure 21 shows the welding head with a fixture similar to that shown in Fig. 19. However, this fixture was designed to be held stationary while the plate and three spacer wires were passed through it. Guides were provided to maintain proper spacing between the wires and to locate them on the plate. In operation, the spacers on one edge were welded flush with the plate edge, while those on the opposite edge overhung the plate edge by 0.046 in.

This fixture worked well with straight wires. However, with knurled wires and their attendant slight twist and bend, it was difficult to pass the plate and three spacer wires through the fixture unless the guides were loosened and thus incapable of maintaining specified dimensional tolerances. As a consequence, the plates were slightly bowed after the wires were spot welded.

To eliminate these difficulties, the next fixture employed was designed to support the spacers over their entire length. With reference to

Fig. 22, the grooved bars which hold the spacers in position were machined from Type 2024-T6 aluminum and anodized for electrical insulation. They could be adjusted to accommodate wires or plates of different widths. The 1/4-in.-dia holes at 1/2-in. intervals provide access for the upper electrode. Type 6061 aluminum was selected for the base plate because of its relatively good electrical conductivity. One lead from the spot welder was connected to this plate.

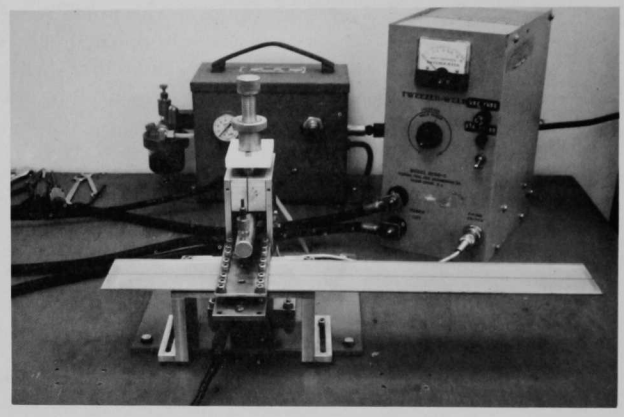

Fig. 21. Air-actuated Welding Head with Modified Spot-welding Fixture Similar to That Shown in Fig. 19

Initial difficulty with proper spacing and degree of parallelism was remedied by making one of the edge grooved bars wider and stiffer, thus providing a reference point for locating the other support bars. After proper adjustments were made, the fixture proved satisfactory in most respects. The spacing between wires could be maintained within the specified tolerance, and the plates remained flat after the wires were spot welded.

When welding with this fixture, the spring in the welding head was adjusted to the lightest load, the air pressure was set at 25 psig, and the welding power ranged from 40 to 50 Wsec. The higher power, compared to that used with the tweezer electrodes, is attributed partially to losses through the base plate and partially to the distribution of energy over a larger contact area.

A study was made of the spot-weld nugget size as a function of welder power and the air pressure to the welding head. The spring was adjusted to the lightest load. As evidenced by the photomicrographs in Fig. 23, there was no significant variation in nugget size under the conditions investigated. The largest nuggests were less than 0.002 in. thick, with equal penetration into the plate and spacer wire.

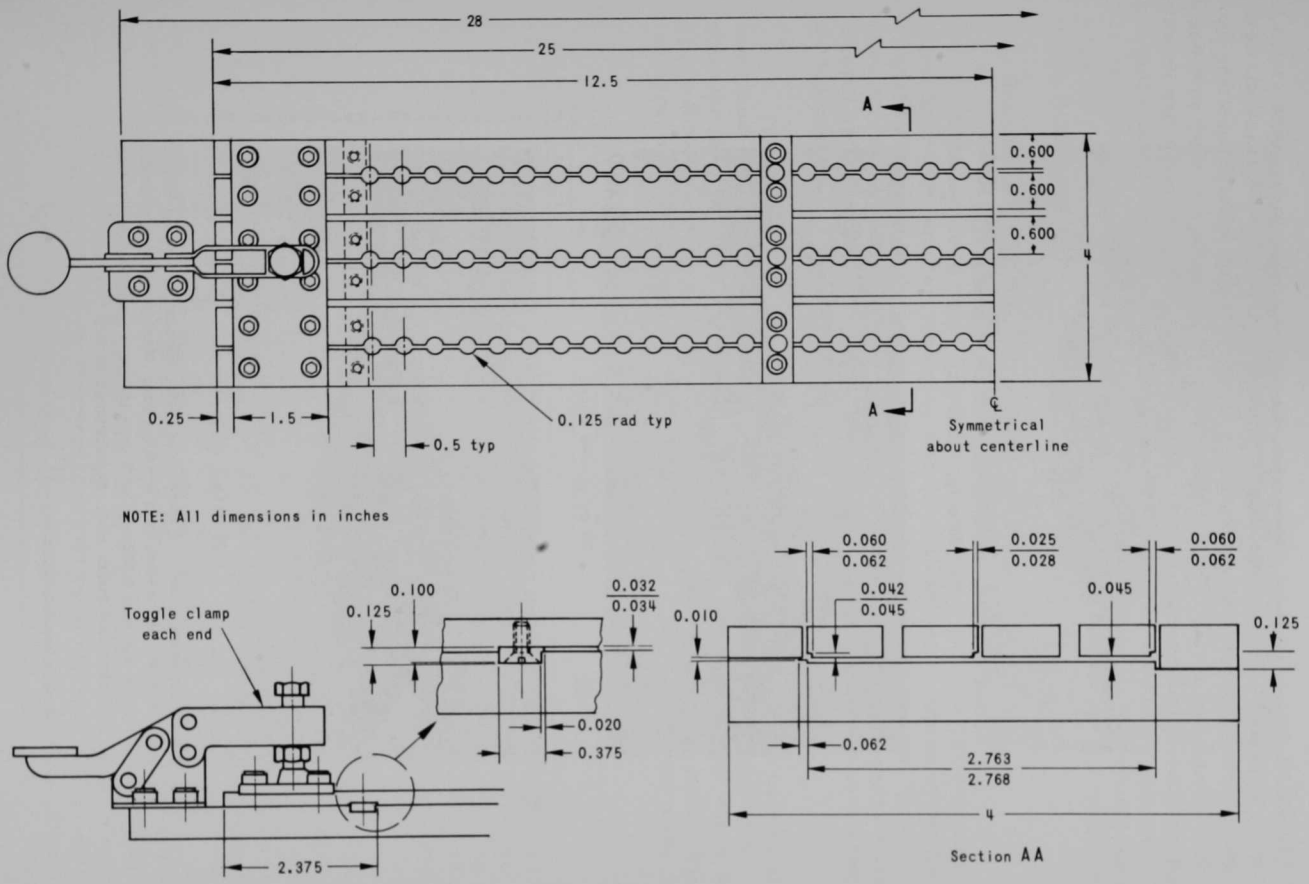

Fig. 22. Details of Adjustable Spot-welding Fixture Designed to Locate and Support Spacer Wires

20 psig, 40 W-sec

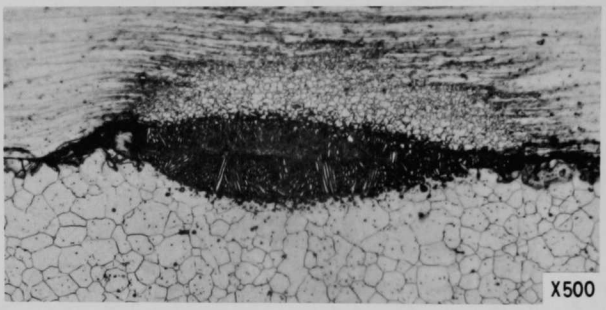

30 psig, 40 W-sec

20 psig, 60 W-sec

Fig. 23. Microstructures of Typical Spot Welds Effected by Varying Welder Power or Air Pressure to Welding Head. Maximum nugget thickness is less than 0.002 in., with approximately equal penetration into plate and spacer wire. Electroetched in 50% HNO_3.

Although the spot-welding system described above was adjudged satisfactory, improvements could be made in a number of areas. For example, copper bars inserted in the base plate would increase conductivity and thus decrease electrical losses. A welding head with greater throat depth should be used, since with the WH-250 system, the electrode reached slightly beyond the center of the fixture. Thus one edge spacer and the center spacer were welded; then the fixture was turned to weld the opposite edge spacer. A longer throat would eliminate this additional manipulation of the fixture.

2.8 Brazing Temperature Distribution

A full-scale, dummy Type-A fuel assembly (No. 452-IIA 8-1) was assembled with ten thermocouples attached at various locations within the 27-plate assembly to determine the temperature distribution during exposure to the standard brazing cycle. In addition, six thermocouples were located on the fixture at positions normally used to monitor temperatures during brazing.

The individual plate thicknesses of the assembly and the overall dimensional characteristics are given in Table V and Fig. 24, respectively. All plate surfaces were machined to a 60 μin. finish. Knurled spacer wires were spot welded to the plates, braze alloy was applied with grooved plastic loading bars, and the aluminum scribing technique was used to control alloy flow.

TABLE V. Individual Measurements of Dummy Fuel-plate Thickness: Subassembly No. 452-IIA 8-1

Plate	Wire No. 1					Wire No. 2					Wire No. 3				
No.	a	b	c	d	e	a	b	c	d	e	a	b	c	d	e
1	0.0810	0.0804	0.0811	0.0802	0.0800	0.0807	0.0807	0.0805	0.0806	0.0808	0.0805	0.0809	0.0809	0.0807	0.0808
2	0.0802	0.0802	0.0802	0.0801	0.0804	0.0801	0.0800	0.0800	0.0800	0.0800	0.0809	0.0802	0.0807	0.0805	0.0804
3	0.0800	0.0798	0.0798	0.0792	0.0790	0.0787	0.0787	0.0787	0.0789	0.0789	0.0794	0.0792	0.0791	0.0791	0.0792
4	0.0798	0.0798	0.0797	0.0792	0.0794	0.0798	0.0788	0.0788	0.0787	0.0788	0.0787	0.0788	0.0788	0.0787	0.0792
5	0.0802	0.0803	0.0802	0.0802	0.0803	0.0804	0.0808	0.0802	0.0803	0.0808	0.0803	0.0807	0.0805	0.0807	0.0802
6	0.0805	0.0802	0.0802	0.0801	0.0800	0.0797	0.0798	0.0800	0.0798	0.0797	0.0802	0.0803	0.0802	0.0806	0.0798
7	0.0802	0.0805	0.0802	0.0806	0.0801	0.0800	0.0798	0.0799	0.0798	0.0798	0.0803	0.0802	0.0802	0.0805	0.0810
8	0.0802	0.0803	0.0800	0.0801	0.0802	0.0809	0.0806	0.0802	0.0807	0.0805	0.0807	0.0808	0.0806	0.0809	0.0810
9	0.0792	0.0789	0.0791	0.0789	0.0788	0.0789	0.0786	0.0786	0.0785	0.0785	0.0788	0.0792	0.0788	0.0790	0.0790
10	0.0812	0.0802	0.0801	0.0802	0.0804	0.0807	0.0803	0.0802	0.0801	0.0805	0.0806	0.0805	0.0804	0.0802	0.0805
11	0.0803	0.0800	0.0802	0.0800	0.0802	0.0804	0.0802	0.0802	0.0800	0.0805	0.0812	0.0802	0.0808	0.0810	0.0810
12	0.0802	0.0805	0.0801	0.0805	0.0802	0.0802	0.0802	0.0801	0.0798	0.0802	0.0803	0.0802	0.0802	0.0802	0.0810
13	0.0794	0.0789	0.0792	0.0790	0.0791	0.0785	0.0788	0.0789	0.0785	0.0788	0.0788	0.0788	0.0787	0.0785	0.0786
14	0.0802	0.0805	0.0802	0.0796	0.0798	0.0804	0.0801	0.0801	0.0801	0.0800	0.0806	0.0805	0.0805	0.0807	0.0805
15	0.0809	0.0802	0.0808	0.0800	0.0802	0.0793	0.0790	0.0790	0.0790	0.0790	0.0800	0.0800	0.0802	0.0808	0.0808
16	0.0802	0.0802	0.0801	0.0801	0.0804	0.0792	0.0791	0.0792	0.0795	0.0795	0.0805	0.0807	0.0807	0.0806	0.0805
17	0.0785	0.0791	0.0790	0.0789	0.0790	0.0772	0.0770	0.0773	0.0771	0.0770	0.0790	0.0789	0.0789	0.0789	0.0790
18	0.0802	0.0802	0.0810	0.0799	0.0810	0.0795	0.0792	0.0790	0.0790	0.0795	0.0805	0.0805	0.0800	0.0800	0.0800
19	0.0801	0.0805	0.0803	0.0806	0.0810	0.0791	0.0791	0.0791	0.0791	0.0795	0.0800	0.0804	0.0805	0.0806	0.0803
20	0.0802	0.0803	0.0802	0.0805	0.0805	0.0788	0.0788	0.0787	0.0786	0.0806	0.0800	0.0806	0.0801	0.0800	0.0806
21	0.0799	0.0791	0.0798	0.0799	0.0790	0.0781	0.0776	0.0778	0.0773	0.0773	0.0792	0.0788	0.0786	0.0789	0.0785
22	0.0802	0.0802	0.0805	0.0808	0.0805	0.0796	0.0792	0.0793	0.0792	0.0791	0.0810	0.0809	0.0813	0.0812	0.0813
23	0.0810	0.0810	0.0815	0.0811	0.0815	0.0792	0.0795	0.0794	0.0790	0.0790	0.0811	0.0810	0.0815	0.0812	0.0810
24	0.0809	0.0809	0.0808	0.0811	0.0811	0.0790	0.0788	0.0782	0.0788	0.0782	0.0808	0.0805	0.0802	0.0802	0.0809
25	0.0809	0.0802	0.0801	0.0809	0.0808	0.0791	0.0790	0.0789	0.0788	0.0788	0.0810	0.0807	0.0802	0.0808	0.0802
26	0.0808	0.0808	0.0803	0.0802	0.0803	0.0807	0.0800	0.0802	0.0800	0.0801	0.0805	0.0805	0.0810	0.0805	0.0809
27	0.1197	0.1191	0.1191	0.1195	0.1197	0.1191	0.1188	0.1188	0.1185	0.1185	0.1199	0.1198	0.1199	0.1195	0.1199
Total:	2.206	2.202	2.204	2.202	2.203	2.187	2.185	2.181	2.179	2.184	2.194	2.204	2.2035	2.2034	2.206

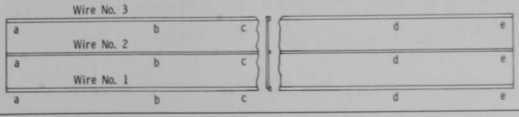

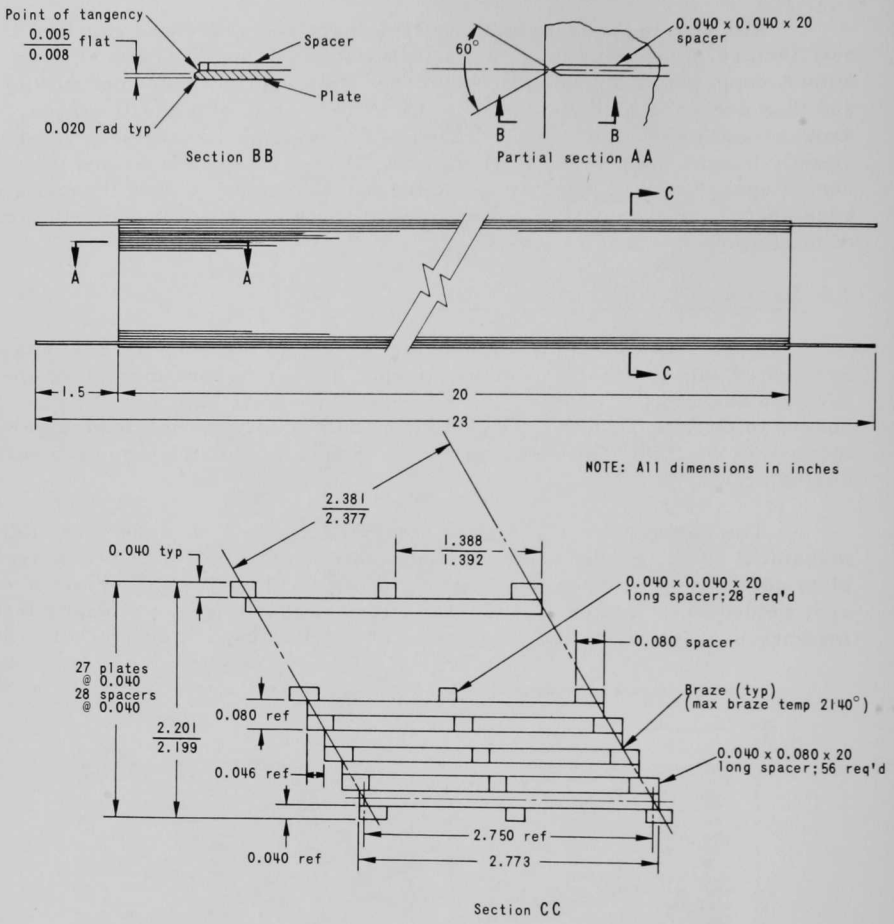

Fig. 24. Overall Dimensional Characteristics of Dummy Type-A Fuel-plate Assembly Used to Determine Brazing Temperature Distribution

The thermocouples were made from 28-gage Chromel/Alumel wire and insulated with Mullite tubes of 0.035-in. OD with a 0.006-in. wall. The thermocouples were attached to selected plate areas by spot welding the bead with a stored-energy welder. In the following tabulation, the thermocouple locations are relative to orientation of the plates and fixture during brazing.

Thermocouple	Location
A	Outside plate, center, adjacent to bottom edge spacer
B	Outside plate, center, adjacent to center spacer
C	Center plate, hydrogen inlet end, center spacer
D	Center plate, center, bottom edge spacer
E	Center plate, center, center spacer
F	Center plate, center, top edge spacer
G	Center plate, hydrogen exit end, center spacer
H	Seventh plate from outside, center, center spacer
I	Outside plate, center, center spacer
J	Outside plate, center, bottom edge spacer
K	End fixture frame, top center
L	Middle fixture frame, top center
M	Middle fixture frame, bottom center
N	End fixture frame, bottom center
O	Against outside of outer plate A-B in center
P	Against outside of outer plate I-J in center

Figure 25 shows an outer plate and a center plate with the thermocouples attached. Figure 26 shows the instrumented assembly installed in the brazing retort.

As anticipated, the maximum temperature differences occurred during the initial heating and final cooling phases. The temperature at the top center of the end fixture frame [Thermocouple (K)] increased the fastest and that at the subassembly center (E) the slowest. For example, when (E) was reading 555°F, (K) was reading 760°F, that is, 205°F higher. This temperature difference decreased to 70° during the equalizing hold at 800-900°F, and both thermocouples registered the same temperature during the 0.5-hr hold at 1950°F. When the temperature was increased to the final brazing value (2120-2130°F), Thermocouple (K) again led by approximately 30°F. However, both temperatures equalized within a few minutes and remained

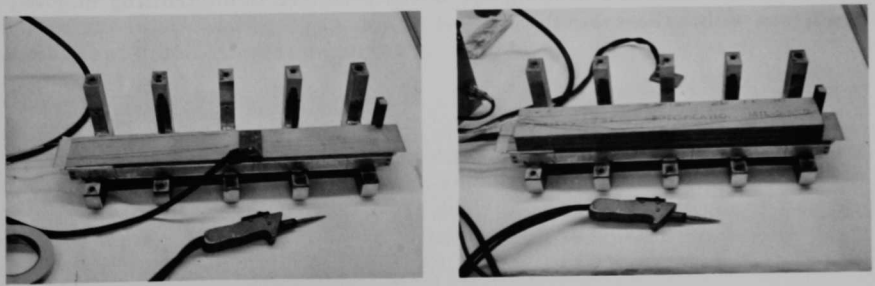

Fig. 25. Outer Plate and Center Plate with Thermocouples Attached

Fig. 26. Instrumented Assembly Installed in Brazing Retort

within 5°F of each other during the 2-hr hold. During the furnace cooling period, the end frame cooled slightly faster, its temperature ranging from 20-30°F lower than that at the assembly center.

The temperature registered by Thermocouple (M) at the bottom center of the middle fixture closely approximated the assembly center temperature, while Thermocouple (L) at the top center of the same fixture led by 5-10°F during most of the brazing cycle.

There was no significant temperature gradient along the center plate from the hydrogen inlet side to the outlet side. Temperatures at both ends of this plate remained within 10°F of each other during heating and cooling above 1650°F, and within 5°F of each other at the brazing temperature. Temperatures across the plate width also were essentially constant. When there was a measurable difference, the top edge was 5°F hotter than the bottom edge.

During transient conditions, the temperature gradient across the assembly was concentrated in the outer plates. For example, during heating, the outer plate registered 1930°F, the seventh plate 1905°F, and the center plate 1900°F. Equalization occurred rapidly, and after a few minutes at the 1950°F equalizing hold and during the 2-hr hold at braze temperature, the gradient across the assembly was only 5°F.

This test indicated that thermocouples attached to selected areas on the brazing fixture and on the outside of the assembly could yield temperatures that correlated well with values prevailing within the subassembly. Also, that the standard brazing cycle was effective in controlling thermal gradients within the assembly.

3.0 BRAZING OF FULL-SCALE DUMMY FUEL-PLATE ASSEMBLIES

Brazing of these plate assemblies is treated separately in this report since it involved either an evaluation of the state-of-the-art or an extension of the brazing development program consistent with modifications of subassembly design that were effected during the program. In both instances the end objective was a fabrication procedure that would yield a quality product. This procedure may be divided into three basic operations: (1) assembly of individual plates with spacer wires; (2) fixturing of the multiplate assembly; and (3) furnace brazing of the unit.

At the time of these tests, the AARR fuel subassembly contained 27 fuel plates (each 20 in. long, 2.810 in. wide, and 0.040 in. thick) stacked with a 60° offset and 0.040-in. spacing between plates. Spacer wires of 0.040-in.-square cross section were continuous at the centers of the plates and intermittent at the edges, i.e., 3/8-in.-long wires were positioned $2\frac{5}{64}$ in. apart.

3.1 State-of-the-Art Techniques

3.1.1 Specimen Assemblies

Six, full-scale dummy fuel-plate assemblies were assembled and brazed, using GE J8100 braze powder, Nicrobraz cement, and Nicrobraz Green Stopoff. Five had single, full-length, center spacer wires between plates. The sixth had two, full-length, center spacer wires located so that three equal-width channels were formed between the plates.

The fuel plates were simulated by Type 347 stainless steel sheets sheared from nominally 0.040-in.-thick stock and machined 20 ± 0.005 in. long and 2.810 ± 0.002 in. wide. The actual thickness varied ~0.001 in. Plates with an average thickness of 0.0395 in. were used.

Type 347 stainless steel was used for the spacer wires. Center spacer wires were obtained in three sizes: 0.0385-, 0.0395-, and 0.0405-in.-square cross section by 20 in. long. Edge spacers were of the same thicknesses, but 0.060 in. wide by 0.375 in. long.

3.1.2 Fixturing

The brazing fixture also was fabricated from Type 347 stainless steel to match the thermal expansion characteristics of the plate assembly. As shown in Fig. 27, the plates were confined laterally between the stepped side supports, but could move 0.020 in. vertically so that close joint gaps could be maintained.

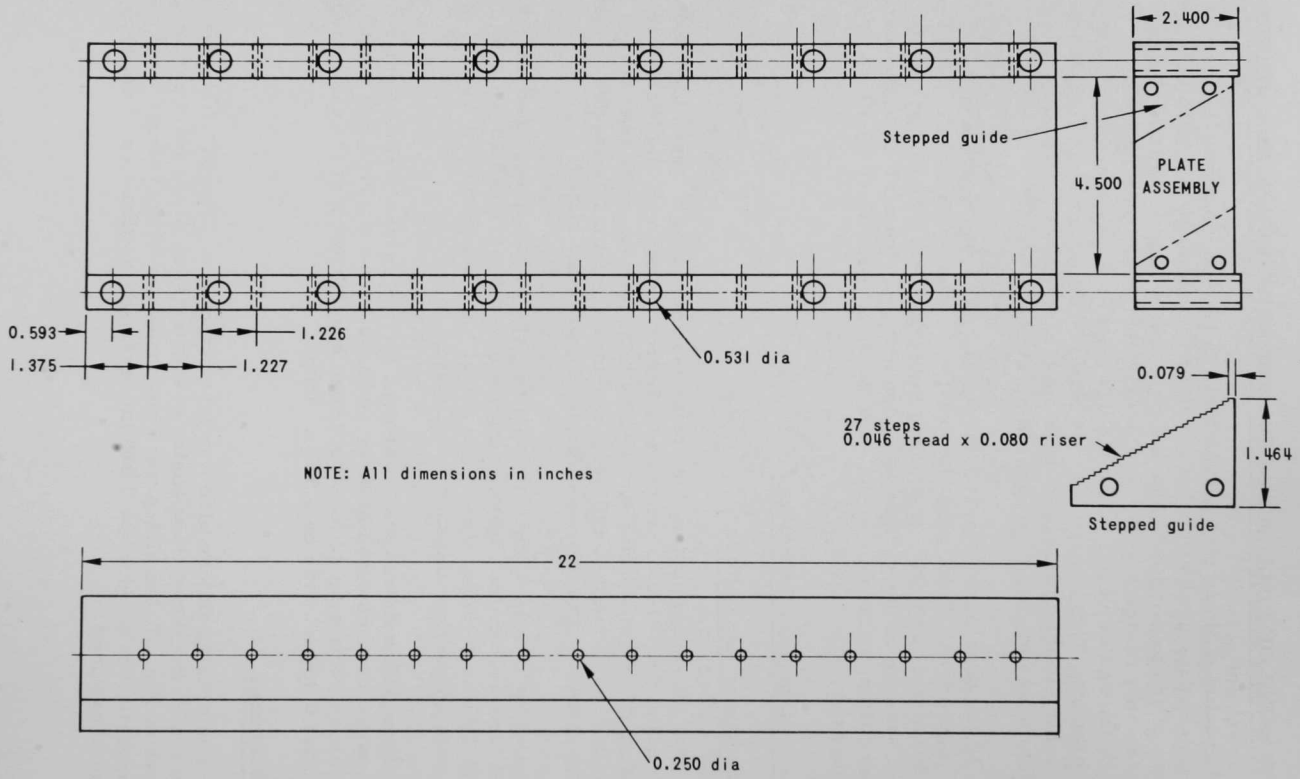

Fig. 27. Brazing Fixture for Full-scale Dummy Fuel-plate Assemblies

The sidewalls of the fixture were machined to a height such that the height of the subassembly could be controlled by bolting the top plate tightly against the tops of the sidewalls. Sufficient space was allowed at the top and bottom of the subassembly for insertion of thin plates coated with stop-off. These plates prevented brazing of the subassembly to the fixture.

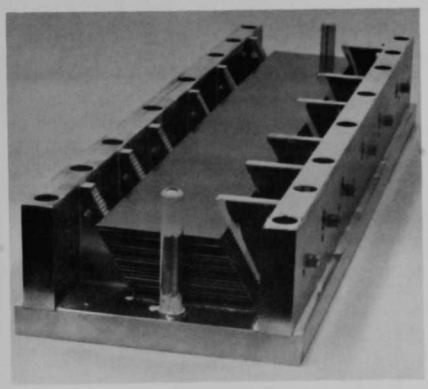

Fig. 28. Partially Assembled Plate Assembly in Brazing Fixture

Each assembly was fixtured as follows. The stepped guides were bolted to the sidewalls and the bottom stopoff-coated plate was inserted. Next, the dummy fuel plates were stacked, with the spacer wires on the underside. In this position, braze alloy flow could be assisted by gravity. Finally, the top stopoff-coated plate was installed and bolted against the tops of the sidewalls. Figure 28 shows a partially assembled unit.

3.1.3 Brazing

Five of the assemblies in this group were furnace brazed in weld-sealed retorts containing a dry hydrogen atmosphere. Assembly S/N 327-5 was brazed in a cold-wall, high-vacuum furnace evacuated to $>10^{-4}$ Torr.

The brazing cycle used in these initial evaluations was that previously developed at ANL and ORNL. Each subassembly was heated to 2135-2145°F and held for 2 hr at temperature to allow the silicon to diffuse away from the joints and thus eliminate the hard brittle phase. Natural furnace cooling was employed to minimize thermal gradients that could cause distortion. Subsequent metallographic examinations and microhardness surveys confirmed the effectiveness of this cycle in producing sound, ductile, brazed joints.

3.1.4 Results

3.1.4.1 Assembly S/N 327-1

The primary purpose in brazing this assembly was to check the fixture design and assembly procedures. Thin plates (0.0365 in. thick) were used; therefore, the overall dimensions were not expected to be correct. Moreover, the plates near the top of the stack did not fit squarely into the stepped fixture guides; hence, some of the plate edges were bent. Except for a few of the edge spacer wires, the joints appeared sound.

3.1.4.2 Assembly S/N 327-2

Some gaps were found in the edge spacer joints. Nicrobraz 50 alloy was applied to these areas and the assembly was rebrazed at 1875°F.

Subsequent metallographic examination revealed all edge spacer joints were sound and complete. A typical brazed joint is shown in Fig. 29. Some joints (see Fig. 30) were bonded on both sides with braze alloy, with very tight wire-to-plate contact in between. The bonding in the latter area appeared to be partially by diffusion.

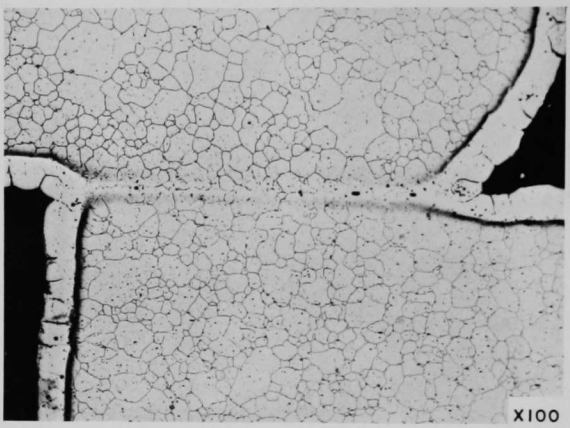

Fig. 29. Typical Edge Spacer Joint in Assembly S/N 327-2. Electroetched with 50% HNO_3.

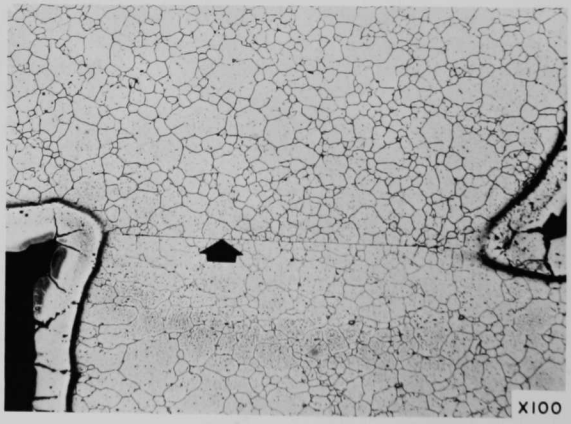

Fig. 30. Arrow Points to Partially Diffusion-bonded Joint in Assembly S/N 327-2. Electroetched with 50% HNO_3.

With respect to the center spacer-to-plate joints, the majority were complete; imcomplete alloy flow on one side of the joint was observed in a few instances. To alleviate this problem, knurling of the spacer wires was incorporated into the assembly procedure.

Some distortion and bending at the plate ends was also evident in this subassembly.

3.1.4.3 Assembly S/N 327-3

This assembly was assembled and brazed using 18 comb-type edge spacers (see Fig. 31) instead of individually spot welded spacer wires.

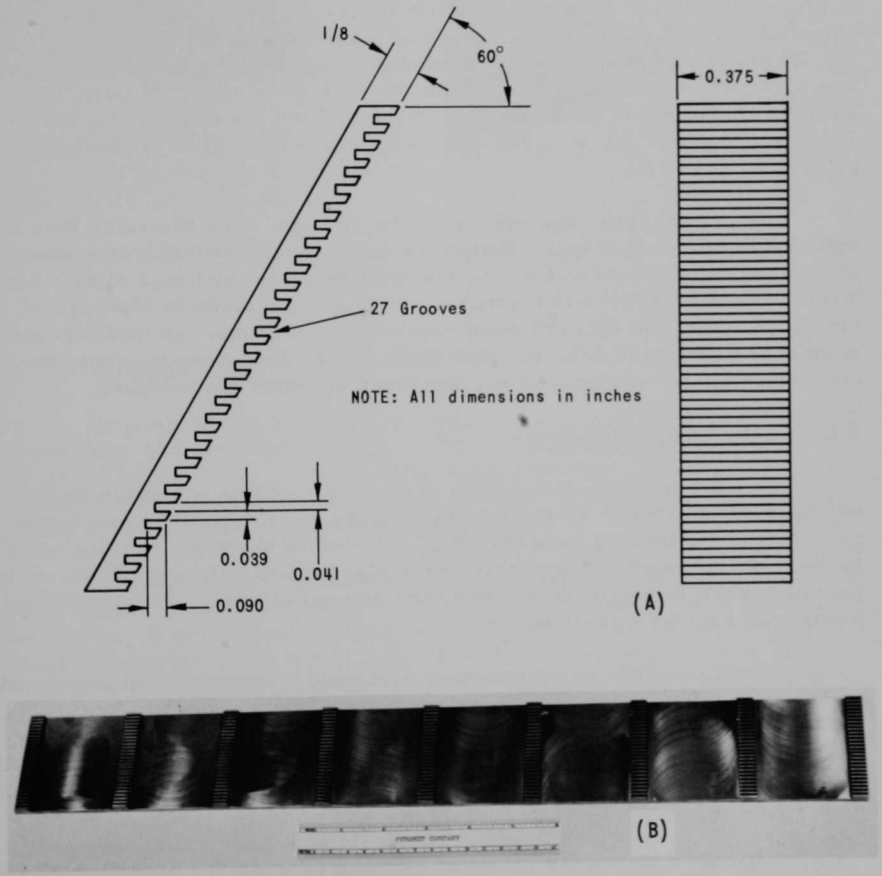

Fig. 31. (A) Individual Comb-type Edge Spacer Used on Assembly S/N 327-3; (B) Multiple Edge Spacer Design Which Was Removed from Consideration due to Difficulties in Machining and Alloy Placement

One of the problems with the individual comb spacers was holding them during machining. Therefore, the feasibility of machining nine spacers on one side of a subassembly from a single sheet of stainless steel was investigated. It was believed that the sheet would be easier to hold and that the distance between spacers could be controlled precisely. However, this design proved more difficult to machine and presented greater problems of placement of the braze alloy.

Preparatory to assembly, the center spacer wires were spot welded to the plates and braze alloy applied to the joint area. Next, the 27 plates were stacked in rough approximation to the 60° offset. Braze alloy was applied to the inner edges of the comb "teeth" of each edge spacer and held in place with Nicrobraz cement. Each spacer was slipped over the plate edges and tapped in place. The stack of plates was accurately adjusted to the 60° offset as the spacers were affixed. Additional braze alloy and binder was applied to the edges of the "teeth" at each plate edge. Finally, the assembly was brazed in the same fixture used for the other units, but with 18 straight-edged, 60° wedges for side supports instead of the stepped guides.

The comb-type edge spacers were adjudged less desirable than the individual spot-welded type. Numerous gaps were observed in the joint areas, probably because of the difficulty in applying the braze alloy. There was no gain with regard to control of spacing dimensions or warpage of plates. Finally, the spacers were expensive to machine and would require postbraze grinding to achieve final dimensions. For these reasons, the comb-type spacer design was not employed on other assemblies.

3.1.4.4 Assembly S/N 327-4

The brazing characteristics of the joints in this assembly were adjudged satisfactory. Of the four differently sized, specially machined, grooved plastic loading bars (see Fig. 11) used to apply the brazing alloy to the center spacer wires of this assembly, the bar with a 0.030-in.-square groove appeared to provide the optimum amount of braze alloy powder to the joints with knurled spacer wires.

Metallographic examination of sectioned joints revealed sound and complete bonding. However, the braze alloy was not contained by the scratches inscribed along the joints for that purpose. There was a very slight degree of sag in the plates between the edge spacers. Final overall height of the assembly varied between 2.164 and 2.170 in. along the length, with the minimum at the center section.

Figure 32 shows the extent of alloying between the braze metal and the stainless steel plate. The reaction zone is observed to extend ~0.002 in. below the original surface of the plate. A surface-alloy layer ~0.002 in. thick extends 1/8 in. or more from the spacer wire. This layer does not

represent a net increase in plate thickness; rather, it is a diffusion-alloyed zone between the braze metal and the stainless steel. Microhardness measurements (see Fig. 33) made on sectioned joints from this and other assemblies indicated that the layer is not significantly harder than the unalloyed stainless steel. The extent of this layer was decreased substantially by the alloy placement and control techniques developed in this program.

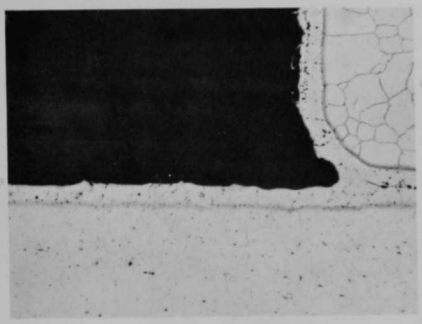

Fig. 32. Typical Brazed Joint in Assembly S/N 327-4, Showing Alloy Zone between Braze Metal and Stainless Steel

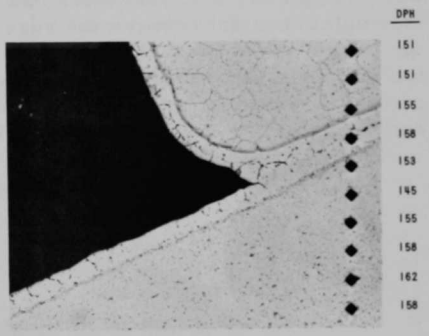

Fig. 33. Microhardness Survey of Spacer Wire-plate Joint in Assembly S/N 327-4 Brazed with GE J8100 Alloy for 2 hr at 2140°F. Electro-etched with 50% HNO_3.

3.1.4.5 Assembly S/N 327-5

Brazing of this assembly in a high vacuum instead of a dry hydrogen atmosphere greatly improved the wetting and flow characteristics of the GE J8100 braze metal. However, the alloy flow from the joint areas and across the plate surfaces was more pronounced on this subassembly than on any previous assembly brazed in dry hydrogen.

Longitudinal scratches inscribed with coarse emery paper parallel to the spacer wires were ineffective in hindering braze alloy flow across the plates. Several small bond gaps were observed in the edge spacer joints and one joint was completely unbonded. Also, there was a slight longitudinal sag of the plates between the edge spacers and a perceptible bending (transversely) near the bottom of the assembly. The overall height of the assembly varied from 2.191 in. at the center to 2.219 in. at each end. Plate distortion was attributed to bending moments incurred by misalignment of the spacers during installation in the fixture.

Nicrobraz 50 alloy was applied to the bond gaps and the assembly was rebrazed for 15 min in a dry hydrogen atmosphere at 1800°F. Subsequent examination revealed that the gaps were completely filled with no further distortion of the plates.

3.1.4.6 Assembly S/N 327-6

Except for the use of two center spacer wires, the plates in this assembly were assembled and brazed by the same procedure employed for Assembly S/N 327-4. The stoppoff scratches inscribed with a scribing tool provided some hindrance to braze alloy flow across the plates, but the degree of restriction was still unsatisfactory. A majority of the joints were completely brazed; others had some very small gaps resulting from incomplete contact between the edge spacers and plates. A slight sag of the plates was observed between the edge spacers; this was attributed to the additional support at the center section. Transverse bending of the plates, observed in plates with single center spacer wires, was not noticeable in this subassembly (see Fig. 34).

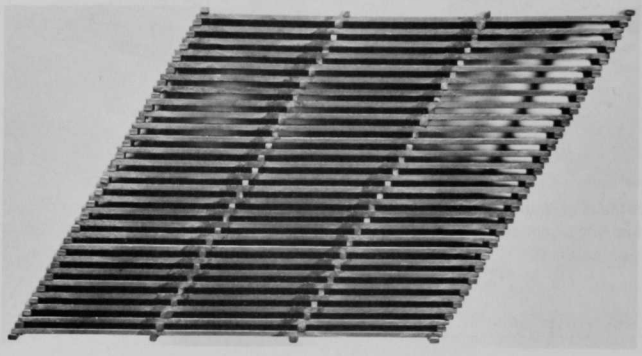

Fig. 34. End View of Assembly S/N 327-6 with Double Center Spacer Wires

As in the case of Assembly S/N 327-5, the small bond gaps were filled with Nicrobraz 50 alloy powder and rebrazed satisfactorily.

3.2 Plasma Spraying of Braze Alloy

Two procedures were evaluated for assemblies equipped with full-length edge spacer wires. For the first assembly tested, the wires were knurled on four sides to promote adherence of the plasma coating, and to improve spot welding and flow characteristics of the braze alloy. After spot welding of the wires to the plates, the plates were assembled and held in the final configuration by stainless steel strips spot welded across the ends. These strips were removed after brazing. Next, the entire assembly, except areas that were to be plasma coated (i.e., edges of plates and spacer wires), was masked with heat-resistant tape. The exposed areas were then sprayed with GE J8100 alloy to a thickness of 0.008-0.010 in. Adherence of the coating was marginal, necessitating great care in subsequent handling of the subassembly to prevent chipping. Finally, the assembly was clamped

in the brazing fixture, loaded into the furnace in the vertical position, and exposed to the standard brazing cycle. After brazing, the assembly was surface-ground to the finished dimensions, and examined visually and metallographically.

The results were encouraging. Joints were sound and complete except for small areas near the edges where the coating had chipped prior to brazing. Figure 35 shows cross sections of a typical brazed joint and

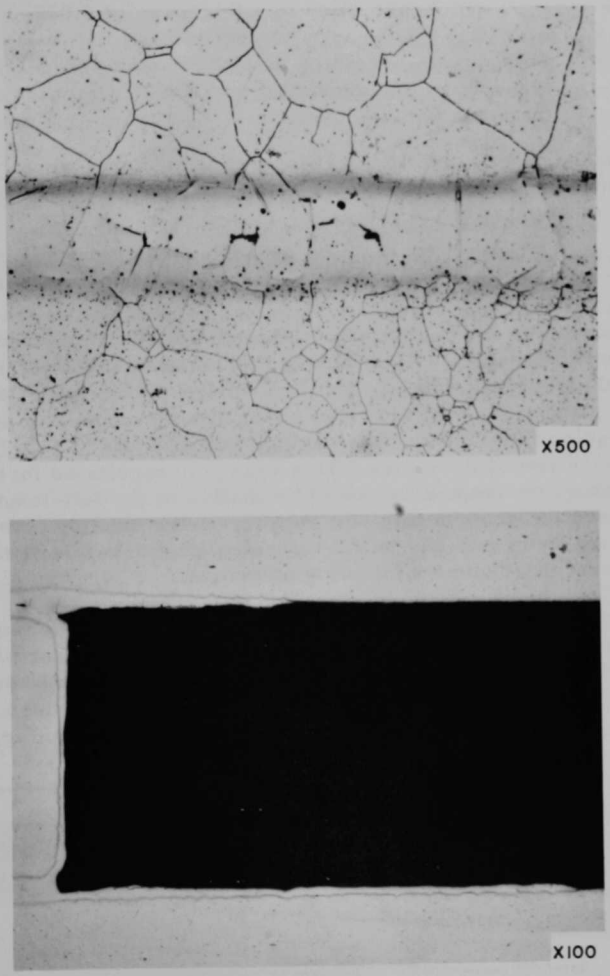

Fig. 35. Cross Sections of (Top) Typical Brazed Joint and (Bottom) Inside Fillet Area from Full-scale Dummy Fuel-plate Assembly on Which Braze Alloy Was Plasma Sprayed

inside fillet area. Alloying between the braze metal and stainless steel is very slight. As discussed previously, the diffusion zone extended to a thickness of 0.002 in.

Several changes were made in the procedure employed for the second assembly. First, the faces of the wires to be plasma sprayed were grit-blasted with chilled iron shot. Next, the wires were pickled in a 40% nitric acid-4% hydrofluoric acid solution before being spot welded to the plates. Red Stopoff was then applied around the areas to be plasma sprayed. These areas were sprayed with braze alloy to a thickness of 0.010-0.012 in. Adherence of the coating was greatly improved over that in Test No. 1. Finally, the assembly was assembled as before, clamped in a fixture, loaded into the furnace, in the horizontal position (i.e., plates on edge), and exposed to the same brazing cycle.

Subsequent examinations revealed that all joints were complete, with no evidence of unbonded areas. There was no measureable warpage, distortion, or sagging of the plates.

3.3 Fabrication of Complete Dummy Fuel Subassemblies

The intent of the preceding tests was to incorporate the findings into procedures for fabrication of a complete AARR dummy fuel subassembly as described in Sect. 3.0. This included fabrication and attachment of end fittings to the plate assembly. However, during the course of these tests, the design of the plate assembly was changed for purposes of hydraulic tests, so as to require full-length edge spacers, with a short (3/8 in. long) center spacer at each end of the plates. This change necessitated further refinement of brazing techniques because elimination of the full-length center spacers posed the problem of plate sagging during brazing. At the same time, however, accessibility to the relocated joint areas facilitated investigation of several techniques for alloy placement.

Accordingly, three, complete, full-scale, dummy fuel subassemblies were fabricated and brazed to investigate: (1) techniques for placement of the braze alloy; (2) effects of varying orientation of the plate assembly during brazing; (3) use of welding or brazing to attach the end fittings to the plate assembly. As a result of this effort, one subassembly (see Fig. 36) was

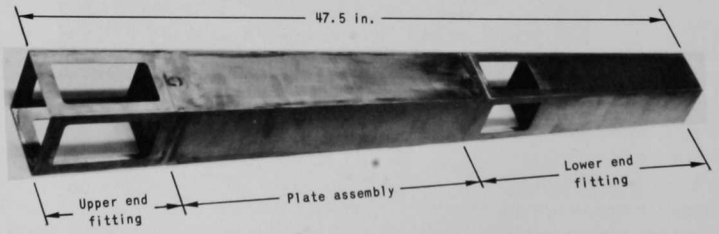

Fig. 36. Full-scale AARR Dummy Fuel Subassembly Fabricated Completely by Brazing

fabricated by means of the brazing techniques developed in this program. Briefly, the plate assembly and each of the upper and lower fittings were fabricated separately and subsequently joined by furnace brazing.

3.3.1 Plate Assembly

Except for the changes cited below, the plate assembly and brazing procedures were the same as those employed for the second test assembly in Sect. 3.2.

The assembly consisted of 27 plates, each 20 in. long, 2.810 in. wide, and 0.040 in. thick, except for the top and bottom plates. The latter were 21 in. long to facilitate subsequent attachment of the box-type end fittings. Each plate was spaced by full-length, knurled wires (20 in. long, 0.080 in. wide, and 0.040 in. thick) spot welded at the side edges, and short wires (0.375 in. long, and 0.040 in. square) similarly attached at the center of each end. Red Stopoff was applied in 1/8-in.-wide strips onto the plate surfaces to control the braze alloy to within 1/16 in. of the joints. GE J8100 alloy was then plasma sprayed along the edge spacers and applied with an acrylic binder at the center spacers.

After brazing, the plate assembly was surface ground to final dimensions and then immersed for 0.5 hr in a 50% nitric acid solution at room temperature to remove the Red Stopoff residue.

3.3.2 Upper and Lower End Fittings

Two methods of joining the corners of the box-type end fittings were evaluated: full-length welding and brazing.

3.3.2.1 Welding

A special fixture was constructed to position the top, bottom, and side plates for full-length welding of both the upper and lower fittings. It consisted of an adjustable, mild steel mandrel machined to fit inside for support, and holddown bars with clamps to provide support from the outside. The tungsten inert gas welding process was used, with argon as the shielding gas.

During welding of the first fitting, fusion occurred between the stainless steel welds and the corners of the mandrel. To alleviate this difficulty, the corners of the mandrel were machined to a radius of ~0.030 in. Very little fusion was encountered during welding of the next fitting.

Plate distortion resulting from weld shrinkage was the primary reason for discarding the welding method; the joint angles increased 3-5°.

In addition, welding posed the problem of smoothing the residual bead to accommodate attachment of full-length spacer wires to the complete subassembly.

3.3.2.2 Brazing

Three upper end and three lower end fittings were fabricated by a combination of tack welding and brazing. The first two fittings fabricated in each group were used for test purposes. As described later, the last set was brazed to the plate assembly to complete the subassembly.

With reference to Fig. 37, the edges of the plates were precisely machined to a 60° bevel, fitted together, and then spot welded with a stored-energy, capacitor-discharge-type welder. The full-length, exterior spacer wires were not included in the first two braze tests, but were attached prior to brazing of the complete subassembly. GE J8100 braze alloy powder was applied to the inside corners and held in place with an acrylic binder. Finally, Red Stopoff was applied adjacent to the joint areas to confine the flow of braze alloy.

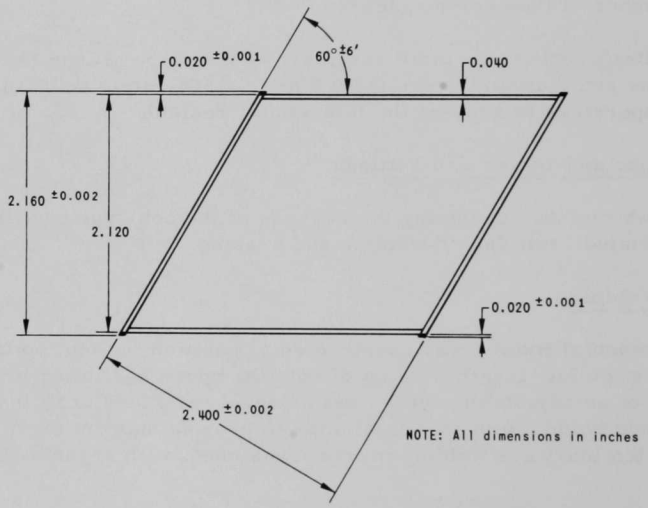

Fig. 37. Cross Section of Box-type End Fitting Assembly Preparatory to Brazing

The first set of fittings (without window slots) were assembled as described above, positioned vertically on stainless steel supports in a weld-sealed retort, and exposed to the brazing cycle. This cycle consisted of heating to 2135-2145°F in a dry hydrogen atmosphere, holding for 2 hr, and then retort-cooling to room temperature.

The external appearance of the brazed joints was very good. Bonds appeared sound and complete along the length of each joint. This was confirmed by metallographic examination of random cross sections. Figure 38 shows a typical cross section.

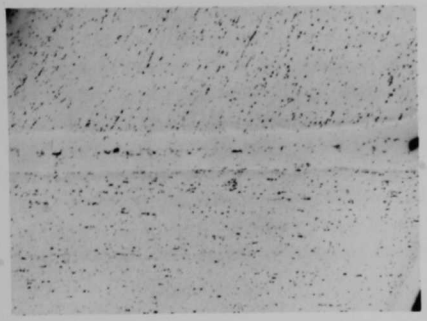

Fig. 38. Typical Cross Section of End Fitting Corner Joint Brazed with GE J8100 Alloy for 2 hr in Dry Hydrogen Atmosphere at 2135-2145°F. Electroetched with 50% nitric acid.

The second set of end fittings were machined as described above, including window slots. In addition, the side plates were made 1/4 in. longer to provide for a lap-joint attachment to the plate assembly. These fittings were then assembled for brazing and then exposed to the same brazing cycle. Subsequent visual and metallographic examinations revealed sound and complete bonds over the length of all brazed joints.

3.3.3 Attachment of End Fittings to Plate Assembly

Tests were conducted using tungsten inert gas welding, brazing, and combinations of each. Brazing was selected because microcracks were observed in welded joints in areas where residual braze alloy had been present during welding.

The ends of the first plate assembly were machined so that the side plates of the end fitting could be attached with a 1/4-in. lap joint. Two side plates were welded to the plate assembly. Sections of the welded joints were then prepared for metallographic examination. As shown in Fig. 39, microcracks were found in the root areas of the weld bead, where braze alloy from

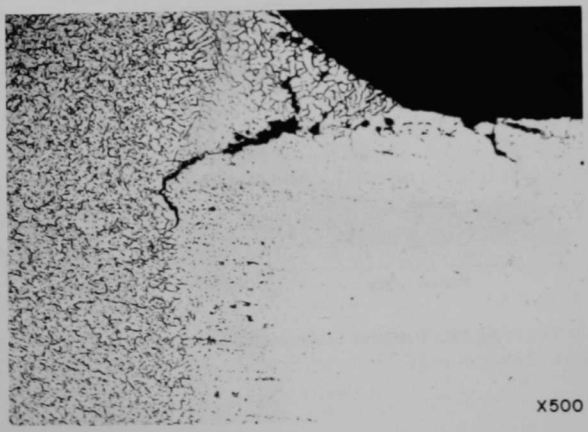

Fig. 39

Root Crack in Area of Welded End Fitting-plate Assembly Joint Caused by Remelting of Braze Alloy on Plate during Welding

the plate assembly had been remelted along with the weld metal. These cracks appeared to result from the lower-strength braze alloy penetrating the interstices of dendrites formed in the weld, then cracking under the stresses set up on cooling.

To avoid the microcracking and to reduce the possibility of plate distortion from nonuniform thermal expansion and weld bead shrinkage, the second subassembly was prepared for brazing. With reference to Fig. 40, the side plates of the upper and lower end fittings were attached to the plate assembly with a 1/4-in. lap joint. A smooth transition fit-up was accomplished by machining the land areas on the plate assembly to a depth of 0.040 in. from the finish-ground surface. The top and bottom plate of the end fittings were joined with a 30° scarf joint to the corresponding plates of the plate assembly. The latter plates were extended 1/4 in. to separate the scarf joints from the channel inlets on the plate assembly.

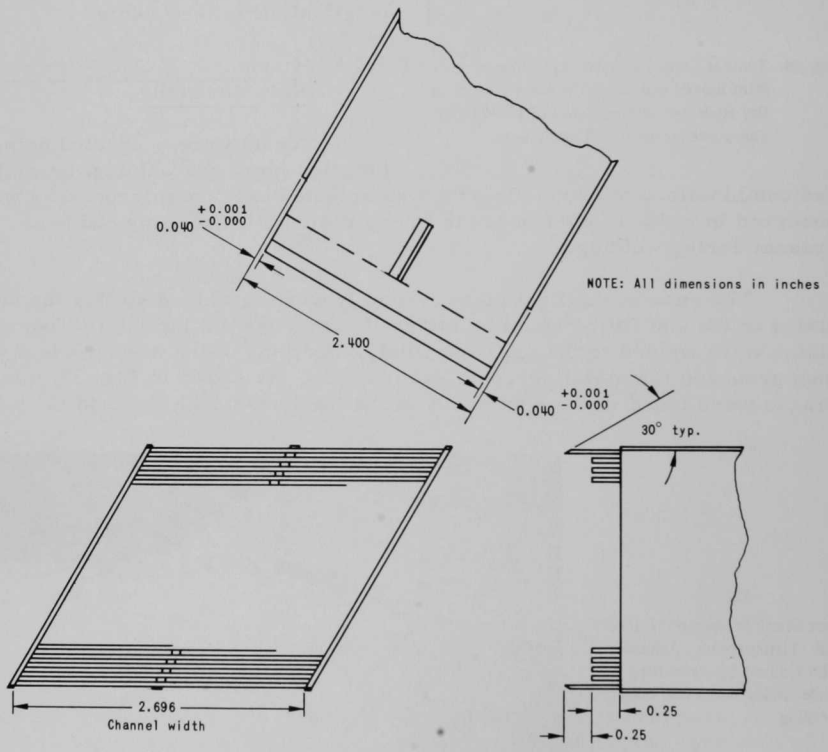

Fig. 40. Design of Transition Joints between End Fittings and Dummy Plate Assembly

3.3.4 Final Assembly Procedures

Preparatory to brazing, full-length end fittings, including full-length edge spacer wires (0.020 in. x 0.065 in.), were tack welded to the plate assembly. GE J8100 braze alloy powder (-150 mesh) was applied along the exterior length of the edge spacer wires with loading bar No. 4, and held in position with an acrylic binder. At the transition joints, the alloy was applied with acrylic binder to both the interior and exterior of the joints. Red Stopoff was used to confine the alloy flow.

This assembly was clamped into the fixture previously used for brazing individual plate assemblies (see Fig. 28), with the end fittings protruding unrestrained at each end, and was then loaded vertically into the brazing retort. The brazing cycle consisted of heating to 2135-2145°F in a dry hydrogen atmosphere, holding for $1\frac{1}{2}$ hr, and then cooling at less than 100°F/hr.

After brazing, the subassembly was examined visually. All end fitting and transition joints appeared to be completely brazed. Figure 41 shows a typical brazed joint between the upper end fitting and the plate assembly. The 1/4-in. lap joints between the end-fitting side plates and those of the plate assembly were difficult to evaluate because of limited visual access. Some runoff of braze alloy had accumulated between plates at the lower end of the plate assembly and at the bottom of the lower end fitting.

Fig. 41. Closeup View of Brazed Joints between Upper End Fitting and Plate Assembly

3.4 Semiproduction of Full-scale Dummy Plate Assemblies

The objective here was to assemble and braze seven full-scale dummy plate assemblies on a semiproduction basis, using the previously developed techniques with certain modifications. These modifications were necessitated by (1) the change from intermittent to continuous edge spacers, which affect both the spot welding and fixturing, and most importantly, (2) the more exacting standards and criteria established for these assemblies. Additional testing and inspection of the previously brazed assemblies had revealed a number of deficiencies in the overall procedure.

In these tests, the basic steps remained the same: spacer wires were spot welded to the

plates with a stored-energy-type welder; braze alloy powder (GE J8100) was applied with grooved plastic loading bars and held in place by Nicrobraz cement; the plates were clamped in a fixture and then exposed to the brazing cycle. The basic cycle involved heating to 2140°F in a dry hydrogen atmosphere (dewpoint = 180°F), holding for 2 hr at temperature, and then furnace cooling.

The procedural changes that were effected related to plate and spacer-wire dimensions employed, combinations of plates and spacer wires used in the assemblies to maintain dimensional tolerances, surface preparation, fixturing for spot welding and brazing, and, eventually, the brazing cycle.

Of the seven assemblies brazed, six were used for testing and evaluation; the first unit was scrapped because of large gaps in the brazed joints and excessive distortion.

3.4.1 Fabrication of Plates and Spacer Wires

Dummy fuel plates were cut from two lots of Type 347 stainless steel sheet stock, each having a nominal thickness of 0.040 in. The measured thickness of the first lot averaged 0.0395 in., and the second lot 0.041 in. Each plate was cut slightly oversize and then machined to final dimensions: 20 ± 0.005 in. long and 2.773 ± 0.001 in. wide. (Modifications in the core design required reduction of plate width from 2.810 to 2.773 in.) The ends were milled to a radius of 0.020 in.

The edge and center spacer wires also were fabricated from Type 347 stainless steel. Wires of two cross-sectional areas were employed as follows:

Edge spacers: 0.080 in. wide, 0.0395 in. thick

0.080 in. wide, 0.0385 in. thick

Center spacers: $0.0380 \, ^{+\,0.0005}_{-\,0.0000}$ in. square

$0.0390 \, ^{+\,0.0005}_{-\,0.0000}$ in. square

Each wire was machined to a length of 19.960 ± 0.005 in. In addition, the ends of the center spacer wires were tapered 60°.

3.4.2 Combinations of Plates and Spacer Wires

Combinations of plates and spacer wires were selected so that the sum of the 27 plate thicknesses plus the sum of the 28 wire thicknesses equalled the desired total assembly height less an allowance for the

brazed-joint thicknesses. The approximate allowance was 0.00025 in. per brazed joint. Variations in tolerances of plate and wire thicknesses prevented precise control of this factor.

The first two assemblies (S/N 452-IA-1 and 2) contained plates which averaged 0.041 in. in thickness; these were machined from the lot of sheets which was on the high side of the nominal 0.040-in. thickness. Spacer wires used with these plates were 0.0385 in. thick. With two exceptions, the remaining assemblies contained plates machined from both lots of sheets (0.041 in. thick and 0.0395 in. thick). The thicker plates were combined with the thinner wires (0.0385 in.) and the thinner plates with the thicker wires (0.0395 in.). These combinations were aimed at a spot-welded unit thickness (plate and attached wire) of ~0.0795 in., thereby allowing 0.00025 in. for each brazed joint. The combinations in the last two assemblies included eight thick plates with thick spacer wires. These combinations were intended to prevent gaps in the brazed joints which had been observed in earlier assemblies.

3.4.3 Surface Preparation

The joint surfaces of each spacer wire were knurled to a depth of 0.001 in., with a density of 64 grooves per linear inch. Preparatory to assembly, all components were vapor degreased with trichlorethylene, pickled for 15 min in a hot (120°F) solution of 40% HNO_3-2% HF, washed in acetone, and dried in air.

3.4.4 Spot Welding of Spacer Wires

One center spacer and two edge spacers were spot welded to each plate, as shown in Fig. 19. Wire No. 3 was welded in position first, using the plate edge as a reference. The fixture shown in Fig. 42 was then used to locate the other two wires relative to wire No. 3.

Spot welding was accomplished with a stored-energy capacitor-discharge-type spot welder equipped with tweezer electrodes. Welds were spaced at 0.5-in. intervals along the wire lengths; 30 and 25 Wsec of power, respectively, were required for welding the edge and center spacer wires.

Several problems were encountered during welding. The points of electrode contact on the wires and plates were depressed due to localized softening and melting. Adjacent to each depression, one or more projections were incurred by expulsion of molten metal from beneath the area of electrode contact (of ~0.030-in. diameter). It was necessary to file these projections to maintain specified stack height dimensions. Finally, lack of sufficient electrode pressure resulted in misalignment between spacer wires of adjacent plates, since many of the wires remained cocked after welding.

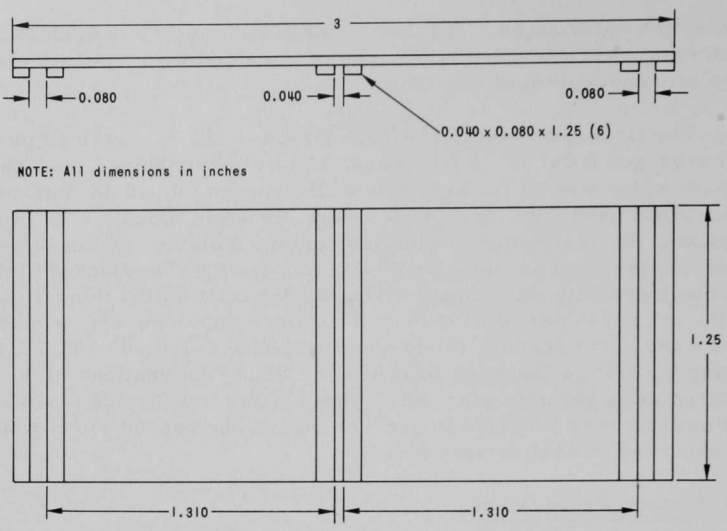

Fig. 42. Fixture Used for Spot Welding Spacer Wires to Plates with Tweezer Electrodes

3.4.5 Application of Braze Alloy

Precise quantities of GE J8100 braze powder (-150 mesh) were measured out and applied along each wire with grooved plastic loading bars. The groove size used for No. 2 and No. 3 spacer wires was 20 in. long and 0.030 in. square. For joints involving No. 1 spacer wires, the braze alloy was applied in the corner formed by the wire overhang and the plate edge. On Assemblies S/N 452-IB-5, -6, and -7, the quantity of braze powder was reduced 20% at each joint by removing 1/4 in. of powder over a $1\frac{1}{4}$ in. joint length. The objective here was to reduce alloy runoff during brazing.

Nicrobraz acrylic binder, diluted 50% with acetone, was used to cement the alloy powder in place. Excess powder was wiped from the plate surfaces with cotton swabs soaked with acetone. Finally, Nicrobraz Green Stopoff was applied with cotton swabs in very thin films parallel to the joint areas.

3.4.6 Unit Thickness

The total thickness of each assembled plate was measured at 15 evenly spaced intervals along each spacer wire. The values for plate Assemblies Nos. 452-IB-2 to 7 are listed in Table VI.

TABLE VI. Individual Plate-spacer Thickness Measurements: Full-scale Dummy Fuel Plate Assemblies

Note: See sketch at end of Table V

Plate No.	Wire No. 1					Wire No. 2					Wire No. 3				
	a	b	c	d	e	a	b	c	d	e	a	b	c	d	e
						Assembly No. S/N 452-1B-2									
1	0.1175	0.1165	0.1170	0.1175	0.1172	0.1165	0.1163	0.1173	0.1181	0.1165	0.1163	0.1163	0.1163	0.1166	0.1165
2	0.0796	0.0791	0.0786	0.0788	0.0792	0.0795	0.0792	0.0792	0.0789	0.0792	0.0790	0.0790	0.0788	0.0786	0.0785
3	0.0790	0.0785	0.0787	0.0785	0.0789	0.0797	0.0794	0.0792	0.0793	0.0797	0.0790	0.0792	0.0790	0.0787	0.0790
4	0.0793	0.0796	0.0795	0.0797	0.0799	0.0803	0.0799	0.0796	0.0797	0.0802	0.0799	0.0799	0.0793	0.0795	0.0798
5	0.0794	0.0796	0.0801	0.0800	0.0804	0.0798	0.0796	0.0797	0.0795	0.0795	0.0795	0.0797	0.0798	0.0795	0.0795
6	0.0788	0.0789	0.0788	0.0788	0.0786	0.0792	0.0792	0.0795	0.0793	0.0795	0.0792	0.0787	0.0787	0.0789	0.0788
7	0.0788	0.0788	0.0787	0.0786	0.0791	0.0796	0.0795	0.0794	0.0796	0.0795	0.0790	0.0785	0.0788	0.0786	0.0788
8	0.0785	0.0785	0.0782	0.0783	0.0791	0.0793	0.0792	0.0792	0.0793	0.0790	0.0795	0.0791	0.0789	0.0791	0.0791
9	0.0792	0.0795	0.0794	0.0793	0.0796	0.0796	0.0794	0.0795	0.0805	0.0795	0.0786	0.0786	0.0791	0.0787	0.0785
10	0.0788	0.0788	0.0791	0.0791	0.0791	0.0795	0.0796	0.0795	0.0796	0.0793	0.0790	0.0792	0.0792	0.0792	0.0790
11	0.0790	0.0785	0.0786	0.0786	0.0790	0.0797	0.0794	0.0794	0.0795	0.0796	0.0788	0.0790	0.0792	0.0792	0.0791
12	0.0790	0.0792	0.0791	0.0795	0.0790	0.0795	0.0795	0.0795	0.0795	0.0795	0.0785	0.0795	0.0793	0.0785	0.0783
13	0.0790	0.0790	0.0790	0.0795	0.0790	0.0790	0.0788	0.0790	0.0790	0.0788	0.0782	0.0789	0.0785	0.0786	0.0786
14	0.0788	0.0787	0.0788	0.0784	0.0786	0.0796	0.0792	0.0790	0.0795	0.0795	0.0788	0.0786	0.0787	0.0792	0.0788
15	0.0785	0.0800	0.0795	0.0790	0.0785	0.0796	0.0794	0.0790	0.0790	0.0794	0.0786	0.0788	0.0788	0.0794	0.0785
16	0.0785	0.0795	0.0785	0.0788	0.0785	0.0800	0.0800	0.0795	0.0791	0.0795	0.0790	0.0785	0.0790	0.0789	0.0788
17	0.0795	0.0795	0.0790	0.0791	0.0793	0.0793	0.0795	0.0798	0.0790	0.0795	0.0790	0.0786	0.0790	0.0781	0.0791
18	0.0785	0.0782	0.0782	0.0785	0.0785	0.0794	0.0796	0.0790	0.0793	0.0795	0.0795	0.0790	0.0790	0.0793	0.0792
19	0.0790	0.0795	0.0793	0.0793	0.0796	0.0796	0.0795	0.0793	0.0795	0.0790	0.0797	0.0792	0.0790	0.0796	0.0795
20	0.0790	0.0792	0.0792	0.0793	0.0793	0.0796	0.0796	0.0797	0.0795	0.0799	0.0792	0.0793	0.0793	0.0795	0.0790
21	0.0787	0.0791	0.0792	0.0792	0.0792	0.0791	0.0791	0.0792	0.0792	0.0793	0.0788	0.0785	0.0785	0.0783	0.0783
22	0.0790	0.0790	0.0788	0.0785	0.0803	0.0792	0.0790	0.0790	0.0790	0.0793	0.0785	0.0788	0.0789	0.0788	0.0790
23	0.0785	0.0785	0.0790	0.0787	0.0787	0.0794	0.0799	0.0793	0.0792	0.0798	0.0794	0.0786	0.0792	0.0793	0.0789
24	0.0796	0.0798	0.0780	0.0790	0.0788	0.0793	0.0795	0.0789	0.0790	0.0796	0.0785	0.0785	0.0784	0.0785	0.0787
25	0.0795	0.0800	0.0800	0.0800	0.0802	0.0801	0.0805	0.0802	0.0801	0.0802	0.0800	0.0805	0.0798	0.0798	0.0798
26	0.0780	0.0782	0.0783	0.0783	0.0785	0.0792	0.0795	0.0795	0.0792	0.0795	0.0795	0.0792	0.0795	0.0790	0.0792
27	0.0780	0.0784	0.0784	0.0784	0.0785	0.0792	0.0792	0.0792	0.0800	0.0790	0.0790	0.0787	0.0785	0.0785	0.0785
Total:	2.169	2.172	2.170	2.171	2.165	2.184	2.183	2.181	2.182	2.182	2.172	2.170	2.171	2.171	2.169
						Assembly No. S/N 452-1B-3									
1	0.1185	0.1190	0.1198	0.1190	0.1196	0.1193	0.1185	0.1188	0.1192	0.1198	0.1196	0.1192	0.1185	0.1185	0.1192
2	0.0798	0.0797	0.0792	0.0794	0.0799	0.0793	0.0794	0.0786	0.0788	0.0800	0.0793	0.0795	0.0791	0.0792	0.0796
3	0.0803	0.0794	0.0798	0.0794	0.0797	0.0802	0.0797	0.0796	0.0798	0.0794	0.0798	0.0796	0.0792	0.0795	0.0793
4	0.0799	0.0791	0.0794	0.0793	0.0788	0.0793	0.0792	0.0788	0.0792	0.0793	0.0794	0.0791	0.0788	0.0793	0.0791
5	0.0804	0.0807	0.0795	0.0794	0.0800	0.0786	0.0782	0.0782	0.0780	0.0780	0.0791	0.0792	0.0792	0.0790	0.0793
6	0.0790	0.0786	0.0789	0.0786	0.0788	0.0790	0.0786	0.0786	0.0786	0.0786	0.0803	0.0800	0.0795	0.0797	0.0801
7	0.0790	0.0788	0.0788	0.0790	0.0788	0.0792	0.0793	0.0790	0.0786	0.0783	0.0795	0.0794	0.0793	0.0790	0.0794
8	0.0797	0.0795	0.0793	0.0798	0.0795	0.0792	0.0791	0.0788	0.0792	0.0797	0.0788	0.0793	0.0796	0.0793	0.0794
9	0.0798	0.0794	0.0798	0.0791	0.0799	0.0803	0.0801	0.0808	0.0796	0.0796	0.0797	0.0800	0.0798	0.0796	0.0796
10	0.0793	0.0794	0.0790	0.0792	0.0788	0.0786	0.0793	0.0790	0.0788	0.0789	0.0796	0.0795	0.0790	0.0794	0.0796
11	0.0790	0.0791	0.0790	0.0786	0.0794	0.0790	0.0785	0.0786	0.0784	0.0787	0.0795	0.0788	0.0792	0.0793	0.0793
12	0.0802	0.0803	0.0798	0.0795	0.0800	0.0798	0.0798	0.0796	0.0796	0.0796	0.0798	0.0800	0.0796	0.0794	0.0796
13	0.0787	0.0790	0.0793	0.0793	0.0790	0.0801	0.0796	0.0795	0.0794	0.0800	0.0800	0.0804	0.0798	0.0795	0.0802
14	0.0794	0.0795	0.0798	0.0796	0.0800	0.0794	0.0796	0.0793	0.0796	0.0796	0.0798	0.0796	0.0793	0.0793	0.0793
15	0.0787	0.0787	0.0787	0.0788	0.0790	0.0800	0.0800	0.0798	0.0803	0.0806	0.0793	0.0795	0.0796	0.0794	0.0796
16	0.0802	0.0807	0.0795	0.0798	0.0797	0.0809	0.0803	0.0799	0.0798	0.0806	0.0802	0.0798	0.0798	0.0808	0.0800
17	0.0796	0.0794	0.0796	0.0793	0.0794	0.0798	0.0798	0.0797	0.0797	0.0794	0.0798	0.0800	0.0798	0.0795	0.0793
18	0.0808	0.0800	0.0796	0.0796	0.0800	0.0804	0.0797	0.0798	0.0800	0.0797	0.0800	0.0798	0.0799	0.0800	0.0796
19	0.0794	0.0792	0.0793	0.0793	0.0797	0.0799	0.0795	0.0797	0.0796	0.0798	0.0810	0.0811	0.0810	0.0812	0.0812
20	0.0797	0.0799	0.0798	0.0795	0.0796	0.0806	0.0797	0.0797	0.0795	0.0799	0.0801	0.0802	0.0796	0.0798	0.0802
21	0.0800	0.0803	0.0798	0.0800	0.0802	0.0796	0.0796	0.0794	0.0796	0.0798	0.0795	0.0794	0.0793	0.0790	0.0795
22	0.0793	0.0790	0.0795	0.0794	0.0792	0.0806	0.0796	0.0795	0.0797	0.0796	0.0796	0.0795	0.0796	0.0794	0.0796
23	0.0787	0.0799	0.0790	0.0790	0.0785	0.0793	0.0793	0.0796	0.0797	0.0796	0.0803	0.0800	0.0794	0.0800	0.0790
24	0.0794	0.0798	0.0802	0.0802	0.0800	0.0803	0.0794	0.0800	0.0795	0.0803	0.0807	0.0804	0.0806	0.0803	0.0797
25	0.0795	0.0798	0.0797	0.0796	0.0802	0.0796	0.0797	0.0797	0.0794	0.0795	0.0796	0.0802	0.0800	0.0800	0.0804
26	0.0800	0.0797	0.0802	0.0793	0.0794	0.0800	0.0798	0.0797	0.0795	0.0801	0.0806	0.0797	0.0803	0.0707	0.0798
27	0.0787	0.0789	0.0789	0.0789	0.0788	0.0799	0.0804	0.0804	0.0804	0.0803	0.0813	0.0815	0.0810	0.0808	0.0808
Total:	2.187	2.187	2.185	2.182	2.186	2.192	2.186	2.184	2.183	2.189	2.196	2.195	2.190	2.190	2.182

TABLE VI (Contd.)

Plate No.	Wire No. 1					Wire No. 2					Wire No. 3				
	a	b	c	d	e	a	b	c	d	e	a	b	c	d	e
						Assembly No. S/N 452-1B-4									
1	0.1175	0.1170	0.1175	0.1170	0.1176	0.1170	0.1176	0.1166	0.1170	0.1172	0.1173	0.1167	0.1165	0.1163	0.1167
2	0.0801	0.0797	0.0797	0.0793	0.0790	0.0792	0.0782	0.0787	0.0792	0.0796	0.0792	0.0792	0.0798	0.0794	0.0803
3	0.0788	0.0793	0.0788	0.0789	0.0786	0.0793	0.0788	0.0786	0.0785	0.0787	0.0786	0.0793	0.0788	0.0790	0.0787
4	0.0790	0.0787	0.0785	0.0790	0.0788	0.0793	0.0785	0.0785	0.0786	0.0785	0.0792	0.0789	0.0792	0.0787	0.0795
5	0.0806	0.0800	0.0803	0.0797	0.0798	0.0785	0.0780	0.0790	0.0790	0.0795	0.0793	0.0795	0.0795	0.0802	0.0810
6	0.0788	0.0786	0.0785	0.0780	0.0785	0.0785	0.0780	0.0778	0.0776	0.0781	0.0786	0.0786	0.0790	0.0791	0.0789
7	0.0794	0.0794	0.0794	0.0794	0.0797	0.0800	0.0794	0.0792	0.0792	0.0800	0.0796	0.0796	0.0797	0.0796	0.0797
8	0.0798	0.0792	0.0794	0.0793	0.0790	0.0792	0.0788	0.0792	0.0792	0.0798	0.0796	0.0792	0.0792	0.0792	0.0795
9	0.0792	0.0798	0.0797	0.0796	0.0795	0.0798	0.0801	0.0800	0.0798	0.0799	0.0798	0.0791	0.0801	0.0798	0.0796
10	0.0796	0.0792	0.0793	0.0791	0.0793	0.0798	0.0800	0.0795	0.0800	0.0797	0.0796	0.0793	0.0796	0.0792	0.0797
11	0.0794	0.0788	0.0789	0.0795	0.0788	0.0802	0.0798	0.0800	0.0798	0.0798	0.0798	0.0796	0.0798	0.0796	0.0800
12	0.0799	0.0793	0.0793	0.0795	0.0798	0.0798	0.0794	0.0796	0.0797	0.0797	0.0794	0.0794	0.0791	0.0794	0.0798
13	0.0798	0.0796	0.0792	0.0788	0.0788	0.0802	0.0798	0.0799	0.0793	0.0801	0.0796	0.0791	0.0795	0.0796	0.0797
14	0.0794	0.0792	0.0795	0.0788	0.0794	0.0800	0.0801	0.0799	0.0796	0.0800	0.0797	0.0794	0.0794	0.0794	0.0797
15	0.0795	0.0792	0.0797	0.0793	0.0798	0.0804	0.0798	0.0794	0.0794	0.0798	0.0802	0.0794	0.0794	0.0798	0.0798
16	0.0791	0.0789	0.0792	0.0791	0.0794	0.0793	0.0797	0.0798	0.0798	0.0800	0.0795	0.0789	0.0792	0.0789	0.0790
17	0.0792	0.0790	0.0789	0.0789	0.0792	0.0793	0.0795	0.0795	0.0797	0.0798	0.0792	0.0795	0.0791	0.0802	0.0793
18	0.0801	0.0800	0.0796	0.0797	0.0798	0.0800	0.0797	0.0797	0.0796	0.0798	0.0799	0.0795	0.0796	0.0796	0.0798
19	0.0798	0.0794	0.0795	0.0794	0.0793	0.0793	0.0793	0.0745	0.0790	0.0787	0.0798	0.0796	0.0795	0.0798	0.0805
20	0.0798	0.0800	0.0805	0.0795	0.0795	0.0795	0.0793	0.0793	0.0797	0.0795	0.0798	0.0793	0.0795	0.0796	0.0796
21	0.0798	0.0793	0.0790	0.0792	0.0787	0.0790	0.0791	0.0792	0.0790	0.0792	0.0800	0.0795	0.0795	0.0797	0.0797
22	0.0795	0.0797	0.0794	0.0792	0.0788	0.0792	0.0785	0.0785	0.0790	0.0785	0.0800	0.0797	0.0802	0.0803	0.0800
23	0.0807	0.0808	0.0807	0.0803	0.0803	0.0795	0.0787	0.0794	0.0791	0.0792	0.0790	0.0790	0.0794	0.0792	0.0792
24	0.0804	0.0805	0.0790	0.0796	0.0798	0.0795	0.0795	0.0795	0.0795	0.0795	0.0797	0.0802	0.0797	0.0797	0.0792
25	0.0780	0.0776	0.0774	0.0774	0.0777	0.0788	0.0777	0.0785	0.0778	0.0778	0.0783	0.0786	0.0780	0.0785	0.0786
26	0.0792	0.0796	0.0795	0.0793	0.0794	0.0798	0.0800	0.0798	0.0796	0.0793	0.0797	0.0795	0.0792	0.0793	0.0793
27	0.0804	0.0806	0.0800	0.0801	0.0801	0.0806	0.0802	0.0804	0.0805	0.0806	0.0794	0.0793	0.0793	0.0794	0.0796
Total:	2.187	2.182	1.182	2.177	2.179	2.185	2.178	2.179	2.179	2.172	2.184	2.179	2.181	2.183	2.187
						Assembly No. S/N 452-1B-5									
1	0.1192	0.1190	0.1188	0.1192	0.1204	0.1180	0.1181	0.1181	0.1175	0.1176	0.1193	0.1187	0.1191	0.1194	0.1200
2	0.0787	0.0787	0.0786	0.0786	0.0790	0.0792	0.0792	0.0791	0.0791	0.0792	0.0793	0.0798	0.0790	0.0796	0.0791
3	0.0787	0.0789	0.0791	0.0787	0.0788	0.0793	0.0788	0.0793	0.0792	0.0788	0.0796	0.0798	0.0794	0.0793	0.0797
4	0.0792	0.0792	0.0787	0.0795	0.0799	0.0792	0.0795	0.0792	0.0797	0.0790	0.0794	0.0796	0.0791	0.0793	0.0799
5	0.0791	0.0793	0.0792	0.0796	0.0795	0.0801	0.0798	0.0799	0.0798	0.0796	0.0797	0.0798	0.0798	0.0799	0.0795
6	0.0783	0.0783	0.0783	0.0782	0.0783	0.0793	0.0790	0.0792	0.0786	0.0783	0.0785	0.0792	0.0787	0.0786	0.0792
7	0.0794	0.0790	0.0788	0.0790	0.0792	0.0790	0.0788	0.0791	0.0789	0.0788	0.0793	0.0792	0.0793	0.0793	0.0793
8	0.0796	0.0793	0.0796	0.0799	0.0796	0.0795	0.0794	0.0792	0.0796	0.0793	0.0797	0.0797	0.0799	0.0796	0.0796
9	0.0797	0.0792	0.0794	0.0793	0.0781	0.0797	0.0795	0.0790	0.0790	0.0789	0.0798	0.0797	0.0796	0.0795	0.0805
10	0.0796	0.0798	0.0798	0.0797	0.0797	0.0794	0.0796	0.0798	0.0796	0.0798	0.0800	0.0800	0.0798	0.0798	0.0797
11	0.0802	0.0795	0.0797	0.0796	0.0796	0.0793	0.0795	0.0781	0.0788	0.0794	0.0797	0.0795	0.0795	0.0798	0.0803
12	0.0793	0.0791	0.0792	0.0788	0.0795	0.0791	0.0791	0.0792	0.0793	0.0793	0.0793	0.0796	0.0797	0.0794	0.0793
13	0.0794	0.0793	0.0793	0.0792	0.0793	0.0793	0.0790	0.0781	0.0792	0.0794	0.0789	0.0796	0.0791	0.0796	0.0797
14	0.0788	0.0791	0.0791	0.0791	0.0791	0.0796	0.0795	0.0794	0.0797	0.0798	0.0791	0.0788	0.0796	0.0794	0.0793
15	0.0794	0.0797	0.0793	0.0794	0.0796	0.0794	0.0794	0.0795	0.0797	0.0797	0.0797	0.0797	0.0796	0.0797	0.0793
16	0.0797	0.0797	0.0790	0.0790	0.0794	0.0793	0.0796	0.0796	0.0791	0.0794	0.0797	0.0797	0.0794	0.0796	0.0794
17	0.0795	0.0797	0.0796	0.0795	0.0795	0.0794	0.0793	0.0793	0.0792	0.0792	0.0797	0.0794	0.0791	0.0793	0.0795
18	0.0795	0.0795	0.0796	0.0796	0.0793	0.0795	0.0795	0.0795	0.0795	0.0792	0.0796	0.0794	0.0797	0.0797	0.0797
19	0.0794	0.0794	0.0792	0.0794	0.0793	0.0792	0.0794	0.0793	0.0793	0.0796	0.0793	0.0792	0.0791	0.0796	0.0795
20	0.0790	0.0787	0.0793	0.0790	0.0798	0.0793	0.0793	0.0793	0.0793	0.0790	0.0797	0.0797	0.0797	0.0798	0.0794
21	0.0793	0.0793	0.0796	0.0796	0.0795	0.0790	0.0795	0.0785	0.0787	0.0790	0.0793	0.0795	0.0787	0.0787	0.0793
22	0.0797	0.0794	0.0796	0.0797	0.0796	0.0793	0.0786	0.0787	0.0792	0.0790	0.0797	0.0797	0.0781	0.0792	0.0790
23	0.0793	0.0793	0.0793	0.0796	0.0796	0.0793	0.0797	0.0793	0.0792	0.0790	0.0797	0.0800	0.0800	0.0797	0.0797
24	0.0789	0.0789	0.0789	0.0788	0.0791	0.0785	0.0786	0.0787	0.0787	0.0787	0.0793	0.0796	0.0790	0.0796	0.0788
25	0.0802	0.0796	0.0796	0.0796	0.0797	0.0790	0.0791	0.0788	0.0785	0.0783	0.0798	0.0800	0.0797	0.0801	0.0806
26	0.0793	0.0792	0.0796	0.0789	0.0793	0.0794	0.0796	0.0793	0.0790	0.0790	0.0796	0.0793	0.0793	0.0791	0.0793
27	0.0805	0.0805	0.0808	0.0802	0.0805	0.0791	0.0792	0.0792	0.0794	0.0792	0.0794	0.0793	0.0797	0.0793	0.0796
Total:	2.183	2.180	2.180	2.181	2.185	2.180	2.180	2.177	2.177	2.176	2.186	2.186	2.184	2.187	2.188

TABLE VI (Contd.)

Plate No.	Wire No. 1					Wire No. 2					Wire No. 3				
	a	b	c	d	e	a	b	c	d	e	a	b	c	d	e
						Assembly No. S/N 452-1B-6									
1	0.1195	0.1195	0.1195	0.1195	0.1192	0.1190	0.1190	0.1190	0.1191	0.1190	0.1192	0.1192	0.1196	0.1191	0.1197
2	0.0797	0.0799	0.0792	0.0794	0.0793	0.0801	0.0800	0.0803	0.0803	0.0805	0.0802	0.0801	0.0799	0.0802	0.0801
3	0.0796	0.0793	0.0801	0.0803	0.0803	0.0795	0.0797	0.0797	0.0799	0.0797	0.0806	0.0802	0.0808	0.0809	0.0802
4	0.0802	0.0801	0.0800	0.0800	0.0800	0.0802	0.0799	0.0800	0.0802	0.0806	0.0803	0.0804	0.0803	0.0804	0.0805
5	0.0792	0.0788	0.0792	0.0790	0.0796	0.0790	0.0791	0.0790	0.0794	0.0791	0.0793	0.0800	0.0799	0.0800	0.0791
6	0.0807	0.0798	0.0798	0.0805	0.0801	0.0795	0.0791	0.0791	0.0788	0.0792	0.0802	0.0799	0.0798	0.0802	0.0802
7	0.0791	0.0798	0.0798	0.0790	0.0802	0.0795	0.0791	0.0788	0.0788	0.0790	0.0798	0.0795	0.0797	0.0797	0.0797
8	0.0797	0.0795	0.0793	0.0795	0.0799	0.0788	0.0788	0.0789	0.0788	0.0789	0.0806	0.0800	0.0800	0.0801	0.0798
9	0.0798	0.0796	0.0793	0.0798	0.0795	0.0795	0.0794	0.0791	0.0792	0.0798	0.0801	0.0799	0.0795	0.0798	0.0795
10	0.0788	0.0789	0.0793	0.0788	0.0790	0.0788	0.0790	0.0788	0.0792	0.0788	0.0801	0.0800	0.0800	0.0802	0.0801
11	0.0806	0.0801	0.0800	0.0895	0.0802	0.0799	0.0793	0.0793	0.0793	0.0793	0.0803	0.0799	0.0805	0.0800	0.0801
12	0.0795	0.0792	0.0792	0.0792	0.0794	0.0793	0.0794	0.0792	0.0795	0.0797	0.0793	0.0793	0.0790	0.0790	0.0790
13	0.0803	0.0802	0.0801	0.0801	0.0806	0.0800	0.0802	0.0795	0.0795	0.0800	0.0807	0.0803	0.0803	0.0802	0.0806
14	0.0798	0.0798	0.0802	0.0805	0.0801	0.0800	0.0800	0.0802	0.0806	0.0800	0.0806	0.0800	0.0800	0.0800	0.0800
15	0.0791	0.0785	0.0782	0.0791	0.0791	0.0792	0.0790	0.0796	0.0789	0.0798	0.0795	0.0790	0.0795	0.0791	0.0798
16	0.0800	0.0792	0.0790	0.0793	0.0796	0.0790	0.0788	0.0792	0.0795	0.0795	0.0798	0.0790	0.0800	0.0798	0.0801
17	0.0801	0.0795	0.0794	0.0794	0.0801	0.0792	0.0790	0.0790	0.0790	0.0791	0.0800	0.0800	0.0797	0.0799	0.0800
18	0.0795	0.0804	0.0802	0.0805	0.0803	0.0810	0.0805	0.0802	0.0798	0.0802	0.0804	0.0800	0.0802	0.0807	0.0810
19	0.0805	0.0801	0.0805	0.0802	0.0801	0.0803	0.0803	0.0800	0.0802	0.0803	0.0806	0.0800	0.0805	0.0803	0.0803
20	0.0802	0.0801	0.0794	0.0805	0.0795	0.0792	0.0792	0.0791	0.0793	0.0795	0.0795	0.0795	0.0790	0.0800	0.0800
21	0.0795	0.0794	0.0798	0.0790	0.0798	0.0795	0.0790	0.0790	0.0792	0.0790	0.0793	0.0792	0.0795	0.0792	0.0792
22	0.0811	0.0811	0.0812	0.0812	0.0807	0.0807	0.0800	0.0807	0.0800	0.0806	0.0806	0.0798	0.0806	0.0806	0.0806
23	0.0803	0.0801	0.0801	0.0803	0.0800	0.0795	0.0792	0.0792	0.0790	0.0799	0.0802	0.0800	0.0798	0.0797	0.0800
24	0.0798	0.0798	0.0796	0.0792	0.0795	0.0791	0.0791	0.0791	0.0789	0.0789	0.0791	0.0791	0.0780	0.0791	0.0791
25	0.0807	0.0812	0.0810	0.0800	0.0800	0.0792	0.0793	0.0795	0.0795	0.0797	0.0800	0.0800	0.0800	0.0799	0.0800
26	0.0798	0.0800	0.0800	0.0796	0.0798	0.0800	0.0800	0.0798	0.0798	0.0796	0.0805	0.0811	0.0810	0.0800	0.0799
27	0.0793	0.0796	0.0793	0.0791	0.0793	0.0794	0.0793	0.0792	0.0793	0.0798	0.0795	0.0792	0.0796	0.0796	0.0797
Total:	2.196	2.194	2.186	2.193	2.195	2.188	2.185	2.188	2.185	2.190	2.200	2.195	2.198	2.189	2.198
						Assembly No. S/N 452-1B-7									
1	0.1203	0.1205	0.1200	0.1197	0.1190	0.1190	0.1182	0.1191	0.1190	0.1191	0.1212	0.1211	0.1202	0.1200	0.1200
2	0.0795	0.0790	0.0789	0.0795	0.0795	0.0790	0.0785	0.0788	0.0791	0.0789	0.0795	0.0794	0.0795	0.0790	0.0790
3	0.0788	0.0788	0.0789	0.0788	0.0785	0.0791	0.0798	0.0791	0.0788	0.0790	0.0800	0.0798	0.0790	0.0790	0.0790
4	0.0782	0.0790	0.0785	0.0790	0.0792	0.0799	0.0790	0.0786	0.0790	0.0795	0.0793	0.0790	0.0792	0.0785	0.0800
5	0.0787	0.0778	0.0789	0.0786	0.0787	0.0782	0.0786	0.0790	0.0789	0.0786	0.0790	0.0790	0.0793	0.0792	0.0795
6	0.0786	0.0785	0.0790	0.0785	0.0785	0.0789	0.0785	0.0785	0.0783	0.0798	0.0790	0.0787	0.0787	0.0791	0.0791
7	0.0791	0.0790	0.0789	0.0789	0.0792	0.0781	0.0783	0.0782	0.0781	0.0779	0.0787	0.0790	0.0793	0.0796	0.0791
8	0.0788	0.0789	0.0787	0.0785	0.0790	0.0778	0.0778	0.0778	0.0778	0.0780	0.0792	0.0794	0.0799	0.0788	0.0792
9	0.0780	0.0779	0.0781	0.0780	0.0785	0.0785	0.0787	0.0789	0.0800	0.0805	0.0796	0.0785	0.0791	0.0791	0.0790
10	0.0791	0.0785	0.0791	0.0784	0.0782	0.0782	0.0778	0.0778	0.0778	0.0788	0.0796	0.0789	0.0797	0.0790	0.0793
11	0.0790	0.0798	0.0792	0.0791	0.0791	0.0788	0.0790	0.0789	0.0785	0.0785	0.0785	0.0795	0.0794	0.0790	0.0800
12	0.0800	0.0796	0.0792	0.0792	0.0795	0.0805	0.0812	0.0808	0.0809	0.0808	0.0808	0.0803	0.0803	0.0809	0.0807
13	0.0796	0.0790	0.0795	0.0795	0.0800	0.0799	0.0798	0.0795	0.0797	0.0800	0.0795	0.0796	0.0800	0.0795	0.0790
14	0.0802	0.0795	0.0798	0.0791	0.0790	0.0808	0.0805	0.0803	0.0803	0.0809	0.0800	0.0800	0.0800	0.0800	0.0800
15	0.0785	0.0783	0.0780	0.0782	0.0787	0.0800	0.0789	0.0789	0.0795	0.0795	0.0801	0.0787	0.0795	0.0790	0.0790
16	0.0788	0.0785	0.0780	0.0780	0.0782	0.0787	0.0788	0.0785	0.0791	0.0785	0.0790	0.0779	0.0770	0.0772	0.0772
17	0.0791	0.0795	0.0798	0.0797	0.0795	0.0790	0.0885	0.0788	0.0792	0.0795	0.0799	0.0792	0.0798	0.0792	0.0797
18	0.0792	0.0799	0.0791	0.0795	0.0788	0.0800	0.0793	0.0791	0.0789	0.0789	0.0795	0.0806	0.0797	0.0792	0.0797
19	0.0777	0.0776	0.0777	0.0776	0.0772	0.0775	0.0775	0.0773	0.0772	0.0772	0.0774	0.0773	0.0770	0.0773	0.0780
20	0.0788	0.0790	0.0790	0.0790	0.0790	0.0800	0.0798	0.0792	0.0792	0.0789	0.0800	0.0792	0.0797	0.0801	0.0798
21	0.0811	0.0808	0.0803	0.0798	0.0795	0.0803	0.0805	0.0802	0.0804	0.0805	0.0805	0.0805	0.0800	0.0800	0.0800
22	0.0792	0.0792	0.0791	0.0795	0.0790	0.0795	0.0800	0.0800	0.0792	0.0795	0.0799	0.0802	0.0799	0.0796	0.0795
23	0.0808	0.0809	0.0806	0.0802	0.0809	0.0810	0.0808	0.0810	0.0805	0.0809	0.0810	0.0804	0.0803	0.0805	0.0809
24	0.0808	0.0805	0.0800	0.0800	0.0800	0.0806	0.0808	0.0810	0.0808	0.0808	0.0805	0.0810	0.0808	0.0810	0.0809
25	0.0804	0.0805	0.0803	0.0795	0.0799	0.0803	0.0802	0.0807	0.0803	0.0809	0.0806	0.0802	0.0802	0.0808	0.0803
26	0.0800	0.0792	0.0792	0.0800	0.0792	0.0810	0.0811	0.0802	0.0808	0.0805	0.0808	0.0805	0.0808	0.0808	0.0809
27	0.0791	0.0783	0.0790	0.0789	0.0788	0.0791	0.0791	0.0792	0.0789	0.0792	0.0793	0.0788	0.0791	0.0788	0.0789
Total:	2.180	2.178	2.177	2.175	2.175	2.184	2.180	2.180	2.180	2.184	2.192	2.186	2.187	2.184	2.188

3.4.7 Fixturing

Figure 43 shows a plate assembly loaded in the first brazing fixture used in this phase of the program. Each plate was stacked to the 60° offset with the aid of the stepped guides. Stopoff-coated stainless steel shims (0.004 in. thick) were installed above and below the plate assembly to prevent it from being brazed to the fixture. These shims were permitted to braze to the assembly. Similar shims, 0.001 in. thick, were used to prevent brazing of the stepped guides to the plate assembly.

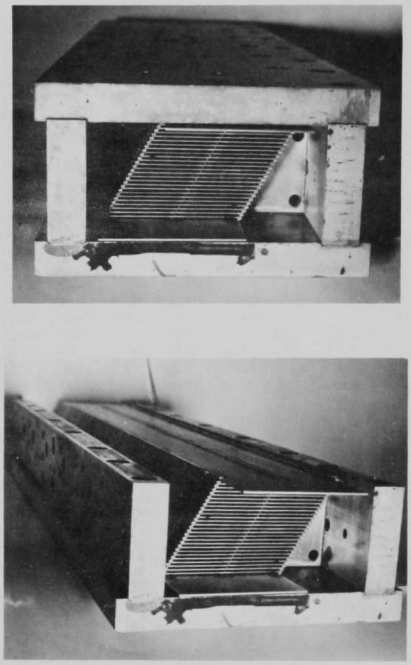

Fig. 43. Views of Dummy Fuel-plate Assembly in Brazing Fixture

3.4.8 Brazing

Each fixtured assembly was loaded into a weld-sealed retort, heated to and held for 2 hr in a dynamic, dry hydrogen atmosphere (-80°F dewpoint) at 2140°F, and then furnace cooled. The retort measured 33 in. in ID by 22-in. high, with a volume of ~11 ft^3. At a hydrogen flow rate of 200 ft^3/hr, approximately 18 atmosphere changes were achieved per hour.

Modifications were made in the brazing cycle after exposure of the first two assemblies because of thermal distortion of both the fixtures and the assemblies. For the remaining assemblies, the heating rate in the range 800-1950°F was slowed to a maximum of 200°F/hr. This change resulted in less distortion. During brazing of Assembly No. 6, the decision was made to decrease the cooling rate to help reduce distortion. A maximum cooling rate of 100°F/hr was specified.

The temperature-time cycles for the respective plate assemblies are plotted in Fig. 44.

3.4.9 Results

As mentioned earlier, Assembly No. 452-IB-1 was scrapped because of large gaps in the brazed joints and excessive distortion. The other six assemblies were photographed and then subjected to rigorous visual inspection and dimensional surveys. Assembly No. 2 was also machined, dye-checked, and then incorporated into a complete dummy fuel subassembly (see Fig. 45).

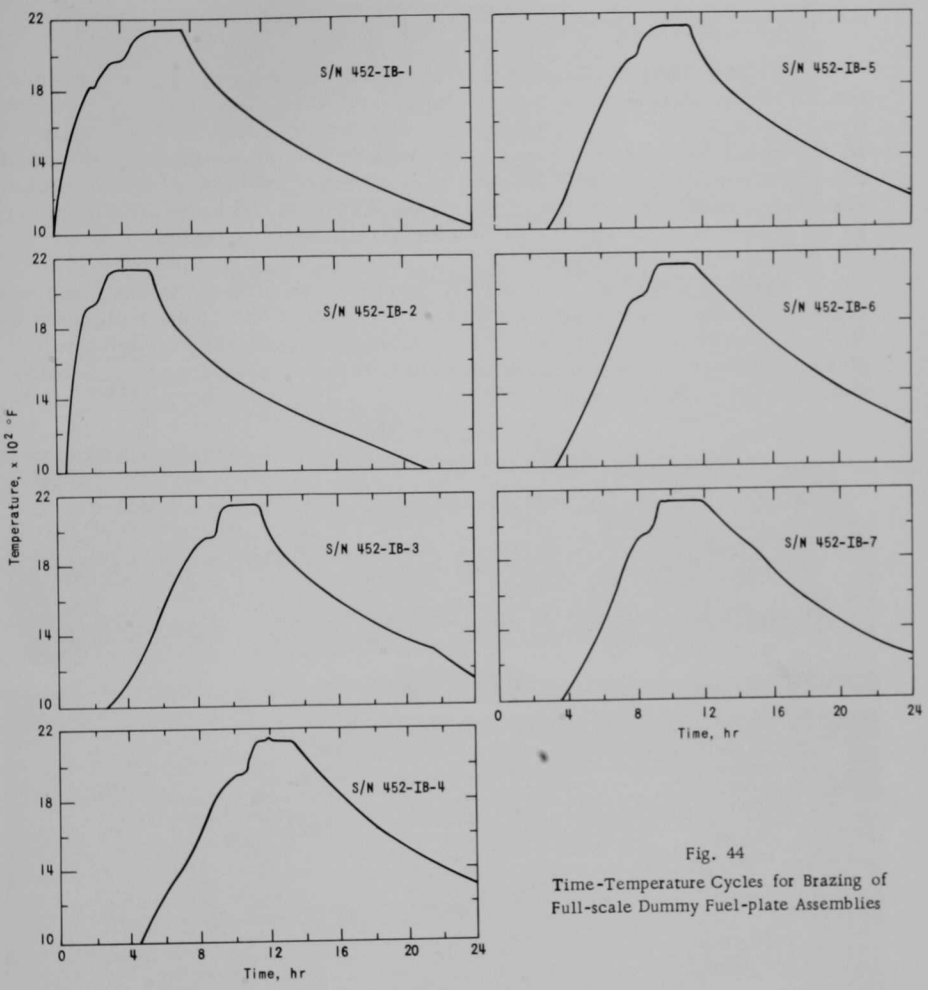

Fig. 44
Time-Temperature Cycles for Brazing of Full-scale Dummy Fuel-plate Assemblies

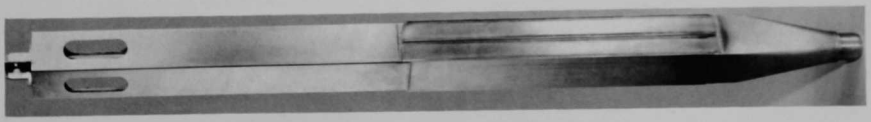

112-7345

Fig. 45. Plate Assembly No. 452-IB-2 with End Fittings Attached

3.4.9.1 Visual Inspection

Photographs of the as-brazed assemblies are shown in Figs. 46 and 47. Assemblies No. 2, 3, and 4 appeared to be completely brazed. Braze alloy flow on the top and bottom plates was marginal, especially on Assembly No. 4; outgassing of the stopoff in these areas was presumed to be responsible. A small amount of alloy runoff was observed on each assembly between the plates at each end of the spacer wires. Two spacers on the top plate of Assembly No. 2 contained nonbrazed areas.

With respect to Assembly No. 5, there was a 5/16-in.-long gap in an edge spacer joint at the 12th plate from the bottom and about 4 in. from the "b" end (see sketch, Table V). Braze alloy flow on the top and bottom plate-to-spacer joints was poor; however, there was no appreciable alloy runoff at the ends of this assembly.

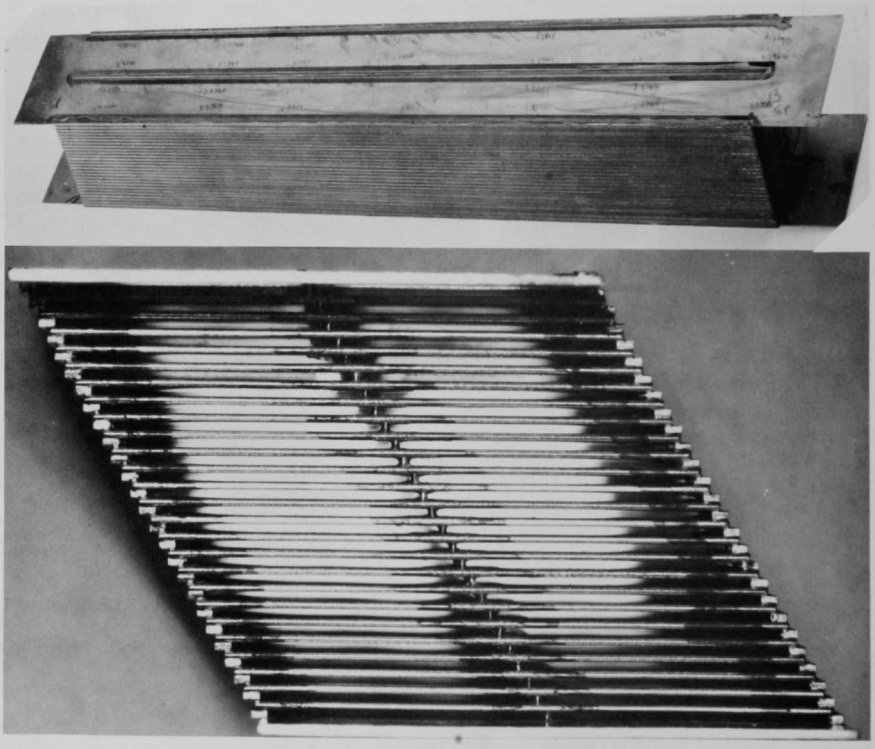

Fig. 46. Side and End Views of Assembly No. S/N 452-IA-2, as Brazed

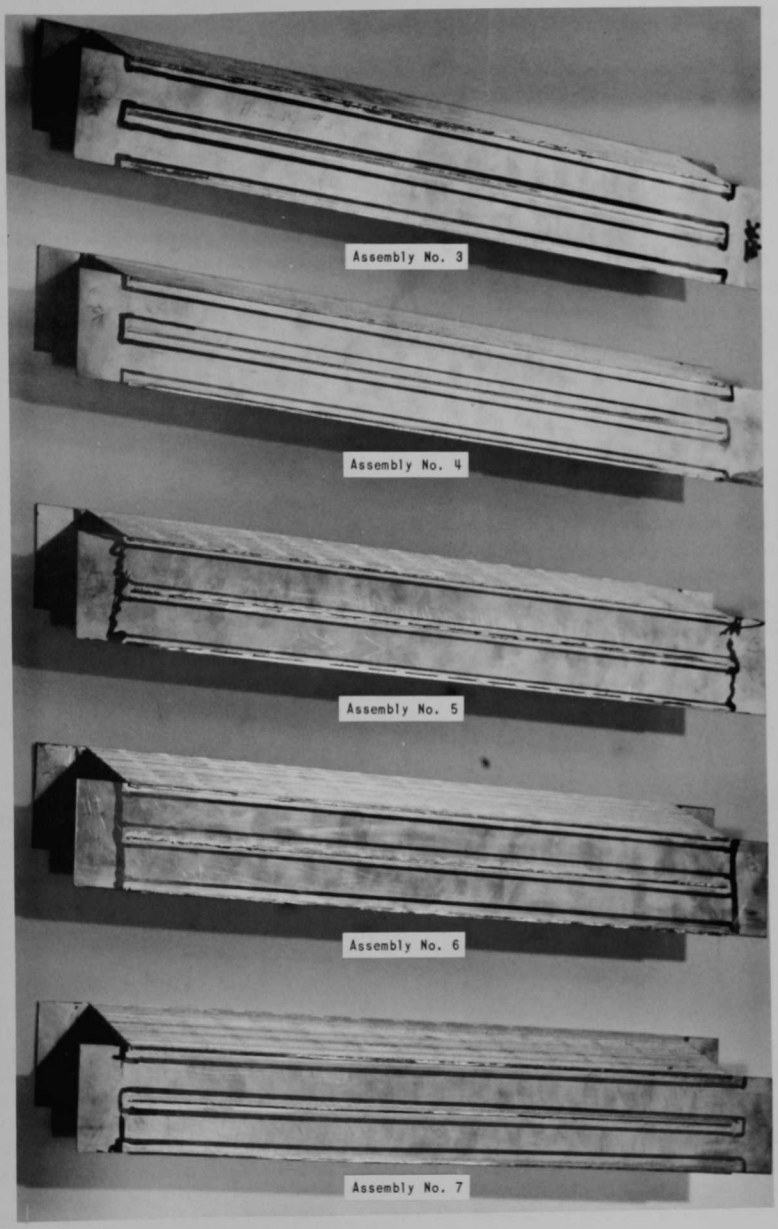

Fig. 47. As-brazed Appearance of Assemblies No. S/N 452-IA-3 to -7

Most joints on Assembly No. 6 appeared to be completely brazed. The top and bottom plate joints were suspect because of poor alloy flow; the plate ends were clear of alloy runoff.

The plates in all assemblies exhibited excessive stopoff residue. Attempts to remove the residue by washing and ultrasonic cleaning were unsuccessful.

Most of the assemblies had small pieces of shim stock brazed to the spacers. This was caused by discontinuities in the stopoff which had been applied to the shim stock prior to assembly in the braze fixture. Final machining of the spacers would remove the attached pieces; however they caused some inaccuracies in the dimensional surveys.

3.4.9.2 Dimensional Surveys

External Dimensions

Table VII lists the nominal and the maximum/minimum external dimensions of each plate assembly. Dimensions A, B, and C are the overall heights measured from a reference plane to the peaks of the plate on spacer edges. Here, excess braze material can appreciably affect the dimensions. The lengths D, E, and F are the overall heights from a reference plane to the tops of the spacer wires. These dimensions were affected by the shim stock pieces as mentioned earlier. The dimensions G and H are the channel widths measured from inside the edge spacer to the center spacer wire. Here, the measurements are affected by the radii formed by the fluid braze alloy.

TABLE VII. Overall Dimensions of Dummy Fuel-plate Assemblies

Location:	A	B	C	D	E	F	G	H	Stack Height
Nominal Dimension, in.		2.459 ± 0.002			2.200 ± 0.001		1.310 ± 0.002		2.120 + 0.001
Assembly No.									
2	2.485/2.470	2.474/2.461	2.470/2.463	2.210/2.207	2.210/2.200	2.211/2.200	1.325/1.308	1.324/1.290	2.124/2.118
3	2.475/2.467	2.476/2.468	2.473/2.466	2.208/2.203	2.207/2.201	2.205/2.199	1.325/1.299	1.325/1.298	2.119/2.115
4	2.469/2.458	2.475/2.462	2.467/2.456	2.203/2.198	2.201/2.197	2.198/2.195	1.335/1.306	1.320/1.297	2.123/2.118
5	2.480/2.463	2.481/2.460	2.480/2.460	2.199/2.196	2.196/2.192	2.194/2.187	1.325/1.302	1.321/1.297	2.120/2.116
6	2.469/2.463	2.470/2.462	2.469/2.462	2.211/2.207	2.207/2.204	2.204/2.201	1.328/1.303	1.324/1.302	2.122/2.116
7	2.470/2.463	2.471/2.465	2.464/2.458	2.211/2.209	2.212/2.209	2.211/2.208	1.322/1.300	1.324/1.307	2.123/2.119
		A, B, and C			D, E, and F		G and H		
Average:		2.4679			2.2038		1.3128		2.1194
Mean:		2.467-2.468			2.203-2.204		1.314-1.315		2.119

One dimension which was carefully measured was the plate stack height. It was gauged at points along the length and represents the perpendicular distance from the top of plate No. 1 at the left of the center spacer wire to the bottom of plate No. 27 at the right of the center spacer wire.

Channel Gaps

The spacing between plates was measured with tandem, strain gauge-type probes, as shown in Fig. 48. Both gauges were calibrated on each pass by driving them through a set of blocks having 0.035, 0.040, and 0.045-in. openings before entering the flow channels of the plate assembly. The probes had different sensitivities and, at the dimensions measured, tended to operate in a nonlinear region. At best, the probe, chart, and drift errors at 0.037 in. were ±0.0005 in. for Probe A and ±0.001 in. for Probe B. At worst, Probe B was within ±0.0015 in. at 0.035 in.

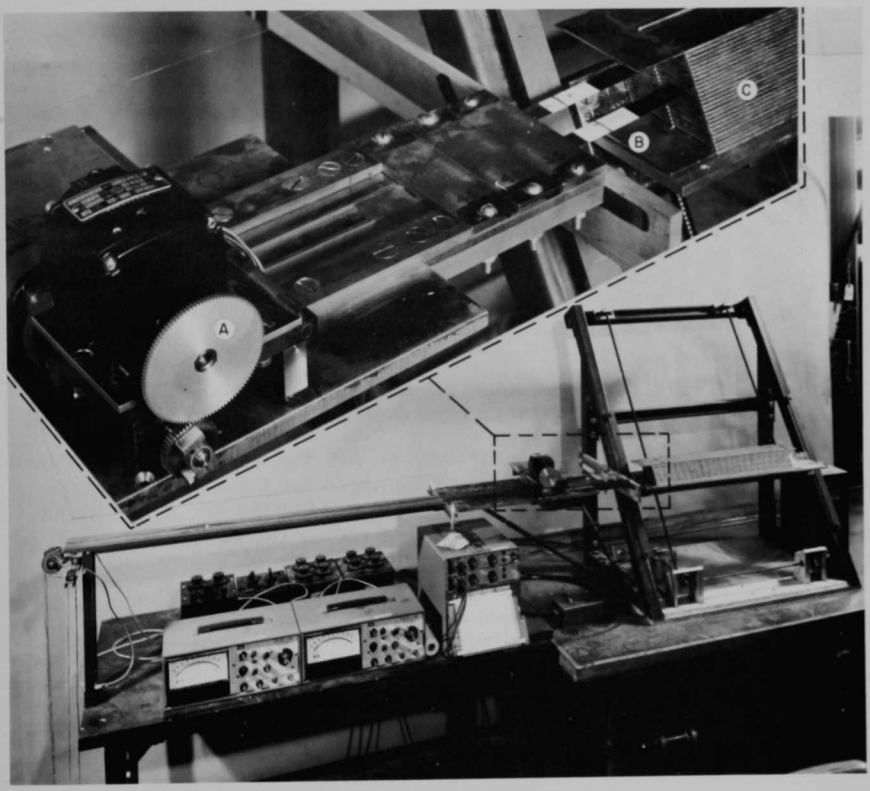

Fig. 48. Apparatus Used to Measure Channel Gaps in Plate Assemblies. Inset shows (A) probe drive, (B) tanden probes, and (C) plate assembly.

Initial probing produced very erratic readings. Closer examination of the plate assembly, both visually and by touch, revealed a residue on the plate surfaces. Since the plates as fabricated had a smooth surface, the residue was incurred either during assembly or subsequent brazing. In any

event, the residue could be scraped off, and the channels ultimately cleaned with emery paper followed by an air blast or water rinse. Figure 49 shows the probe traces before and after cleaning the channels in Assembly No. 4.

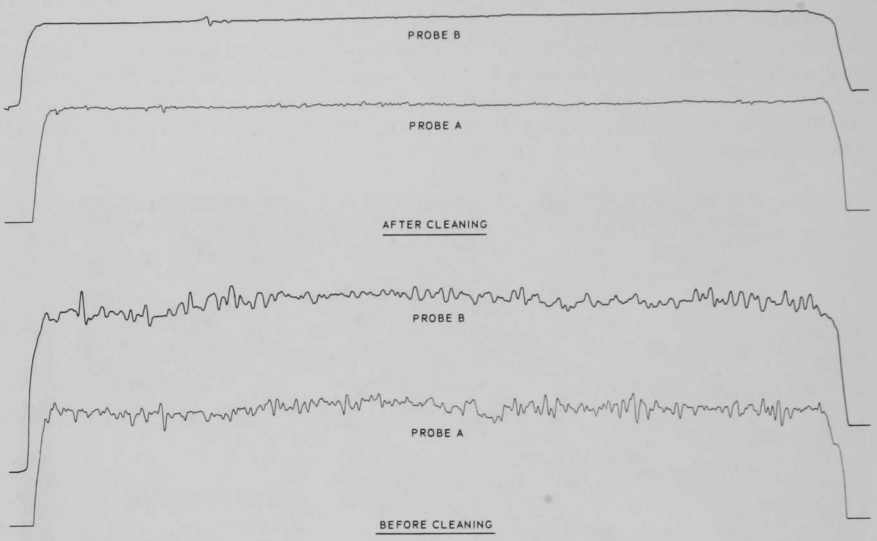

Fig. 49. Comparison of Probe Deflection Traces before and after Cleaning Plate Surfaces in Assembly S/N 452-IB-4

Prior to each subsequent measurement, the channels were cleaned as described above. Gap values were averaged for the individual half-channels. The average of all half-channels was 0.0369 in., with a standard deviation (σ) of 0.878 mil (0.000878 in.). Data for the respective plate assemblies are summarized in Table VIII.

TABLE VIII. Averaged Channel Gaps in Dummy Fuel-plate Assemblies

Assembly No.:	2	3	4	5	6	7
Mean Dimension, in.:	0.0365	0.037	0.037	0.036	0.037	0.037
Avg Dimension, in.:	0.03646	0.03701	0.0369	0.03626	0.03691	0.03735
σ, mil	0.83	0.65	0.53	1.06	0.76	0.93

A plot of the individual channel average dimensions determined with each probe is shown in Fig. 50. The majority of data indicated that channel cleaning was not as complete as desired. Some channels also had longitudinal deviations. A typical example is shown in Fig. 51.

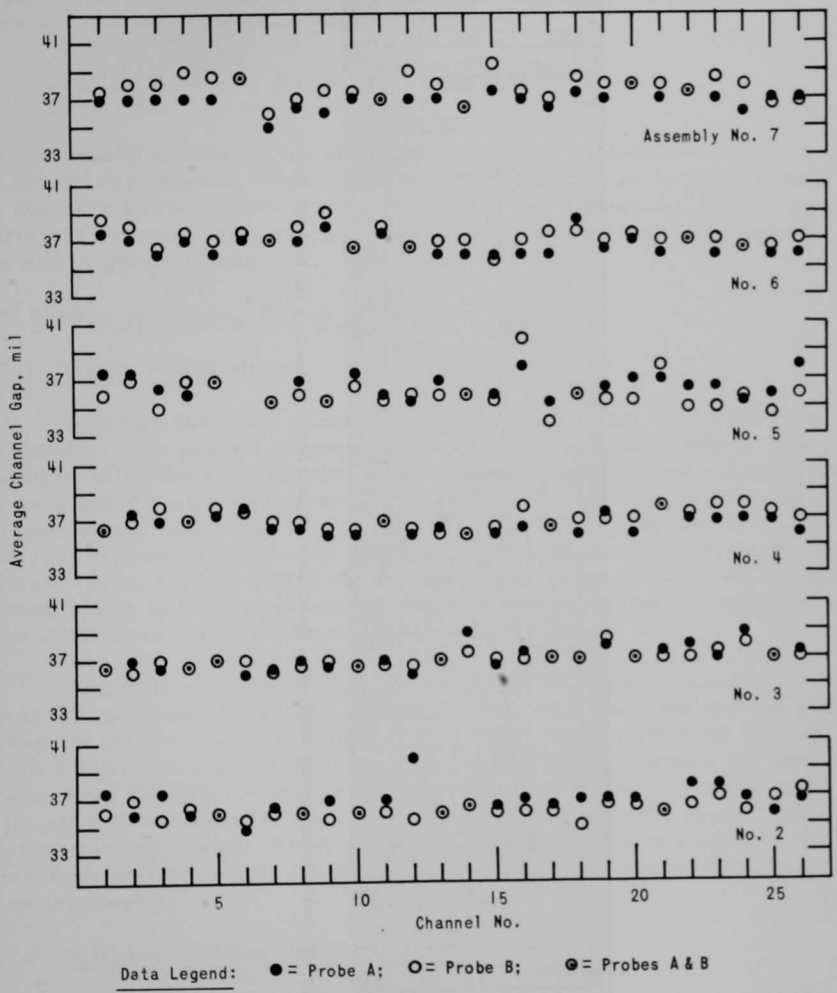

Fig. 50. Average Channel-gap Dimensions of Dummy Fuel-plate Assemblies

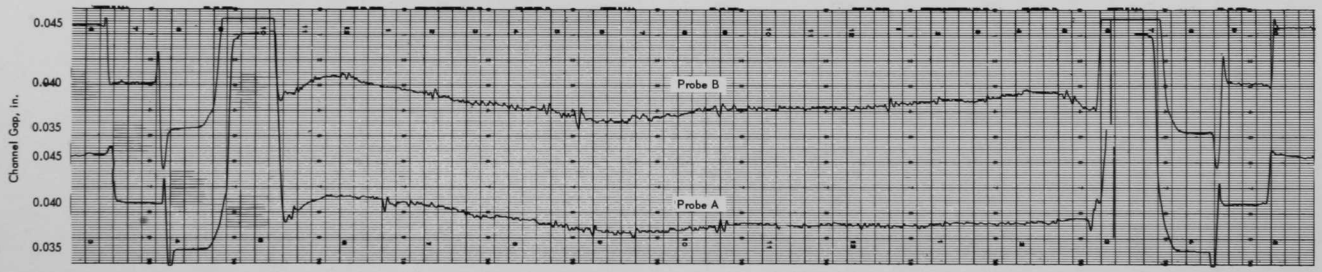

Fig. 51. Probe Traces Showing Longitudinal Variations in Channel No. 25 of Assembly No. S/N 452-IB-4

Measurement of the extended end plates gave a material thickness of 0.041^{+} in. On the assumption that the balance of the plates were similarly oversize (by $+0.001^{+}$ in.), the total for the 27 plates was 1.107^{+} in. Thus the average channel gap should have been:

$$\frac{2.119 - 1.107^{+}}{26} = 0.0389 \text{ in.}$$

The measured average of all channels was 0.0369, or a difference of -0.002 in. per channel. This difference can be attributed to the residue on the plate surfaces, small scratches on the same surfaces, or cumulative errors in the measuring process, i.e., plate thickness and/or errors in the strain-gauge probes.

3.5 Studies of Brazing-fixture Modification

3.5.1 Design Modifications

Although the fixture (see Fig. 43) used in brazing full-scale plate assemblies have proved adequate, it did have certain deficiencies. For example, after the solid closure plate was affixed, visual and manual access to the stacked plates was severely restricted. During brazing, the top and bottom dummy fuel plates tended to bow longitudinally, apparently under stresses generated by thermal gradients within the plate assembly and the fixture. Also, stopoff-coated shims used to prevent brazing of the top and bottom plates to the fixture emitted gases which restricted melting and flow of the braze alloy in the adjacent joints.

The fixture shown in Figs. 52 and 53 was designed to overcome these deficiencies. First, the open-beam structure made the stacked plate assembly visible and accessible for minor adjustments after the two halves of the fixture were assembled. Second, the beams that support the loads transmitted through the spacer wires were made thicker: approximately 1 in. square, compared to the 3/4-in. thickness of the solid closure plates on the previous design. Finally, ceramic beads, ground to a uniform thickness were used to isolate the plates from the fixture, thereby obviating the need for stopoff.

3.5.2 Design-evaluation Tests

Four full-scale dummy fuel-plate assemblies were brazed during the course of these tests. The measured thicknesses of the units (plate-spacer wire) in three of these assemblies are listed in Table IX. Similar data for the fourth assembly (S/N 452-IIA-8-1) are listed in Table V. The latter assembly was used primarily to determine brazing temperature distributions, as described in Sect. 2.8. Data pertinent to the new fixture are included in the appropriate subsections which follow.

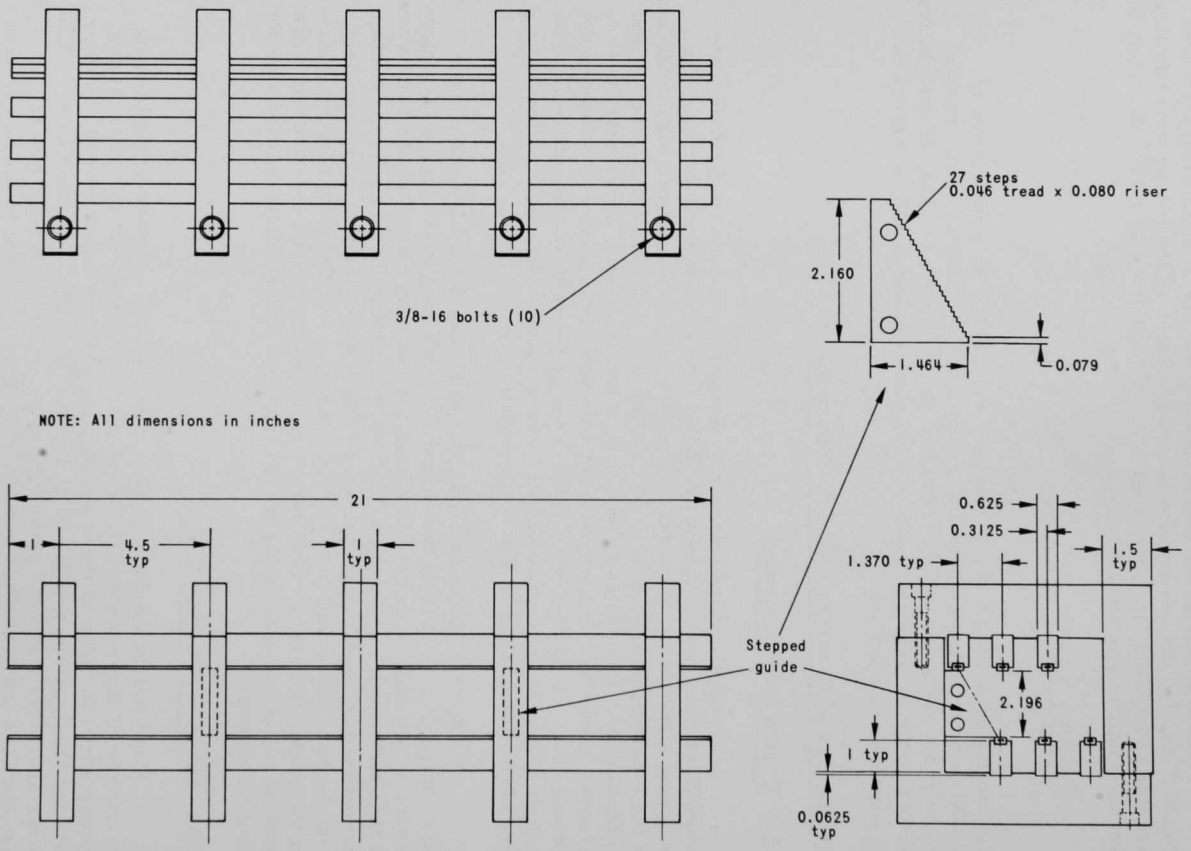

Fig. 52. Design Characteristics of Open-beam Fixture for Brazing Full-scale Dummy Plate Assemblies

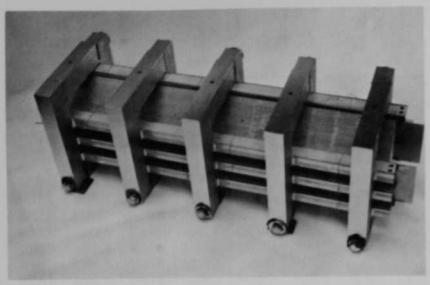

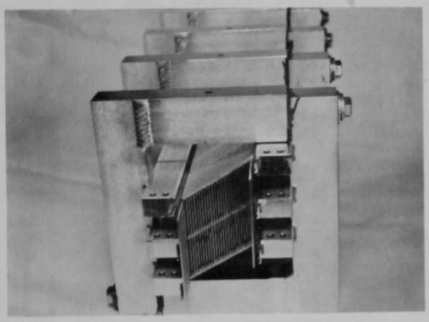

Fig. 53
Views of Open-beam Brazing Fixture with Plate Assembly Installed

TABLE IX. Measured Thicknesses of Plate-spacer Units Brazed in Open-beam Fixture

Plate No.	Wire No. 1*					Wire No. 2*					Wire No. 3*				
	a	b	c	d	e	a	b	c	d	e	a	b	c	d	e
						Assembly No. 452-IIA 7-1									
1	0.0806	0.0803	0.0802	0.0803	0.0805	0.0801	0.0802	0.0800	0.0801	0.0801	0.0801	0.0806	0.0802	0.0806	0.0804
2	0.0806	0.0804	0.0802	0.0808	0.0808	0.0806	0.0803	0.0805	0.0805	0.0808	0.0806	0.0801	0.0804	0.0805	0.0802
3	0.0800	0.0800	0.0800	0.0798	0.0801	0.0808	0.0808	0.0809	0.0810	0.0812	0.0803	0.0802	0.0803	0.0806	0.0805
4	0.0801	0.0800	0.0803	0.0802	0.0805	0.0801	0.0800	0.0801	0.0800	0.0804	0.0812	0.0803	0.0807	0.0808	0.0810
5	0.0801	0.0806	0.0804	0.0805	0.0805	0.0810	0.0808	0.0810	0.0810	0.0809	0.0808	0.0804	0.0804	0.0803	0.0805
6	0.0803	0.0803	0.0800	0.0802	0.0801	0.0799	0.0801	0.0796	0.0793	0.0796	0.0810	0.0804	0.0804	0.0808	0.0808
7	0.0809	0.0806	0.0808	0.0802	0.0804	0.0807	0.0802	0.0807	0.0803	0.0807	0.0808	0.0806	0.0806	0.0804	0.0805
8	0.0802	0.0807	0.0807	0.0803	0.0800	0.0811	0.0810	0.0811	0.0811	0.0812	0.0806	0.0808	0.0806	0.0807	0.0805
9	0.0802	0.0809	0.0802	0.0806	0.0806	0.0810	0.0811	0.0811	0.0811	0.0810	0.0804	0.0806	0.0803	0.0806	0.0807
10	0.0810	0.0809	0.0809	0.0805	0.0808	0.0806	0.0803	0.0803	0.0804	0.0806	0.0808	0.0808	0.0806	0.0808	0.0809
11	0.0804	0.0802	0.0806	0.0802	0.0803	0.0797	0.0799	0.0800	0.0800	0.0801	0.0802	0.0802	0.0801	0.0802	0.0800
12	0.0802	0.0800	0.0802	0.0801	0.0805	0.0802	0.0800	0.0802	0.0801	0.0804	0.0802	0.0805	0.0801	0.0804	0.0812
13	0.0802	0.0801	0.0796	0.0802	0.0800	0.0800	0.0800	0.0801	0.0802	0.0802	0.0802	0.0803	0.0800	0.0802	0.0802
14	0.0806	0.0802	0.0801	0.0800	0.0808	0.0802	0.0800	0.0800	0.0801	0.0801	0.0805	0.0800	0.0802	0.0802	0.0808
15	0.0806	0.0808	0.0803	0.0809	0.0805	0.0806	0.0801	0.0802	0.0803	0.0800	0.0803	0.0803	0.0801	0.0802	0.0801
16	0.0802	0.0801	0.0801	0.0801	0.0800	0.0798	0.0800	0.0798	0.0798	0.0798	0.0800	0.0803	0.0801	0.0800	0.0802
17	0.0802	0.0803	0.0806	0.0803	0.0805	0.0803	0.0802	0.0802	0.0801	0.0801	0.0807	0.0805	0.0801	0.0807	0.0803
18	0.0802	0.0802	0.0801	0.0801	0.0802	0.0798	0.0798	0.0799	0.0800	0.0800	0.0802	0.0801	0.0801	0.0805	0.0807
19	0.1196	0.1198	0.1199	0.1198	0.1200	0.1191	0.1193	0.1192	0.1195	0.1193	0.1196	0.1190	0.1188	0.1192	0.1192
20	0.0802	0.0803	0.0802	0.0800	0.0801	0.0802	0.0803	0.0803	0.0802	0.0802	0.0804	0.0804	0.0801	0.0805	0.0803
21	0.0808	0.0808	0.0808	0.0807	0.0808	0.0802	0.0802	0.0802	0.0802	0.0802	0.0803	0.0802	0.0801	0.0807	0.0809
22	0.0797	0.0798	0.0797	0.0798	0.0797	0.0789	0.0789	0.0786	0.0788	0.0790	0.0788	0.0790	0.0788	0.0783	0.0790
23	0.0790	0.0790	0.0789	0.0789	0.0789	0.0788	0.0786	0.0787	0.0787	0.0788	0.0788	0.0789	0.0790	0.0788	0.0791
24	0.0790	0.0786	0.0786	0.0788	0.0787	0.0789	0.0785	0.0786	0.0787	0.0788	0.0792	0.0788	0.0788	0.0786	0.0791
25	0.0792	0.0792	0.0788	0.0788	0.0793	0.0783	0.0785	0.0786	0.0787	0.0789	0.0790	0.0788	0.0790	0.0791	0.0786
26	0.0789	0.0789	0.0788	0.0788	0.0783	0.0788	0.0788	0.0785	0.0787	0.0788	0.0788	0.0788	0.0789	0.0786	0.0789
27	0.0793	0.0789	0.0789	0.0788	0.0790	0.0791	0.0786	0.0787	0.0790	0.0792	0.0791	0.0788	0.0790	0.0791	0.0787
Total:	2.2018	2.2019	2.199	2.197	2.2019	2.1988	2.1965	2.1979	2.1977	2.2004	2.2029	2.1997	2.1976	2.2014	2.2030

TABLE IX (Contd.)

Plate No.	Wire No. 1*					Wire No. 2*					Wire No. 3*				
	a	b	c	d	e	a	b	c	d	e	a	b	c	d	e
						Assembly No. 452-IIA 7-2									
1	0.0786	0.0790	0.0786	0.0792	0.0800	0.0789	0.0786	0.0788	0.0789	0.0789	0.0790	0.0786	0.0790	0.0784	0.0784
2	0.0782	0.0785	0.0785	0.0784	0.0790	0.0790	0.0789	0.0790	0.0788	0.0789	0.0780	0.0780	0.0780	0.0781	0.0780
3	0.0792	0.0789	0.0790	0.0788	0.0790	0.0786	0.0786	0.0790	0.0789	0.0790	0.0798	0.0795	0.0791	0.0798	0.0792
4	0.0808	0.0800	0.0806	0.0807	0.0805	0.0801	0.0805	0.0801	0.0809	0.0809	0.0809	0.0805	0.0802	0.0809	0.0802
5	0.0800	0.0801	0.0800	0.0807	0.0800	0.0795	0.0795	0.0795	0.0795	0.0808	0.0804	0.0804	0.0806	0.0801	0.0805
6	0.0809	0.0805	0.0805	0.0809	0.0806	0.0801	0.0801	0.0805	0.0795	0.0801	0.0809	0.0807	0.0812	0.0805	0.0809
7	0.0810	0.0802	0.0809	0.0810	0.0808	0.0801	0.0800	0.0799	0.0799	0.0800	0.0807	0.0802	0.0805	0.0802	0.0806
8	0.0809	0.0805	0.0809	0.0810	0.0809	0.0800	0.0800	0.0800	0.0800	0.0800	0.0805	0.0805	0.0806	0.0801	0.0806
9	0.0801	0.0801	0.0808	0.0800	0.0802	0.0798	0.0800	0.0799	0.0803	0.0805	0.0800	0.0800	0.0800	0.0801	0.0801
10	0.0803	0.0803	0.0803	0.0803	0.0804	0.0800	0.0800	0.0800	0.0801	0.0805	0.0803	0.0801	0.0808	0.0805	0.0803
11	0.0801	0.0799	0.0801	0.0800	0.0790	0.0797	0.0797	0.0799	0.0798	0.0798	0.0803	0.0800	0.0805	0.0803	0.0802
12	0.0807	0.0802	0.0805	0.0802	0.0801	0.0800	0.0800	0.0802	0.0802	0.0800	0.0808	0.0807	0.0807	0.0808	0.0803
13	0.0805	0.0804	0.0804	0.0806	0.0802	0.0806	0.0807	0.0807	0.0802	0.0803	0.0809	0.0809	0.0808	0.0808	0.0807
14	0.0805	0.0805	0.0807	0.0805	0.0806	0.0806	0.0801	0.0801	0.0801	0.0802	0.0800	0.0808	0.0807	0.0807	0.0807
15	0.0809	0.0808	0.0808	0.0801	0.0808	0.0808	0.0805	0.0805	0.0805	0.0804	0.0807	0.0806	0.0806	0.0805	0.0806
16	0.0804	0.0798	0.0800	0.0802	0.0800	0.0800	0.0799	0.0797	0.0799	0.0802	0.0807	0.0808	0.0802	0.0807	0.0800
17	0.0799	0.0799	0.0797	0.0796	0.0797	0.0793	0.0788	0.0788	0.0788	0.0788	0.0789	0.0792	0.0788	0.0793	0.0791
18	0.0789	0.0792	0.0792	0.0787	0.0792	0.0791	0.0789	0.0788	0.0792	0.0793	0.0791	0.0798	0.0797	0.0792	0.0797
19	0.0805	0.0802	0.0799	0.0802	0.0802	0.0805	0.0810	0.0809	0.0806	0.0806	0.0802	0.0808	0.0808	0.0803	0.0807
20	0.0802	0.0802	0.0800	0.0803	0.0802	0.0802	0.0805	0.0801	0.0806	0.0805	0.0805	0.0808	0.0804	0.0805	0.0807
21	0.0810	0.0804	0.0804	0.0804	0.0805	0.0795	0.0798	0.0796	0.0798	0.0799	0.0812	0.0803	0.0801	0.0800	0.0802
22	0.0799	0.0802	0.0802	0.0799	0.0801	0.0800	0.0798	0.0802	0.0811	0.0800	0.0800	0.0799	0.0803	0.0800	0.0802
23	0.0812	0.0806	0.0809	0.0809	0.0808	0.0801	0.0806	0.0802	0.0805	0.0805	0.0801	0.0805	0.0803	0.0805	0.0809
24	0.0806	0.0806	0.0800	0.0807	0.0800	0.0801	0.0802	0.0800	0.0800	0.0800	0.0801	0.0801	0.0799	0.0801	0.0799
25	0.0801	0.0800	0.0799	0.0802	0.0799	0.0799	0.0800	0.0800	0.0799	0.0800	0.0802	0.0800	0.0804	0.0806	0.0800
26	0.0806	0.0802	0.0805	0.0806	0.0808	0.0800	0.0798	0.0799	0.0798	0.0800	0.0802	0.0808	0.0806	0.0805	0.0809
27	0.1191	0.1193	0.1196	0.1191	0.1196	0.1190	0.1188	0.1180	0.1177	0.1180	0.1192	0.1199	0.1191	0.1191	0.1192
Total:	2.205	2.2007	2.2029	2.2032	2.2037	2.1955	2.1953	2.1943	2.1955	2.1981	2.2036	2.2044	2.2039	2.2026	2.2028
						Assembly No. 452-IIA 7-3									
1	0.0808	0.0808	0.0808	0.0804	0.0808	0.0810	0.0808	0.0808	0.0807	0.0810	0.0812	0.0809	0.0808	0.0810	0.0808
2	0.0795	0.0800	0.0799	0.0799	0.0799	0.0800	0.0798	0.0798	0.0797	0.0794	0.0794	0.0798	0.0795	0.0798	0.0798
3	0.0805	0.0805	0.0808	0.0805	0.0805	0.0807	0.0808	0.0805	0.0807	0.0805	0.0803	0.0801	0.0804	0.0804	0.0800
4	0.0809	0.0805	0.0805	0.0802	0.0802	0.0802	0.0802	0.0800	0.0799	0.0800	0.0803	0.0803	0.0802	0.0803	0.0806
5	0.0809	0.0810	0.0808	0.0808	0.0805	0.0799	0.0799	0.0800	0.0800	0.0798	0.0802	0.0802	0.0800	0.0803	0.0801
6	0.0809	0.0809	0.0804	0.0805	0.0809	0.0800	0.0800	0.0798	0.0798	0.0800	0.0806	0.0806	0.0802	0.0808	0.0805
7	0.0789	0.0791	0.0792	0.0789	0.0789	0.0785	0.0788	0.0788	0.0789	0.0789	0.0788	0.0785	0.0785	0.0785	0.0788
8	0.0788	0.0788	0.0788	0.0788	0.0789	0.0785	0.0785	0.0785	0.0783	0.0782	0.0789	0.0789	0.0789	0.0789	0.0789
9	0.0789	0.0790	0.0795	0.0790	0.0793	0.0790	0.0790	0.0790	0.0790	0.0789	0.0795	0.0795	0.0792	0.0791	0.0792
10	0.0789	0.0790	0.0789	0.0791	0.0791	0.0790	0.0789	0.0785	0.0785	0.0786	0.0790	0.0790	0.0790	0.0790	0.0790
11	0.0788	0.0788	0.0788	0.0788	0.0788	0.0785	0.0783	0.0785	0.0785	0.0785	0.0788	0.0785	0.0788	0.0788	0.0788
12	0.0799	0.0800	0.0799	0.0800	0.0799	0.0799	0.0798	0.0798	0.0795	0.0799	0.0801	0.0800	0.0800	0.0799	0.0801
13	0.0800	0.0799	0.0801	0.0800	0.0801	0.0795	0.0800	0.0798	0.0797	0.0795	0.0803	0.0802	0.0801	0.0800	0.0803
14	0.0810	0.0808	0.0809	0.0803	0.0809	0.0805	0.0805	0.0802	0.0802	0.0802	0.0810	0.0808	0.0808	0.0811	0.0809
15	0.0809	0.0809	0.0812	0.0809	0.0810	0.0808	0.0803	0.0805	0.0809	0.0807	0.0809	0.0809	0.0810	0.0809	0.0809
16	0.0809	0.0807	0.0808	0.0808	0.0808	0.0807	0.0803	0.0805	0.0809	0.0809	0.0812	0.0808	0.0806	0.0810	0.0811
17	0.0808	0.0807	0.0808	0.0808	0.0808	0.0808	0.0808	0.0805	0.0805	0.0806	0.0805	0.0805	0.0803	0.0807	0.0808
18	0.0809	0.0807	0.0807	0.0811	0.0809	0.0805	0.0802	0.0805	0.0803	0.0803	0.0808	0.0809	0.0808	0.0809	0.0808
19	0.0795	0.0788	0.0789	0.0790	0.0789	0.0793	0.0795	0.0792	0.0792	0.0794	0.0792	0.0792	0.0794	0.0795	0.0795
20	0.0795	0.0795	0.0797	0.0797	0.0798	0.0798	0.0796	0.0798	0.0797	0.0794	0.0795	0.0799	0.0797	0.0797	0.0798
21	0.0798	0.0798	0.0798	0.0798	0.0795	0.0795	0.0796	0.0798	0.0797	0.0798	0.0797	0.0798	0.0797	0.0798	0.0799
22	0.0795	0.0795	0.0795	0.0792	0.0792	0.0798	0.0798	0.0798	0.0798	0.0795	0.0799	0.0798	0.0798	0.0799	0.0798
23	0.0800	0.0802	0.0802	0.0803	0.0802	0.0808	0.0802	0.0805	0.0802	0.0805	0.0808	0.0802	0.0805	0.0805	0.0802
24	0.0808	0.0801	0.0808	0.0805	0.0802	0.0808	0.0802	0.0802	0.0805	0.0802	0.0805	0.0807	0.0803	0.0807	0.0805
25	0.0807	0.0809	0.0805	0.0808	0.0807	0.0810	0.0808	0.0812	0.0812	0.0807	0.0802	0.0808	0.0808	0.0807	0.0805
26	0.0802	0.0808	0.0803	0.0805	0.0802	0.0801	0.0802	0.0802	0.0802	0.0805	0.0803	0.0807	0.0808	0.0804	0.0810
27	0.1208	0.1202	0.1203	0.1204	0.1199	0.1180	0.1180	0.1177	0.1188	0.1193	0.1201	0.1194	0.1198	0.1197	0.1205
Total:	2.2030	2.2017	2.2009	2.2010	2.1999	2.1971	2.1948	2.1944	2.1953	2.1952	2.2020	2.2009	2.1999	2.2023	2.2030

*See sketch at end of Table V.

3.5.2.1 Prebraze Procedures

Prior to each test, the brazing fixture was completely assembled without the plate assembly. Spacings between the ground ceramic beads were measured at several locations along the longitudinal beams with a set of adjustable parallels and feeler gauges. These spacings were then adjusted to a constant value by inserting shims between the two halves of the fixture where the frames are bolted together.

For Assembly No. 7-1, the spacing was adjusted to 2.200 in., which is the final overall stack height specified for the plate assembly. The spacing for the other three assemblies was adjusted to 2.196 in.

The basic steps for each plate assembly consisted of spot welding the knurled spacer wires to the plates, applying GE J8100 braze alloy powder with grooved plastic loading bars, and adding the acrylic binder. Nicrobraz Green Stopoff was used on Assembly No. 7-1, and aluminum scribing on the others. Except for Assembly No. 7-3, the scribing was done after the braze alloy powder and binder were applied.

The surfaces of plates in the six production assemblies that were brazed (see Sect. 3.4) had exhibited a rough condition caused by adherent particles approximately 0.001 to 0.002 in. high. These particles were believed to be braze alloy powder that was not completely cleaned from the plate, or alloy particles that were loosened and scattered during assembly. Therefore, the plates of Assembly No. 7-2 were vacuum cleaned immediately before they were stacked in the brazing fixture. After installation in the fixture, the plate surfaces were again cleaned by drawing lint-free paper through the channels. Assemblies No. 7-3 and 8-1 were also vacuum cleaned, but the swabbing after assembly was eliminated.

Except for Assembly No. 7-2, the edges of the plates were supported on the stepped wedges used with the old fixture. Rectangular Al_2O_3 ceramic inserts were used on each step to prevent brazing of the assembly to the wedges. For Assembly No. 7-2, the stepped wedges were replaced with straight-sided, 60° wedges. A flat ceramic bar was laid on the edge of each wedge to provide a nonwettable support for the plate edges. With this method of edge support and the 0.080-in.-wide edge spacer wires, the weight of each plate was carried essentially by the spot welds in the lower edge spacer wire.

3.5.2.2 Braze Cycle

Each fixtured assembly was heated to and held in a dry hydrogen atmosphere at 800-900°F until the temperature equalized within the assembly. At that time, the temperature was increased at 200°F/hr to 1950°F, held for 1/2 hr at temperature, and then heated to and held for 2 hr at 2100-2120°F. Initial cooling was accomplished by decreasing the furnace temperature at

a rate of 100°F/hr to 1800°F. The furnace power was then turned off and the assembly allowed to cool naturally to 800°F. At that point, the furnace was removed to expose the retort to ambient air. When the plate-assembly temperature had cooled to 200-250°F, the retort was purged of hydrogen with exothermic gas or nitrogen, and opened.

3.5.2.3 Results

Assembly No. 7-1, with the fixture spacing adjusted to 2.200 in., was 0.003-0.004 in. oversize according to measurements made across the outermost plates. Overall measurements, including spacer wires, were precluded by the uneven flow of braze alloy onto the outer surface of the wires. The excess height of the brazed stack could be accounted for by the difference in thermal expansion between the ceramic beads and an equal thickness of stainless steel. By comparison, the height of the three assemblies brazed in the fixtures adjusted to 2.196 in. was within ±0.001 in. of the specified 2.200 in. after brazing.

Because of the 60° offset in the plates, there was only one narrow strip along which micrometer measurements could be made across identical points on the top and bottom plates. The plate-to-plate dimensions measured along this strip at 5-in. intervals (overall stack height less the outer 0.040-in.-thick spacers) are listed below.

	Plate-to-plate Dimension, in.				
Assembly	a	b	c	d	e
S/N 452-IIA 7-1	2.123	2.124	2.125	2.124	2.123
S/N 452-IIA 7-2	2.119	2.120	2.121	2.120	2.119
S/N 452-IIA 7-3	2.120	2.119	2.121	2.120	2.120
S/N 452-IIA 8-1	2.119	2.121	2.119	2.120	2.120

Assembly No. 7-1 was twisted to the extent that a 0.015-in.-thick shim could be inserted under one corner when the assembly was placed on a flat surface. Several plates in Assembly No. 7-2 had shifted during brazing because of spot-weld failures and consequent bending of the spacer wires. The other two assemblies were flat and conformed to the 60° angle.

The surfaces of all plates that had been vacuumed appeared clean and smooth. As shown in Fig. 54, scribing of the plates before application of the braze alloy and binder resulted in more effective control of the alloy flow.

The fixture maintained its original dimensions through the four brazing heats in which it was used. Some of the ceramic beads cracked during each heat and were replaced. The ceramic inserts for the step wedges also were susceptible to chipping and cracking, and some had to be replaced after each heat. It was observed that the inserts in which

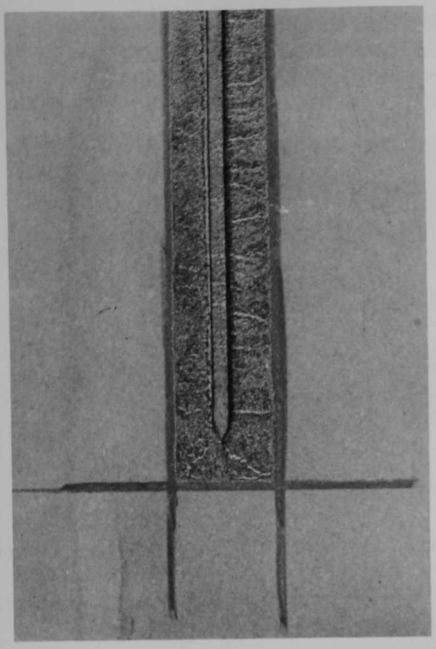

Fig. 54. End of Center Spacer in Assembly S/N 452-IIA-7-3 Showing Effectiveness of Aluminum Scribing in Confining Flow of Braze Alloy. Scribing was performed before alloy and binder were applied.

alloy penetration was most prevalent were those that fit deeply into the corners formed by the offset in adjacent plates and spacers. The useful life of these inserts could probably be extended by adjusting the position of the stepped wedges to keep the inserts away from the corners.

3.6 Irradiation Tests

Sixteen shear-test specimens and seven 3-plate microassemblies were fabricated for irradiation tests in the Engineering Test Reactor. Thirteen of the shear-test specimens were brazed with GE J8100 alloy and three with Nicrobraz 50 alloy. Five of the microassemblies were fabricated with solid, Type 347 stainless steel dummy fuel plates and two with enriched UO_2 fuel plates. Special braze fixtures also were fabricated, and procedures were adapted from the reference program process to assure a high-quality end product.

To yield the most meaningful test data, the fabrication procedure for the microassemblies followed as close as possible that employed for the full-scale subassemblies. The principal change was in the fixturing. Shear-test specimens were simply laid flat on a ceramic plate during brazing. A new stainless steel brazing fixture was designed for the microassemblies.

3.6.1 Preparation of Specimens

3.6.1.1 Shear-test Specimens

After irradiation, these specimens were to be cut into shorter lengths for test purposes. Sufficient unirradiated specimens were also prepared for use as controls.

As shown in Fig. 55, each specimen consisted of a single, stainless steel spacer wire (of 0.040-in. square cross section) brazed to a 5.750 x 1.250 x 0.040-in. plate. Each plate was sheared slightly oversize from 19-gauge sheets of annealed Type 347 stainless steel having a 2D surface

finish, and then machined to final length and width. Each spacer wire was knurled to produce transverse grooves approximately 0.001 in. deep at 1/64-in. intervals along the surfaces to be brazed, and then cut to length and tapered at each end.

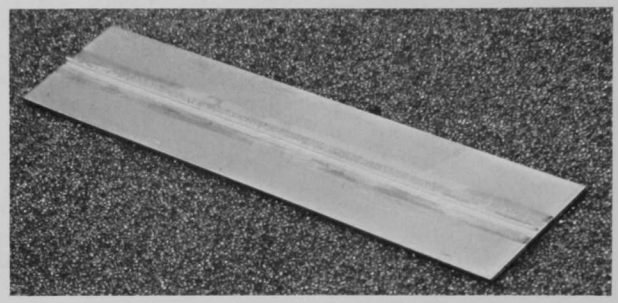

Fig. 55. Typical Specimen for Studying Effect of Radiation on Shear Strength of Brazed Joints

Each wire was spot welded along the center of a plate using a stored-energy welder and tweezer electrodes. The welding fixture consisted of a stainless steel straight edge with stops at the appropriate distance from the edge. In operation, the edge of the plate was placed against the stops and the spacer wire was laid along the straight edge. Spot welds were made at 1/2-in. intervals along the spacer wire, using 40 Wsec welder power. Strips of OFHC copper (0.040 in. thick) were placed between the electrodes and the stainless steel to prevent the surfaces from being marred.

GE J8100 braze alloy powder was applied with a plastic loading bar having a 0.030 x 0.017-in. groove. Nicrobraz cement was used to hold the powder in place. Finally, Nicrobraz Green Stopoff was brushed on the plate surface parallel to and about 1/8 in. from each side of the spacer wire.

The assembled specimens were laid on flat ceramic plates and exposed to the brazing cycle in a dry hydrogen atmosphere (-80°F dewpoint at the retort inlet). This cycle was essentially the same as used previously except for slightly faster heating rates. Specifically, the specimens were heated to 2135-2145°F, held for 2 hr at temperature, and then furnace cooled to below 800°F. The cooling cycle, including furnace cooling, required about 12 hr.

All units prepared with GE J8100 alloy were brazed in two furnace heats of 7 and 6 specimens, respectively. After brazing, one specimen from each heat was selected at random and sectioned for metallographic examination. A transverse cross section and a longitudinal section (~3/4 in. long) from each specimen were examined. A peel test was performed on the remaining portion of each specimen to determine bond

continuity. These investigations indicated complete bonding in the specimens from both heats. Figure 56 shows typical transverse and longitudinal sections of the brazed joints that were affected. Braze alloy flow across the plate surfaces was effectively retarded by the stopoff.

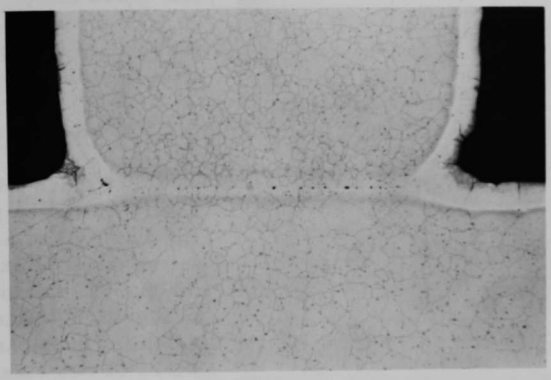

X75

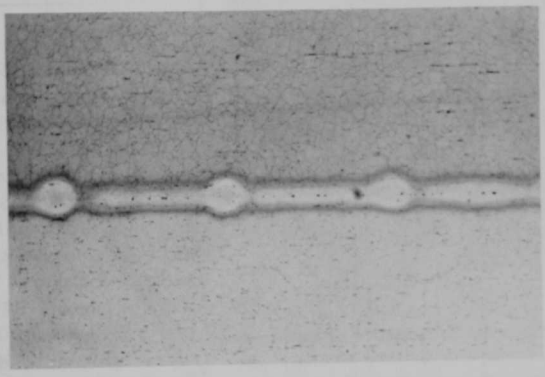

X75

Fig. 56. Transverse (Top) and Longitudinal Cross Sections of Joint in Shear-test Specimen Brazed with GE J8100 Alloy. Electroetched with 50% HNO_3.

Except for the brazing cycle, the same assembly and furnace-loading procedures were employed for the three specimens brazed with the lower melting point Nicrobraz 50 alloy. In this instance, the specimens were heated to 1850°F in a dry, hydrogen atmosphere, held at temperature for 30 min, and then retort cooled.

One specimen was evaluated by metallography and peel test, and the other two by nondestructive tests. These tests revealed sound and continuous

brazed joints. A typical transverse cross section is shown in Fig. 57. Although the test was only qualitative, the peel strength of the Nicrobraz 50 joint was significantly less than the strength of joints brazed with GE J8100 alloy. The grain size in both the spacer and plate was much finer in the specimen brazed with Nicrobraz 50 alloy.

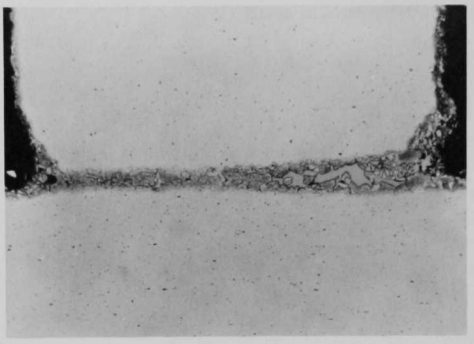

X75

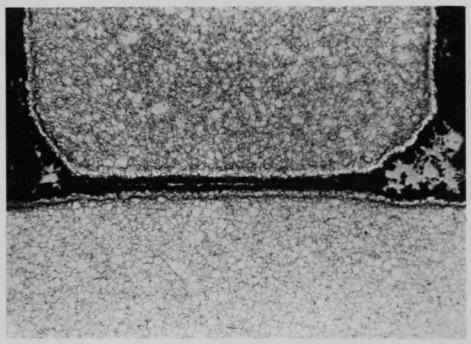

X75

Fig. 57. Typical Transverse Cross Section of Shear-test Specimen Brazed with Nicrobraz 50 Alloy. The etching procedure used to reveal the grain size led to severe attack of the brazed joint.

3.6.1.2 Microassemblies

Figure 58 shows the configuration employed for both the dummy and active fuel microassemblies. Each plate measured (nominally) 5.750 in. in length, 1.250 in. in width, and 0.040 in. in thickness. Spacer wires of two sizes were used.

Dummy Microassemblies

As for the shear-test specimens, the dummy fuel plates were sheared slightly oversize from 19-gauge stainless steel sheets and then machined to size. Spacer wires were knurled, cut to length, tapered at the ends, and then spot welded to the plates using the same welding equipment and conditions. With reference to Fig. 52, two 0.040-in.-square and two 0.040 x 0.100-in. spacers were spot welded to the top plate; two 0.040 x 0.100-in. spacers to the center plate; and two 0.040-in.-square spacers to the bottom plate. The spacer near the plate edge was attached first. Then a set of adjustable parallels was used to locate the second spacer at the desired channel width.

GE J8100 braze alloy powder was applied with grooved plastic loading bars. The bar used for the smaller spacers on the top and bottom plates had a 0.030 x 0.017-in. groove, and the one for the center plate a 0.030 x 0.035-in. groove. The powder was held in place by Nicrobraz acrylic cement applied with an eye dropper. Finally, Nicrobraz Green Stopoff was applied on the plate surfaces 1/8 in. distant from and parallel

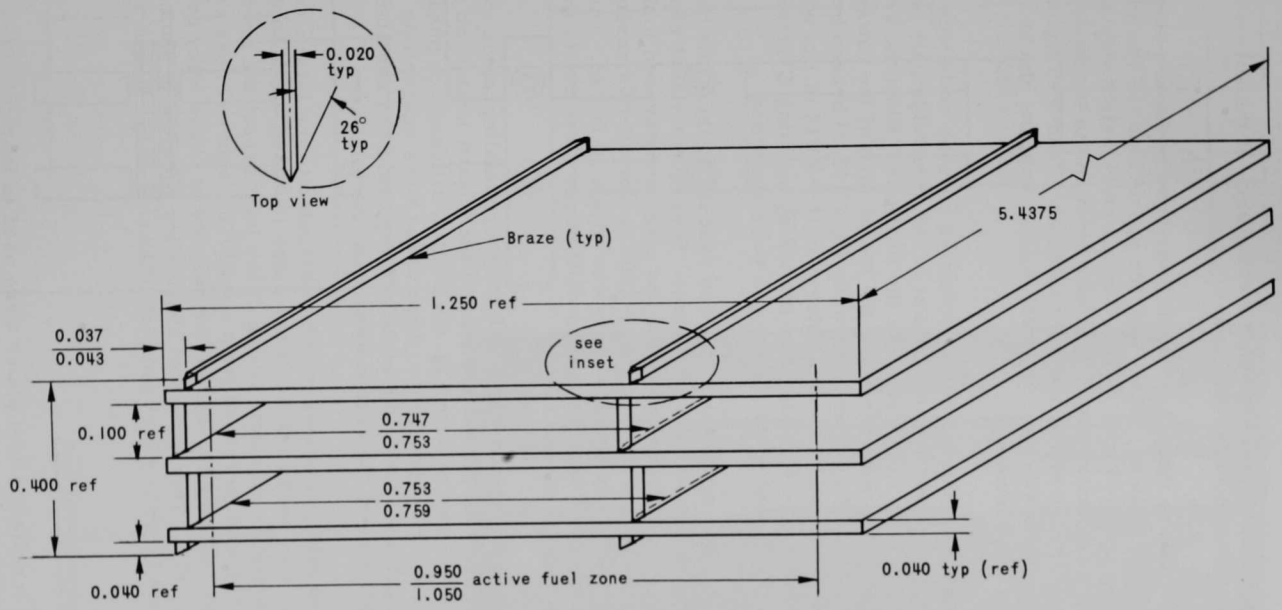

NOTE: All dimensions in inches

Fig. 58. Configuration of Dummy and Active Fuel-plate Microassemblies

to both sides of the center spacers and matching area of the adjacent plate, but only on the inside of the edge spacers.

Three plates were then assembled in the brazing fixture shown in Fig. 59. The parallel rails in contact with the spacers on the top and bottom plates were plasma-sprayed with Al_2O_3. Overall stack height was established by inserting 0.400-in.-thick measuring blocks between the top adjustable rails of the fixture at each end of the microassembly, and then tightening the set screws until the rails were in equal contact with the blocks. At that time, the blocks were removed.

One problem encountered during fixturing of these units was caused by lack of restraint upon vertical movement of the adjustable pair of rails. The bottom surface of the rails rested on the U-frame. When the set screws were tightened, there was a tendency for the inside face of the rails to rise and lift the adjacent fuel plate. One assembly (S/N 433-2) brazed before this problem was recognized showed a lateral shift (~0.012 in.) of one plate. This was corrected in the remaining assemblies by applying C-clamps to restrain vertical movement while the screws were tightened.

Each fuel dummy microassembly was exposed to the same brazing cycle employed for the shear-test specimens. Subsequent visual examination at up to 30X magnification revealed sound and continuous brazed joints. Overall stack height ranged from 0.400 to 0.403 in. for all five assemblies; end-to-end variation for any one assembly was within ±0.001 in. The only notable dimensional defect was the lateral shift of one plate due to the fixturing problem discussed above.

The visual observations were confirmed by metallographic examination of transverse and longitudinal sections of the brazed joints: no voids were found. However, as shown in Fig. 60, brittle, silicon-rich phases were observed in some of the larger fillets; these areas were susceptible to microcracks. In previous tests, the same brazing cycle had resulted in more complete diffusion of the silicon away from the joint area.

These residual hard phases may be attributed to the larger amount of braze alloy that was used because of the wider (0.100 in. versus 0.040 in.) spacer wires. To ensure complete filling of the joint areas, the groove of the alloy loading bar was increased from a 0.030-in.-square cross section to 0.030 x 0.035 in., thereby increasing the quantity of braze alloy by slightly more than 15%. This excess of braze alloy resulted in some fillets that were too large to effect complete diffusion of the silicon formed in certain areas.

Active Microassemblies

Six AARR irradiation-test plates were used to fabricate the two active microassemblies. As shown in Fig. 61, each plate had an active

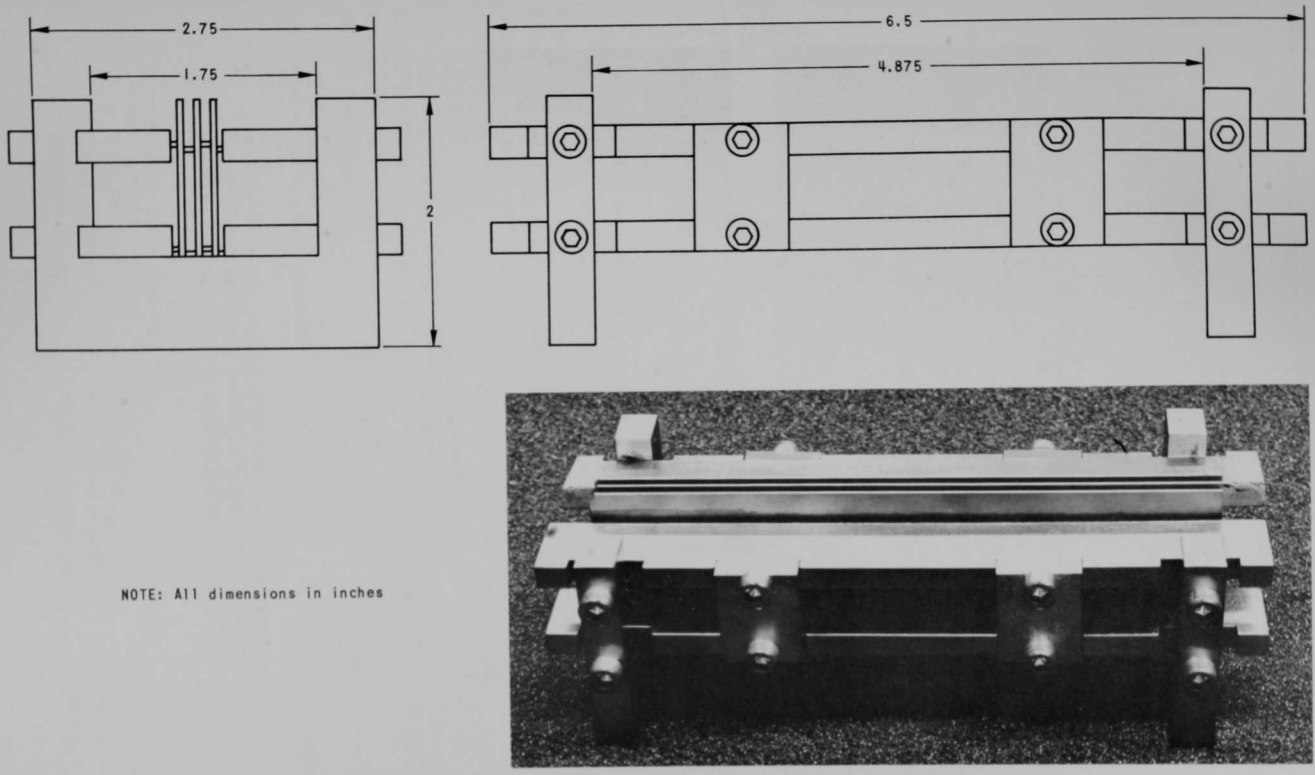

Fig. 59. Brazing Fixture Used for Dummy Microassemblies

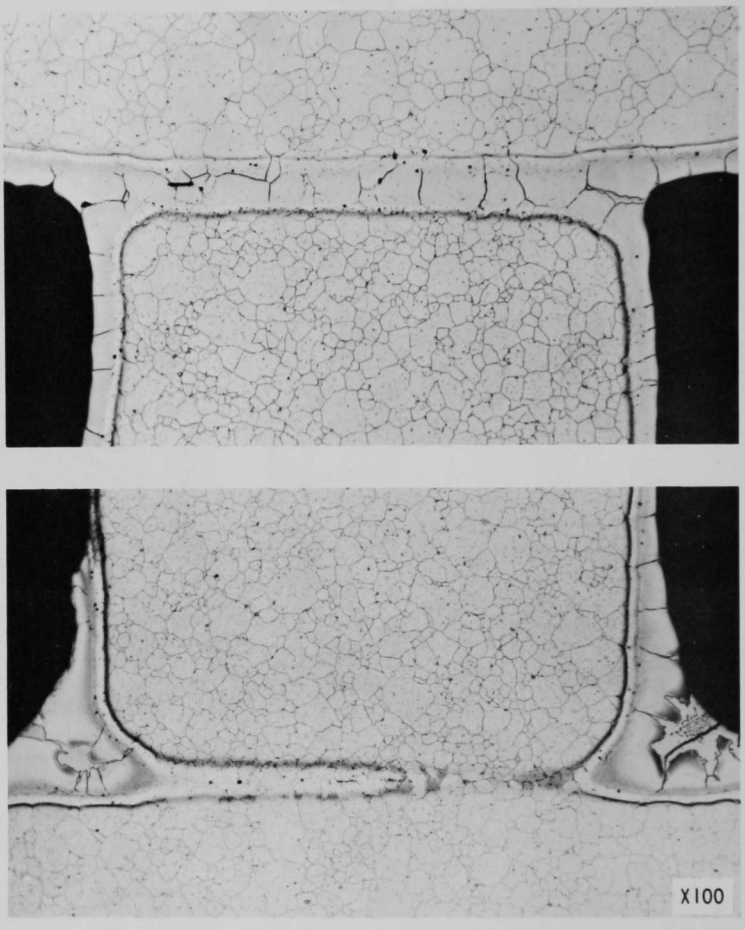

Fig. 60. Transverse Cross Section of Brazed Joint of Dummy Microassembly, Showing Microcracking in Residual Hard Phase in the Fillets. Electroetched with 50% HNO_3.

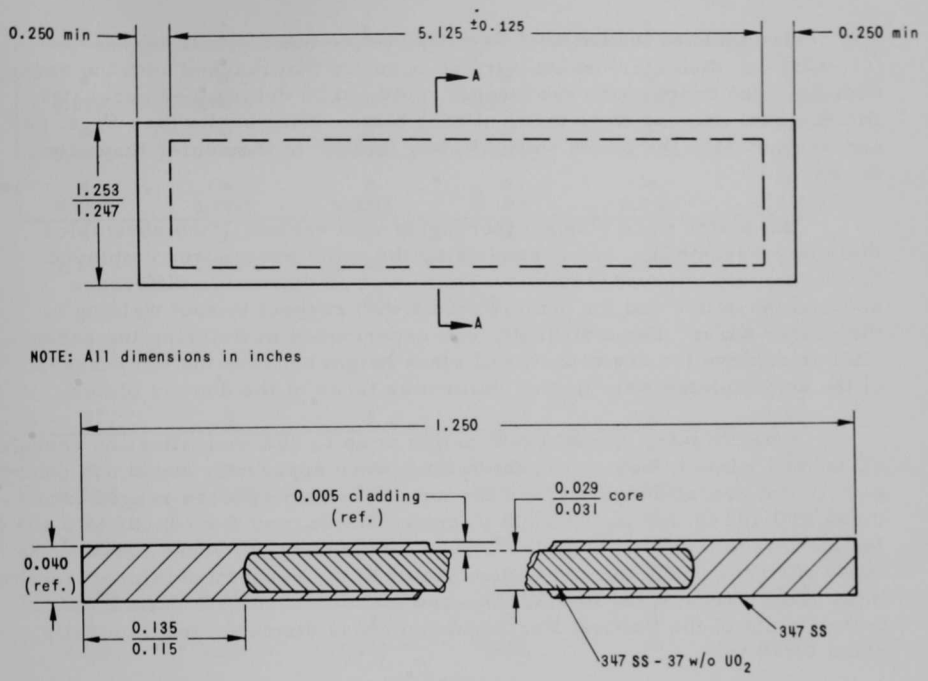

Fig. 61. Composition and Dimensional Characteristics of AARR Irradiation-test Plate

fuel region consisting of 37 w/o UO_2 (fully enriched) in a Type 347 stainless steel matrix clad on both sides with 0.005 in. of Type 347 stainless steel. The nominal overall dimensions of each plate were 5.750 in. in length, 1.250 in. in width, and 0.040 in. in thickness.

Preparatory to assembly, each plate was identified with a serial number and then assigned to either the ETR Critical Facility Sample or the ETR-G12 Irradiation Test Sample. In addition, each plate was positioned within the assembly according to the U^{235} loading, as listed below.

Critical Facility Sample	Plate No.	U^{235} Loading, gm
Top Plate	S/N 18-A15-918	6.79
Center Plate	S/N 20-A15-920	6.81
Bottom Plate	S/N 51-A16-951	5.88
Irradiation Test Sample		
Top Plate	S/N 34-A15-934	6.75
Center Plate	S/N 32-A15-932	6.76
Bottom Plate	S/N 54-A16-954	5.85

The center plate of the Critical Facility Sample had a small depression (of ~1/32-in. diameter) on the surface opposite that marked with the serial number. The depth of the depression could not be determined accurately. Dimensional surveys were made of each plate. The results (see Figs. 62 and 63) indicated the plates were slightly thicker in the center than along the edges.

All plates were cleaned thoroughly with acetone, then assembled into microassemblies, and brazed using the same procedures employed for the dummy microassemblies. There was no detectable difference between the active and the dummy plates with respect to spot welding of the spacer wires. Some difficulty was experienced in fixturing the assemblies to achieve the desired overall stack height because the thicknesses of the active plates were not as uniform as those of the dummy plates.

After brazing, visual examination at up to 30X magnification revealed all brazed joints in both microassemblies were apparently sound and complete. The overall height across the top and bottom spacers ranged from 0.400 to 0.402 in. for the Critical Facility Sample, and from 0.402 to 0.403 in. for the Irradiation Test Sample. The corresponding distances between the outer surfaces of the top and bottom plates of the respective microassemblies ranged from 0.321 to 0.322 in., and from 0.320 to 0.322 in. The bottom plate of the Critical Facility Sample was displaced longitudinally about 0.010 in.

3.6.2 Nature of Irradiations

Four of the shear-test specimens brazed with GE J8100 alloy were irradiated in the ETR-G12 Test Loop for two cycles. The irradiations were programmed so that two of the specimens received one-half and two specimens the highest fluence as listed in Table X. Peak fluence of ~1 x 10^{21} nvt (>1 MeV) was still significantly lower than the ~1 x 10^{22} nvt (>0.9 MeV) expected in the AARR Mark-I core. However, gross changes in the behavior of stainless steel had been reported in the test range. Therefore, these tests would provide some insight, since it was anticipated that potential problems with irradiation damage to the brazed joint would begin to appear in this range, if indeed there was a problem.

TABLE X. Irradiation Data for Shear-test Specimens

Specimen No.	Fast Dose nvt > 1 MeV (x 10^{-20})	Fission Flux Dose (x 10^{-20})	Days in Reactor
A-27-900	8.7	19.6	~45
A-27-901	4	9.0	~21
A-27-909	8.7	19.6	~45
A-27-910	4.7	10.6	~25

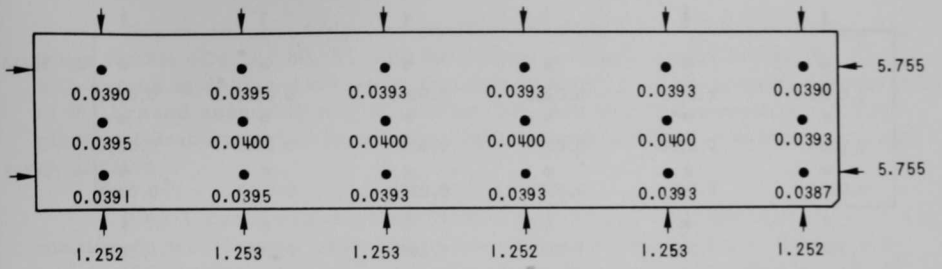

S/N 18-A15-918

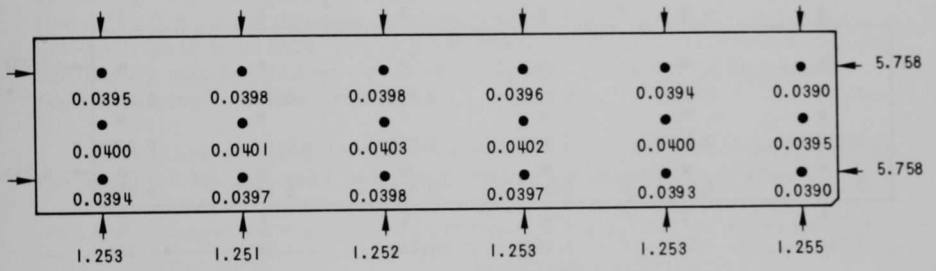

S/N 20-A15-920

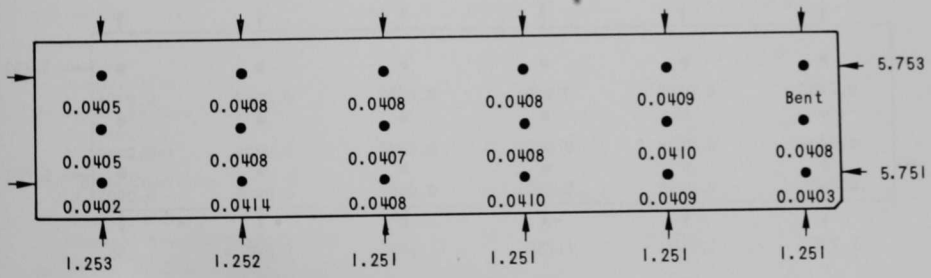

S/N 51-A16-951

Fig. 62. Dimensions of Active Fuel Plates Used in the Critical Facility Sample

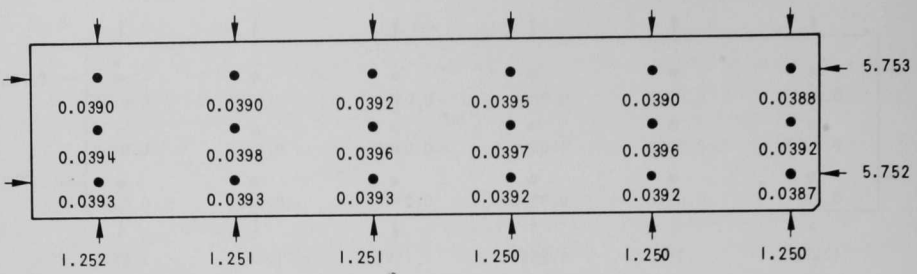

S/N 34-A15-934

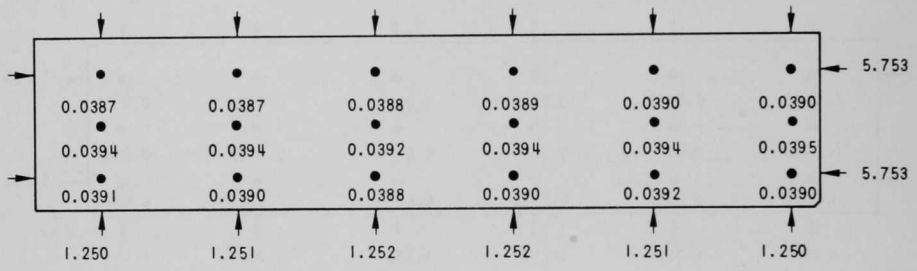

S/N 32-A15-932

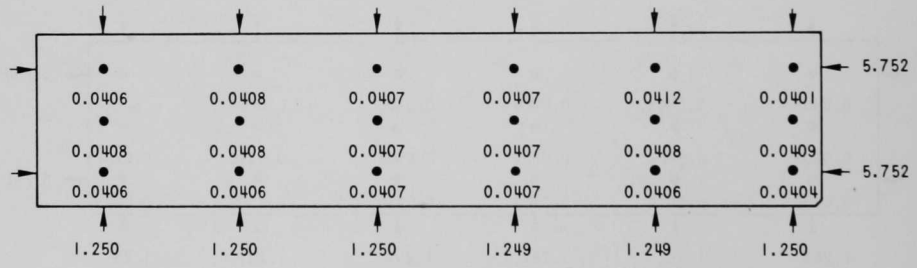

S/N 54-A16-954

Fig. 63. Dimensions of Active Fuel Plates Used in the Irradiation Test Sample

One microassembly was irradiated in the ETR-G12 test facility for three cycles (Cycles 80, 81, and 82). This test was conducted as the first in a series of design-evaluation tests to determine what effect rigid restraint of the brazed assembly might have on irradiation performance of the fuel plates. Basic material-irradiation data were available for comparison and evaluation.

The 3-cycle exposure achieved fuel burnups approximating the maximum peak burnup expected in any part of the AARR Mark-I core, i.e., ~43 to 45% fissioning of U^{235} versus a calculated maximum peak burnup of ~49% U^{235} fissioned in the Mark-I core. Heat fluxes also approached the nominal maximum expected in the Mark-I core; peak heat flux varied between 1.15 and 1.31 x 10^6 Btu/(hr)(ft^2). By comparison, the design operating conditions for the Mark-I reference core were: an average heat flux of ~0.5 x 10^6, a nominal maximum of ~1.5 x 10^6, and a hot-channel, hot-spot, peak heat flux of ~1.9 x 10^6 Btu/(hr)(ft^2). Thus this test, which admittedly was limited on a statistical basis, did afford an opportunity for identifying problem areas.

A more detailed comparison between the ETR test conditions and the expected Mark-I core operating conditions is given in Table XI.

TABLE XI. Comparison of ETR Irradiation Test Conditions with Mark-I Core Operating Conditions

	Engineering Test Reactor					
	Shear-test Specimens		Microassembly			Mark-I
	Cycle 78	Cycle 80	Cycle 80	Cycle 81	Cycle 82	Core
Fuel Coolant Inlet Temp, °F	190	190	190	190	190	135
Coolant pH	4.8-5.2	4.8-5.2	4.8-5.2	4.8-5.2	4.8-5.2	6.5-7.0
Coolant Temp in Fuel Zone, °F						
Average	250	250	255	260	250	160
Nominal Max	250	250	260	265	255	230
Fuel-plate Surface Temp, °F						
Average	250	250	323	326	307	205
Nominal Max	250	250	340	338	325	~320
Fuel-plate Centerline Temp, °F						
Average	250	250	460	470	430	270
Nominal Max	250	250	510	435	475	510
Nominal Max under Spacer Wire	250	250	550	530	510	~580
Heat Flux, 10^6 Btu/(hr)(ft^2)						
Average	0	0	1.13	1.1	0.95	0.5
Nominal Max	0	0	1.31	1.22	1.15	1.5

3.6.3 Nondestructive Evaluations

Nondestructive evaluations included visual examination and measurements of physical dimension and density, all performed by remote control in a high-level cave.

There was no discernible dimensional instability (i.e., twisting, buckling, or warping) of either the individual shear-test specimens or the microassembly. Density measurements of the microassembly (see Fig. 64) indicated a net volume increase of ~6%; this is in agreement with the characteristic fuel-plate swelling observed in the single-plate irradiation tests. There was no observable detrimental effect imposed on the active region of the fuel plates, the plate surfaces, or the microassembly proper by the center spacers or the restraint exercised by the wires and the box-beam configuration.

Destructive testing and analysis were precluded by the untimely termination of the fuel-development program for the Mark-I core.

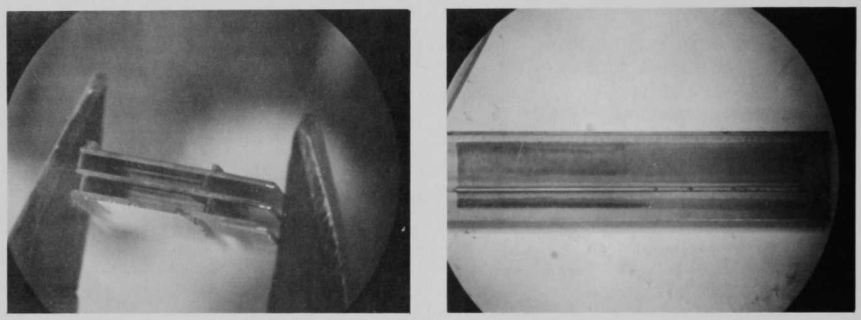

Fig. 64. Views of Microassembly Irradiated to 34% Burnup in ETR. Darker area in right photo is corrosion-product buildup over active fuel region (heat flux = $\sim 10^6$ Btu/(hr)(ft^2).

4.0 REFERENCE FABRICATION PROCEDURE

Based on the findings of the foregoing development activities and test fabrication of full-scale dummy fuel-plate assemblies, a reference procedure was evolved which, if followed, should yield a high-quality, dimensionally reliable product. However, the procedure as outlined below must be evaluated on similar assemblies containing active fuel plates and adjusted as required to produce the optimum results:

(1) Vapor degrease plates and spacer wires.

(2) Knurl spacer wires with 0.001-in.-deep grooves at 1/64-in. intervals.

(3) Cut wires to length (19.960 in.) and taper center spacer wires at both ends.

(4) Pickle plates and spacer wires for 15 min in an aqueous solution containing 40% HNO_3 and 4% HF at 120° F.

(5) Spot weld spacer wires to plates with stored-energy welder.

(6) Measure total thickness of each plate-spacer wire unit at five locations along each wire. Add thickness measurements for all 27 plates in the assembly. Replace plates as necessary to achieve a total stack height of 2.200 ± 0.005 in.

(7) Clean plates and wires with acetone.

(8) Apply GE J8100 braze alloy powder using plastic loading bar with a 0.030 x 0.25-in. groove. On the plate edge with the offset spacer wire, fill the triangular cross section formed by the overhanging spacer wire and the plate edge. Apply binder such as Nicrobraz cement or Coast Plastibond to hold powder in place.

(9) Clean excess binder and braze alloy powder from all plates.

(10) Apply stopoff. The actual sequence will depend on the stopoff material used. For example:

(a) Nickel-plated strips (0.0003-0.0004 in. thick) or vapor-deposited aluminum or titanium should be applied after step (4).

(b) Aluminum scribing of closely spaced, multiple lines should be performed after step (8).

(c) Nicrobraz Green Stopoff should be applied after step (9).

(11) Vacuum clean loose particles from all plate surfaces.

(12) Check dimensions of brazing fixture. Insert shims where appropriate to achieve a spacing of 2.196 in. between ground ceramic flats on the lower and upper levels of the fixture.

(13) Adjust positions of stepped wedges to achieve a spacing of 0.010-0.030 in. between the corners of the ceramic inserts and those of the plate assembly.

(14) Stack plates in bottom half of brazing fixture and shift stack laterally until each plate is firmly against the appropriate ceramic insert on the stepped wedge.

(15) Place top half of fixture over plate assembly and bolt both halves together.

(16) Make final adjustments in location of the plates. Place purge cap over one end of the plate assembly to direct hydrogen flow through the channels.

(17) Load fixtured assembly into retort and level; attach purge line and thermocouples; place stainless steel shroud over the fixture to shield the plate assembly from direct radiation of heat from retort walls.

(18) Seal retort and purge with dry hydrogen (-80°F dewpoint or better). (Throughout the series of brazing cycle tests, a hydrogen flow rate of 200 cfh was maintained during each heating cycle. This provided approximately 18 atmosphere changes per hour in the retort that was used.)

(19) Braze according to the following cycle:

(a) Heat to 800-900°F and equalize, i.e., heat until thermocouple readings at various locations on the plate assembly are within 20°F of each other.

(b) Heat to 1950°F at a rate of 200°F/hr.

(c) Equalize at 1950°F for 30 min.

(d) Heat to 2100-2120°F at a minimum rate of 200°F/hr, and hold for 2 hr. (Reduce to 2090-2110°F for optimum retention of boron in AARR fuel plates.[5])

(e) Decrease temperature to 1800°F at a rate of 100°F/hr by adjusting furnace power input.

(f) Shut off furnace power and allow plate assembly to cool to 800°F. (The cooling rate did not exceed 100°F/hr in this range.)

(g) Remove furnace from retort and allow plate assembly to cool to 250-300°F.

(h) Purge retort with exothermic gas or nitrogen; open retort and remove fixtured plate assembly.

(20) Remove plate assembly from fixture and examine.

5.0 SUMMARY AND CONCLUSIONS

Of the four braze alloys evaluated, GE J8100 alloy was selected. This selection was based on comparative shear tests with individual plate-spacer wire assemblies, pressure tests on brazed multiplate assemblies, and visual and metallographic examination of the brazed joints. In all instances, the GE J8100 alloy flowed more consistently, particularly into the tight joints required to maintain the stringent dimensional tolerances specified for the AARR fuel subassembly; it was stronger and produced better fillets at the junctures. Optimum brazing conditions involved a 2-hr hold at temperatures in the range 2090-2120°F. The higher temperatures appear to produce the higher shear strengths.

Nicrobraz 50, a phosphorus-containing alloy with a lower brazing temperature, was used successfully for rebrazing minor gaps in the GE J8100 brazed joints.

A grooved plastic loading bar is adequate for controlling the amount and placement of the braze alloy powder. Any of the acrylic binders tested will hold the powder in place, with no detrimental effects during the brazing cycle.

Plasma spraying was developed and used successfully as a technique for applying braze alloy to dummy fuel-plate assemblies which had continuous edge spacers. The alloy was sprayed onto the outer edges of both the plates and spacers after the plates were stacked and held in the final configuration by spot-welded strips of stainless steel.

Equivalent alloy flow was achieved by several surface-preparation techniques. These included pickling in a HNO_3-HF solution, nickel plating, stainless steel wire brushing, abrasive sanding, and electrolytic polishing. The pickling technique was selected on the basis of cost and ease of operation.

Several techniques for controlling alloy flow were demonstrated to be feasible, but with some attendant problems, either physical or economical. For example, Nicrobraz Green Stopoff was effective in stopping alloy flow; however, the attendant problems are flaking of the deposited material (which necessitates careful handling during plate assembly), evolution of gases during brazing, and the tenacious residue that forms after brazing. This residue can be removed by swabbing with hot, concentrated H_2SO_4 or by some form of abrasive flow through the channels.

Another promising technique of alloy flow control is scribing the stainless steel plate surface with a pointed, soft aluminum rod. The material is relatively inexpensive, easy to apply accurately, and does not leave any detrimental residue. The chief problems are extreme sensitivity to

surface contaminants (which cause occasional discontinuities in the scribed lines and permit the alloy to flow through) and possibility of reaction with the stainless steel surface if the aluminum deposit is too heavy.

Nickel-plated strips, 0.0002 in. or thicker, were also effective. The major disadvantage was cost: $75.00 for a full-scale, 27-plate fuel assembly.

Vapor-deposited films of aluminum (1000 Å thick) or titanium (100 Å thick) were completely effective in controlling braze alloy flow on single-plate specimens. Again, cost would be an important factor. Vapor deposition of either aluminum or titanium on fuel plates in production quantities was estimated to cost $2 to $3 per plate.

A knurling machine was designed to impress transverse grooves, 0.001-0.002 in. deep and 1/64 in. apart, into two opposing faces of the spacer wires. These grooves resolved the problem of incomplete flow of braze alloy flow between the wires and the plates; they also improved the quality of the spot welds.

A capacitor-discharge welder with tweezer electrodes was adjudged superior to an electronically controlled unit for spot welding the spacer wires to the plates. A spot-welding fixture was designed which located the spacer wires to a dimensional tolerance of ±0.002 in.

Brazing experiments on full-scale dummy plate assemblies indicated that overall stack-height tolerances of ±0.001 in. can be achieved with the open-beam brazing fixture that was ultimately designed and employed in the latter part of the program. Metallographic examination of over 150 brazed joints in a transverse cross section of one assembly revealed a defect incidence rate of slightly over 1%. The defects were in the form of partially brazed joints, i.e., about one-half of the joint was unbonded.

With some modifications, previously developed techniques were used to assemble and braze seven full-scale dummy plate assemblies to AARR Mark-I specifications. Some problems of dimensional control were experienced; these were attributed to thermal distortion of both the assemblies and the fixture during the heating and cooling cycles. Two of the assemblies contained visible gaps in the full-length edge spacer-to-plate brazed joints. These gaps most likely resulted from over allowance of joint thickness tolerance, a value which requires close control.

A full-scale AARR dummy fuel subassembly, including the box-type end fittings, was fabricated completely by brazing. Both tungsten inert gas welding and brazing of the end fittings were evaulated Brazing was selected because it afforded better dimensional control and the desired edge geometry was achieved with less difficulty.

Shear-test specimens, brazed with GE J8100 and Nicrobraz 50 alloy, and three-plate microassemblies, brazed with GE J8100 alloy, were irradiated in the ETR. Preirradiation examination revealed all visible joints were sound and continuous. Also, peel tests performed with the shear-test specimens indicated the GE J8100-brazed joints were significantly stronger.

Assembly procedures and fixturing which produced sound brazed joints with good dimensional control were devloped for the three-plate microassemblies. This was confirmed by metallographic examination of one assembly made with dummy fuel plates. There was no significant difference in behavior of the plates either during spot welding or brazing. However, the fueled plates required considerable effort in fixturing because of variations in plate thickness.

6.0 RECOMMENDED FUTURE EFFORTS

As mentioned in the Introduction, changes in the AARR core design resulted in termination of the brazing research and development activities for the Mark-I fuel subassembly. At the time of termination, the development phase of the contract with Pyromet was almost completed. Fabrication of two dummy fuel subassemblies and one depleted-UO_2-fueled subassembly by the methods and procedure developed was about to begin. Postirradiation examination of the microassembly and the shear-test specimens was also in progress.

Therefore, should interest in the Mark-I core design develop in the future, the following recommendations are made with respect to completing the present program:

(1) Evaluation of the irradiated shear-test specimens and the microassembly should be carried out to completion. These units are presently stored in the ETR-MTR hot cells. All should be tested and examined destructively to ascertain the effects of neutron radiation on the strength of the braze material and the brazed assembly.

(2) Three dummy fuel subassemblies completed and presently in storage at ANL should be inspected in detail to determine channel spacing and to ascertain overall dimensional control.

(3) The possibility of reducing distortion of the fixture and the plate assembly during the brazing cycle should be investigated further.

(4) The grooved plastic loading bar technique proved satisfactory for applying braze metal powder to the continuous outer spacers. However, for large-scale production work, the use of automatic machines for dispersing the braze metal paste should be investigated.

(5) The liquid stopoffs were applied with a swab in this program. Techniques should be developed for more rapid and accurate application of this material, e.g., use of rollers or straight, narrow pads.

(6) Although brazing was used successfully to fabricate and attach the end fittings, other techniques, such as electron beam welding, should be explored.

(7) Because of the critical requirements for joint quality and dimensional control, further development work should include brazing of depleted-UO_2-fueled plates fabricated to dimensional tolerances and surface quality specified for the enriched fuel plates.

(8) A sufficient number of plate assemblies should be fabricated by the brazing procedure developed to permit a statistical evaluation of the fixturing, brazing, and end product.

(9) The radius at the ends of the plates and the taper of the center spacers make it difficult to seal the channels for pressurized leak testing of the brazed joints. Late in the program, a sealing technique was proposed but was not completely evaluated. Briefly, it consisted of pouring a liquid silicon rubber (RTV 21), which can be catalyzed to vulcanize at room temperature, around the ends of the plate assembly, and then inserting a hypodermic needle and pressurizing each channel separately. Bench-type tests indicated the concept was feasible.

ACKNOWLEDGMENTS

The authors gratefully acknowledge the major technical contributions, consultations, and general assistance rendered by personnel from several organizations involved in the program. In particular, T. Hikido of Pyromet Co., the principal contractor, and C. R. Moyer and T. Hunnicut, who assisted Mr. Hikido in the execution of much of the fabrication development work and writing of interim reports; R. Perry of IIT Research Institute, and D. Vetter and J. S. Harmon of ANL for their combined services in developing nondestructive testing techniques and equipment; G. Gibson and M. Graber of Idaho Nuclear Co., for conducting the ETR irradiations and supplying the postirradiation-test data; C. H. Bean of ANL, G. M. Slaughter of ORNL, and R. Bertossa of Pyromet Co. for their consultations throughout the program; J. R. Korn of ANL for supervising preparation of the illustrations; and M. R. Sims of ANL for his editorial assistance.

REFERENCES

1. J. E. Cunningham et al., Specifications and Fabrication Procedures for APPR-1 Core II Stationary Fuel Elements, ORNL-2649 (Jan 1959).

2. W. C. Kramer and C. H. Bean, Fabrication of UO_2-Stainless Steel Dispersion Fuel for BORAX-V, ANL-6649 (Dec 1963).

3. R. G. Donelly, W. C. Thurber, and G. M. Slaughter, Development of Fabrication Procedures for Core B Fuel Elements for the Enrico Fermi Fast Breeder Reactor, ORNL-3475 (July 1964).

4. F. M. Miller, H. S. Gonser, and R. L. Peaslee, Development of Brazing Alloys for Joining Heat Resistant Alloys, WADC TR-55-213 (March 1955).

5. C. V. Pearson, Developments in the Elimination of Boron Loss from UO_2-Stainless Steel Dispersion Fuel Plates for the Argonne Advanced Research Reactor Mark I Core, ANL-7477 (Aug 1968).